CHARACTERIZATION OF THE SUBSTRATE-SPECIFICITY OF BARLEY rHv βII AND RICE BGlu1-LIKE ENZYMES

Teerachai Kuntothom

A Thesis Submitted in Partial Fulfillment of the Requirements for the Degree of Doctor of Philosophy in Biochemistry

Suranaree University of Technology

Academic Year 2008

การศึกษาความจำเพาะต่อสับสเตรตของเอนไซม์ rHv βII ในบาร์เล่ย์และเอนไซม์ในข้าวที่มีสมบัติคล้ายเอนไซม์ BGlu1

นายธีรชัย คุณโทถม

วิทยานิพนธ์นี้เป็นส่วนหนึ่งของการศึกษาตามหลักสูตรปริญญาวิทยาศาสตรดุษฎีบัณฑิต
สาขาวิชาชีวเคมี
มหาวิทยาลัยเทคโนโลยีสุรนารี
ปีการศึกษา 2551

ธีรชัย คุณโทถม : การศึกษาความจำเพาะต่อสับสเตรตของเอนไซม์ rHv βII ในบาเล่ย์และเอนไซม์ในข้าวที่มีสมบัติคล้ายเอนไซม์ BGlu1 (CHARACTERIZATION OF THE SUBSTRATE-SPECIFICITY OF BARLEY rHv βII AND RICE BGlu1-LIKE ENZYMES) อาจารย์ที่ปรึกษา : รองศาสตราจารย์ ดร.เจมส์ เกตุทัต-คาร์นส์, 138 หน้า.

เอนไซม์ (rHv βII) เป็นเอนไซม์ β-mannosidase ในบาเล่ย์พบได้ในเมล็ดข้าวบาเล่ย์ที่งอก เกี่ยวข้องกับการเปลี่ยนแปลงของผนังเซลล์โดยการย่อยสลาย galactomannan ซึ่งเป็นแกนกลางของ hemicellulose โดยทำงานร่วมกับเอนไซม์ β-mannanase จากการเปรียบเทียบความเหมือนของกรดอะมิโนระหว่าง rHv βII และเอนไซม์ β-glucosidaseในข้าว พบว่าเอนไซม์ Os1BGlu1 ในข้าวถูกจัดอยู่ในกลุ่มเดียวกับ rHv βII แสดงให้เห็นว่า เอนไซม์ Os1BGlu1น่าจะมีคุณสมบัติเป็น β-mannosidase เช่นเดียวกับเอนไซม์ rHv βII และเอนไซม์ Os3BGlu8 ถูกจัดให้อยู่ในกลุ่มเดียวกับเอนไซม์ Os3BGlu7 ซึ่งมีคุณสมบัติเป็น β-glucosidase แสดงให้เห็นว่า Os3BGlu8 น่าจะมีคุณสมบัติเป็น β-glucosidase เหมือน Os3BGlu7

cDNA ที่เป็นต้นแบบในการสร้างเอนไซม์ rHv βII ถูกสกัด และใช้เป็นต้นแบบในการสร้างเอนไซม์ rHv βII ในแบคทีเรีย พบว่าเอนไซม์ rHv βII ที่สร้างมีความจำเพาะต่อสับสเตรตเช่นเดียวกับเอนไซม์ Hv βII จากธรรมชาติเพราะทั้งสองเอนไซม์ย่อยสลาย *p*NP-β-(1,4)-D-mannoside ได้ดีกว่า *p*NP-β-(1,4)-D- glucoside และย่อยสลายสับสเตรต β-(1,4)-D-cellobiose ดีกว่า β-(1,4)-D-cellotriose เอนไซม์ rHv βII สามารถย่อยสลาย mannooligosaccharides ที่มีความยาว 2-6 หน่วยได้ดีกว่าเอนไซม์ Os3BGlu7 จากปฏิกริยา transglycosylation พบว่าเอนไซม์ rHv βII สามารถใช้สับสเตรต *p*NPGlc และ cellobiose ในการสังเคราะห์ ผลผลิตที่เชื่อมต่อกันโดย β-(1,2)-, β-(1,3)-, and β-(1,4)-D-linkages ตามลำดับ เอนไซม์ rHv βII สามารถเร่งปฏิกริยา transglycosylation โดยใช้ *p*NP-Glucoside และ cellobiose เป็นสับสเตรตได้ และได้ผลผลิตที่เชื่อมต่อกันพันธะ β-(1,2)-, β-(1,4)-, และ β-(1,6)-linkages แต่ไม่สามารถเร่งปฏิกริยา transglycosylation โดยใช้ สับสเตรตกลุ่ม mannosyl ได้

การศึกษาสมบัติของเอนไซม์ Os1BGlu1 และเอนไซม์ Os3BGlu8 พบว่าเอนไซม์ Os1BGlu1 ไม่มีคุณสมบัติ β-mannosidase ดังที่คาดไว้ข้างต้น แต่เอนไซม์ Os1BGlu1 และเอนไซม์ Os3BGlu8 มีคุณสมบัติเป็น β-glucosidase เหมือนกับเอนไซม์ Os3BGlu7 เนื่องจากเอนไซม์ rHv βII และเอนไซม์ Os3BGlu7 มีความจำเพาะในการย่อยสลายการ *p*NPMan และ *p*NPGlc แตกต่างกัน การเปรียบเทียบโครงสร้างจำลองของเอนไซม์ rHv βII, Os1BGlu1, และ Os3BGlu8 พบว่ากรดอะมิโนบริเวณที่ใช้ในการเร่งปฏิกริยาของเอนไซม์มีความแตกต่างกัน

ระหว่าง rHv βII, Os1BGlu1, Os3BGlu7 และ Os3BGlu8 ดังนั้นกรดอะมิโนที่บริเวณที่ทำหน้าที่จับกับสับสเตรตด้านปลาย (aglycone binding site) ใน subsite +1 และ +2 ในเอนไซม์ rHv βII จึงถูกเปลี่ยนให้เป็นกรดอะมิโนของเอนไซม์ Os3BGlu7 ใน 4 ตำแหน่งคือ V184I, A187L, L246V, และ V250N พบว่าการกลายพันธุ์ที่ตำแหน่งกรดอะมิโนเพียงตัวเดียวนั้น ไม่สามารถเปลี่ยนแปลงความจำเพาะต่อสับสเตรตได้ จากการศึกษาความจำเพาะของ *p*NPMan ต่อ *p*NPGlc พบว่า กรดอะมิโน L246 ทำให้ความจำเพาะต่อ *p*NPMan ลดลง 1.95 เท่าและเพิ่มความจำเพาะต่อ *p*NPGlc จากการศึกษาจลศาสตร์การเร่งปฏิกริยาของเอนไซม์กลายพันธุ์พบว่า L246 จับกับสับสเตรตและเกี่ยวข้องกับการเร่งปฏิกริยาของเอนไซม์

สาขาวิชาชีวเคมี ลายมือชื่อนักศึกษา_____

ปีการศึกษา 2551 ลายมือชื่ออาจารย์ที่ปรึกษา _____

TEERACHAI KUNTOTHOM : CHARACTERIZATION OF THE SUBSTRATE-SPECIFICITY OF BARLEY rHv βII AND RICE BGlu1-LIKE ENZYMES. THESIS ADVISOR : ASSOC. PROF. JAMES R. KETUDAT-CAIRNS, Ph.D. 138 PP.

β-GLCUCOSIDASE/β-MANNOSIDASE

Barley (*Hordeum vulgare*) β-glucosidase isozyme II/HvMANNOS1 (Hv βII), a β-mannosidase purified from germinated barley seed, plays a role in cell wall remodeling by concerted action with β-mannanase in the hydrolysis of galactomannan. Multiple protein sequence alignment of Hv βII with plant glycosyl hydrolase family 1 enzymes shows that it is most similar to plant β-mannosidases and rice BGlu1 β-glucosidase (Os3BGlu7) and related isozymes. Phylogenetically, Hv βII is grouped with the rice isozymes Os1BGlu1 and Os7BGlu26, suggesting that these enzymes should have β-mannosidase activity like Hv βII. Os3BGlu8 is grouped with Os3BGlu7, which suggests that Os3BGlu8 should have β-glucosidase activity like Os3BGlu7.

A cDNA encoding Hv βII was cloned and the Hv βII protein it encodes (rHv βII) was expressed in recombinant *Escherichia coli* and purified. The activity of rHv βII is nearly identical to Hv βII, as they both showed higher efficiency in hydrolysis of *p*NP-β-D-mannopyranoside (*p*NPMan) than *p*NP-β-D-glucopyranoside and in hydrolysis of cellobiose than cellotriose. rHv βII can hydrolyse oligosaccharides with β-(1,2)-, β-(1,3)-, and β-(1,4)-D-linkages, and glycosides, including alcohol glucosides, cyanogenic glucosides, hormonal glucosides, and isoflavonoid glucosides. rHv βII hydrolysed mannooligosaccharides with much higher specific activity than

rice Os3BGlu7 β-glucosidase. The rHv βII enzyme can catalyze transglycosylation using *p*NPGlc and cellobiose as both acceptors and donors to generate transglycosylation products with β-(1,2)-, β-(1,3)-, and β-(1,4)-D-linkages, but could not transglycosylate the corresponding mannosyl substrates. Two inhibitors, *p*NP-thioglucoside and *p*NP-thiomannoside inhibited rHv βII with similar K_i values of approximately 0.2 μM.

Recombinant expression of Os1BGlu1 showed that it does not have β-mannosidase activity, although it is phylogenetically grouped with plant β-mannosidases, while rice Os3BGlu8 is primarily a β-glucosidase like Os3BGlu7. Superposition of homology models of rHv βII, and rice Os1BGlu1, and Os3BGlu8 showed that the certain amino acids expected to interact with the substrate at the active sites are different between the phylogenetically related rHv βII and Os1BGlu1 and the more divergent rice Os3BGlu7 and Os3BGlu8, but no clear correlation of sequence with activity was observed. Four single site-directed mutations, V184I, A187L, L246V, and V250N, were constructed to change the amino acids in rHv βII that are located in subsites +1 and +2 to the corresponding amino acids in rice Os3BGlu7 to see if such changes would decrease the *p*NPMan/*p*NPGlc specific activity ratio of rHv βII. The L246V mutant is promising because it showed lower specific *p*NPMan/*p*NPGlc activity ratio (1.95) and the specific activity toward *p*NPMan decreased, while the specific activity toward *p*NPGlc increased, though not to the level of Os3BGlu7.

School of Biochemistry Student's Signature _____

Academic Year 2008 Advisor's Signature _____

ACKNOWLEDGEMENTS

I would like to express my deepest appreciation to my advisor Assoc. Prof. Dr. James R. Ketudat-Cairns for his patience guidance and encouragement when I had troubles with the experiments. I would also like to express my deepest gratitude to Assoc. Prof. Dr. Maria Hrmova for showing me that protein purification is an easy task, and her support, guidance, and encouragement during my lab works at University of Adelade, Australia.

I would like to thank my colleaguse and friends at the School of Biochemistry, Suranaree University of Technology for helping me with the lab techniques.

I would like to thank the Instutution for Promoting Science Teaching (IPST) for providing me a scholarship since high-school level.

I would like to thank my family for giving me for their unconditional love and full support throughout my studies.

Teerachai Kuntothom

CONTENT

Page

CONTENTS (Continued)

Page

CONTENTS (Continued)

Page

CONTENTS (Continued)

CONTENTS (Continued)

Page

CONTENTS (Continued)

Page

LIST OF TABLES

LIST OF TABLES (Continued)

LIST OF FIGURES

LIST OF FIGURES (Continued)

Figure **Page**

LIST OF FIGURES (Continued)

LIST OF ABBREVIATIONS

A	absorbance
Å	Angstrom
APS	Ammonium persulfate
ºC	degrees Celsius
bis-acryalmide	N,N-methylene-bis-acrylamide
$CaCl_2$	calcium chloride
cDNA	complementary deoxynucleic acid
DIMBOA	2,4-dihydroxy-7-methoxy-1,4-benzoxazin-3-one
DNA	deoxyribonucleic acid
DNaseI	deoxyribonuclease I
DP	degree of polymerization
dsDNA	double strand deoxyribonucleic acid
DTT	1,4-dithio-DL-threitol
EDTA	ethylene diamine tetraacetic acid
g	gravitational acceleration
(μ/m)g	(micro, milli) gram
h	hour
HEPES	4-(2-hydroxyethyl)-1-piperazineethanesulfonic acid
Hv βII	natural barley β-glucosidase
IMAC	immobilized metal-affinity chromatography

LIST OF ABBREVIATIONS (Continued)

IPTG	isopropyl β-D-thioglucopyranoside
K	Kelvin
(k)bp	(kilo) base pair
kDa	kilodalton
(μ/m)l	(micro, milli) liter
(n/μ/m)m	(nano, micro, milli) miter
(μ/m)M	(micro, milli) molar
M_r	molecular weight
min	minute
NaOAc	sodium acetate
PCR	Polymerase chain reaction
PGO	peroxidase-glucose oxidase
PMSF	phenylmethylsulfonylfluoride
*P*NPGlc	*p*-nitrophenyl β-D-glucopyranoside
*P*NPMan	*p*-nitrophenyl β-D-mannopyranoside
*p*NP	*p*-nitrophenol
PAGE	polyacrylamide gel eletrophoresis
PEG	polyethyleneglycol
rHv βII	recombinant barley β-glucosidase
SDS	Sodium dodecyl sulfate
s	second

LIST OF ABBREVIATIONS (Continued)

Tris	Tris-(hydroxymethyl)-aminomethane
T_m	melting temperature
TEMED	N, N, N′, N′-Tetramethylethylenediamine
TLC	Thin layer chromatography
V_M	Matthew's coefficient
V_o	initial velocity
v/v	volume by volume
w/v	weight by volume
xg	relative centrifugal force

CHAPTER I

INTRODUCTION

1.1 Overview of β-glucosidases

β-glucosidases (β-D-glucoside glucosyl hydrolases; EC 3.2.1.21) are enzymes that hydrolyse a broad variety of glycosides, which include aryl and alkyl-β-D-glycosides, or oligosaccharides from which they release glucosyl residues at the nonreducing end. The physiological function of β-glucosidases varies depending on their origin (archea, bacteria, fungi, plants or animals) and substrate specificity.

The roles of β-glucosidases in microorganisms have been identified. Large numbers of bacteria express β-glucosidases, as well as other glycosyl hydrolases including xylanases and endoglucanases, as these enzymes play roles in biomass conversion (Li et al., 2004).

In animals, β-glucosidases have been purified and characterized in several insects and mammalians. In insects, β-glucosidases have been purified from bean blister beetle (*Epicauta gorhami*), bean weevil (*Callosobruchus chinensis*), cockroach (*Periplaneta americana*) (Newcomer, 1954), wood louse (*Porcellio* sp.) (Newcomer, 1952; 1956), locust (*Loczsstami gratoria*), mealworm (*Tenebrio snolitor*) (Robinson, 1956), silkworm (*Bombyx mori*), and wild silkworm (*Dictyoploca japonica*) (Koike, 1954). A study of β-glucosidase purified from *Tenebrio molitor* midgut showed that it is capable of hydrolysing various substrates, including disaccharides, arylglucosides, naturally occurring plant glycosides, alkyl glucosides, oligosaccharides, and polylaminarin (Ferreira et al., 2001)

In mammals, three types of β-glucosidases have been identified; lysosomal glucocerebrosidase, intestinal lactase phlorizin hydrolase (LPH), and cytosolic β-glucosidase, which is expressed predominantly in the liver and kidneys (Gopalan et al., 1989). The deficiency of lysosomal glucocerebrosidase in human leads to Gaucher disease caused by lysosomal accumulation of glycosylceramide. In some adults, the lack of LPH, which is localized to the brush border membrane in the small intestine and hydrolyzes both β-D-galactosides and β-D-glucosides, causes lactose intolerance because lactose cannot be hydrolysed. Interestingly, human cytosolic β-glucosidase showed broad substrate specificity, hydrolyzing various aryl-glycosides (β-D-glucosides, β-D-galactosides, β-L-xylosides, and β-D-arabinosides) (Gopalan et al., 1989). Also, human cytosolic β-glucosidase has significant activity toward many common dietary xenobiotics, including glycosides of phytoestrogens, flavonoids, simple phenolics and cyanogens (Berrin et al., 2002; Berrin et al., 2003).

1.2 Plant β-glucosidases

1.2.1 Plant glycosides

So far, numerous plant glycosides have been identified, such as alcoholic glycosides, anthraquinone glycosides, coumarin glycosides, cyanogenic glycosides, flavonoid glycosides, phenolic glyocosides, saponins, steroidal glycosides or cardiac glycosides, steviol glycosides, and thioglycosides. Salicin is an example of an alcoholic glycoside, which is extracted from willow bark and is toxic to herbivores. Anthraquinone glycosides, which include aloin (barbaloin), isobarbaloin and emodin purified from *Aloe vera*, and aurantio-obtusin, physcion, emodin and chrysophanol purified from *Cassia tora*, have several activities, including antiseptic, laxative, and

viricidal (Kaufman et al., 1998). Several types of coumarin glycosides, such as scopoletin, bergapten from *Glehnia littoralis* and rhamnnopyranoside from *Daphne giraldii*, are economically important because they have antibiotic activities (Kitajima et al., 1998; Su et al., 2008). Flavonoid glycosides, such as rutin and naringin, are also commercially important because they have antioxidant properties (Matsui et al., 2008; Choi et al., 2007; Matsui et al., 2008). Phenolic glucosides, such as flavellagic acid purified from *Phinia glomerata* (Fischer et al., 2008) and hydragenol from *Hydrangea serrata* var. *thunbergii* (Yag et al., 1972), are also antioxidants. Saponins, such as fucostan from *Brufelsia grandiflora* and floratheasaponins from *Cammellia sinensis*, contain insecticidal and antimicrobial properties. Steroidol glycosides, such as tigogenyl glycosides from *Agave utahensis* L., have antifungal activity (Yokosuka and Mimaki, 2007). Stevioside, a major sweet glycoside of *Stevie rebaudiana* leaves, steviobioside, and isosteviol have antimicrobial properties (Lobov et al., 1991; Lin et al., 2004). Thioglucosides such as sinigrin from *Sinapis nigra* and sinalbin from *Sinapis alba*, are biochemical herbicides (Gabrys and Tjallingii, 2002). From the numerous types of identified glycosides, it is highly possible that plants express specific β-glucosidases to hydrolyse these glycosides.

1.2.2 Roles of β-glucosidases in plants

Studies of plant β-glucosidases showed that they act in several biochemical pathways including germination (Leah et al., 1995; Hrmova et al., 1996) and regulation of hormones (Dietz et al., 2000) as well as responses to environmental changes and pest defenses. Overall, plant β-glucosidases are capable of hydrolysis of short oligosaccharides with (1,3)-, (1,4)-, and (1,6)-β-D-linkages, as well as cleavage

the glycosidic bond between saccharides and disaccharides which were linked to various aglycone units.

The main noncarbohydrate component of secondary cell wall in higher plants is lignin, a macromolecule composed of highly cross-linked phenolic molecules. Lignins play roles in strengthening and water-proofing cell wall, providing mechanical support for the plant body, and contributing to defense against microbial attack (Boerjan et al., 2003). In angiosperms, the lignin is derived from the monolignols *p*-coumaryl alcohol, coniferyl alcohol, and sinapyl alcohol by dehydrogenative polymerization (Escamilla-Tevino et al., 2006) and these precursors are transported across the plasma membrane as β-D-glucosides via Golgi-mediated secretion (Ehlting et al., 2005; Samuels et al., 2002). At the cell exterior, which is the lignin deposition site, these transport forms of glucosides are subsequently hydrolysed in the apoplast by specific monlignol glucoside β-glucosidases (Escamilla-Tevino et al., 2006). β-Glucosidases purified from *A. thaliana*, chick pea, and lodgepole pine efficiently hydrolysed phenolic glucosides, including lignin precursors. The β-glucosidase purified from the cell wall of lodgepole pine hydrolyzed coniferin and syringin, with highest activity towards coniferin. In chick pea, a cell wall purified β-glucosidase hydrolysed coniferin and syringin, 218% higher activity was determined in coniferin than for *p*NPGlc. The *A. thaliana* β-glucosidases BGLU45 and BGLU46, like lodgepole pine and chick pea β-glucosidases, should play role in lignification because they showed high activity toward lignin precursors (Escamilla-Tevino et al., 2006). The BGLU45 hydrolysed syringin with highest activity, followed by coniferin with 87% relative activity, and had low activity to *p*-coumaryl alcohol glucoside, while BGLU46 hydrolysed salicin with highest activity, followed by *p*-coumaryl

alcohol glucoside with 71% relative activity, phenyl β-D-glucoside with 62% activity, and had low activity to syringin and coniferin.

In pest defenses, several reports identified β-glucosidases to release phytotoxins and pest repellents from glycoside precursors. 2-O-β-D-glucopyranosyl-4-hydroxy-7-methox-1,4-benzoxaxin-3-one (DIMBOA), a pest defense compound exhibiting antifungal and bacteriostatic activities is found as a β-D-glucoside wheat, maize, and rye (Niemeyer, 1988). The hydroxamic acid is released from DIMBOA-Glc (an inactive form) by specific β-glucosidases in maize (Babcock and Esen, 1994), wheat, and rye (Sue et al., 2000a; Sue et al., 2000b). Another example is the release of the respiratory poison HCN from cyanogenic β-glucosides, which is controlled by β-glucosidases in almond (Grover et al., 1977), cassava (Nambisan, 1999), flax (Fan and Conn, 1988), sorghum (Cicek and Esen, 1998), and rubber plant (Selmar et al., 1987). Plant β-glucosidases also act to release a mixture of terpenoids and indoles that makes herbivores highly attractive to parasitic wasps (Mattiacci et al., 1995).

Plant β-glucosidases also act in response to several environmental changes, including darkness, freezing, and salt stress. In response to darkness, the din2 mRNA, which encodes a β-glucosidase, was accumulated in Arabidopsis thaliana leaves (Fujiki et al., 2001). It was speculated that the β-glucosidase encoded by din2 should allow the plants to utilize β-glucoside conjugates as carbohydrate sources in leaves during dark treatment. In A. thaliana, the mutation in the SFR2 gene, which encodes a β-glucosidase homologue is responsible for the loss of freezing tolerance (Tholby et al., 2004). In determining the gene expression profile during the initial phase of salt stress in the salt tolerant Oryza sativa L. cv Pokkali, an up-regulated transcript encoding a β-glucosidase was detected (Kawasaki et al., 2001).

Also, the regulation of plant hormones is controlled by β-glucosidases, which were identified to release phytohormones in A. thaliana (Lee et al., 2006) and Zea mays (Brzobohaty et al., 1993). A β-glucosidase deficient A. thaliana line showed defective stomatal movement, early germination, abiotic stress-sensitive phenotypes, and lower abscisic acid (ABA) levels, which is different from A. thalianai that expressed ectopic β-glucosidase, which showed higher ABA levels and enhanced tolerance to abiotic stress. In further analysis, it was found that the ER-localized β-glucosidase in A. thaliana responded to the dehydration by releasing of ABA from ABA-glucose conjugate which is stored in shoot, root, and leaves. In H. vulgare cv. Gerbel, β-glucosidase in the intercellular washing fluid is responsible for the release of ABA from ABA-glucose conjugate (Dietz et al., 2000), which are stored in leaf apoplast. In another case, cytokinin from cytokinin-O-glucoside in Z. mays may be released by a β-glucosidase which is localized in plastids (Brzobohaty et al., 1993).

1.3 Classification of β-glucosidases

Glycosyl hydrolases can be classified by several properties, which include enzymatic mechanisms, modes of action, substrate specificities, sequence similarities, and tertiary structures. According to the IUBMB enzyme commission nomenclature, glycosyl hydrolases are designated EC 3.2.1.x, the first digit indicates the enzymes catalyzing hydrolase reactions, the second digit indicates the enzymes are glycosidases and enzymes catalyzing *N*-glycosyl compounds, third digit indicates that the enzymes hydrolyse O-glycosyl linkages are glycosidases, and the last digit indicates the substrates that are recognized.

In early studies when there were small numbers of enzymes, the enzymes with related sequences were classified into families without consistent nomenclature. Henrissat et al. (1991), reported the first broad attempt to classify glycosyl hydrolases into families based on amino acid sequences. A total of 291 amino acid sequences corresponding to 39 EC entries could be classified into 35 families. Only ten sequences could not be assigned to any family. By substrate specificity, eighteen of the thirty-five families were found to be monospecific and 17 were found to be polyspecific. (Henrissat and Bairoch, 1993) updated the classification of glycosyl hydrolases into families based on amino acid sequence similarities. The number of glycosyl hydrolases was increased to 482 entries that were classified into 45 families, of which 22 are polyspecific.

With the increasing numbers of glycosyl hydrolase amino acid sequences and more information on glycosyl hydrolase structures and mode of action, (Henrissat and Davies, 1996) updated the classifications of glycosyl hydrolases based on mechanisms and structures. In classification by mechanisms, glycosyl hydrolases can be broadly classified into groups of enzymes with retaining and inverting mechanisms, respectively. At a second level, groups of families that are thought to have a common ancestry as recognized by significant similarities in tertiary structure, together with conservation of the catalytic residues and catalytic mechanism, are grouped in the same clan.

The introduction of the CAZy carbohydrate active enzymes database website, (http://www.cazy.org/index.html) in which glycosyl hydrolases are classified into families based on amino acid sequences similarities because there is a direct

relationship between sequence and folding similarities, provided an up-to-date listing and classification of glycosyl hydrolases (Coutinho and Henrissat, 1999).

1.4 Glycosyl hydrolase mechanisms

Glycosyl hydrolases are capable of cleavage of the β-glycosidic bonds of their substrates by hydrolysis reactions and transglycosylation reactions in which the nonreducing glycosyl group is joined to oligosaccharides, alcohols or other nucleophilic groups. Two mechanisms, retaining and inverting mechanisms have been identified in glycosyl hydrolases by the retained (Koshland, 1953) and inverted (Zechel and Withers 2000; Withers 2001) configuration of the anomeric carbon of the product.

1.4.1 Retaining mechanism

Koshland (1953) originally proposed that the retaining mechanism occurs via a double displacement mechanism, through the formation of a covalent glycosyl-enzyme intermediate involving two carboxyl groups in the enzyme active site which act as a nucleophile and an acid/base catalyst. In known structures of retaining glycosidases, these carboxyl groups are approximately 5.5 Å apart. In the first step, the carboxyl groups that acts as a general acid protonates the glycosidic oxygen of the substrate. At the same time, the carboxylic acid residue, that acts as a nucleophile attacks the anomeric carbon, forming the glycosyl-enzyme intermediate and cleaving the C-O bond at the anomeric carbon to release the aglycone group (leaving group). The second step starts with the general acid-base deprotonating the incoming water molecule or alcohol at the same time as the water molecule attacks the anomeric

carbon from the β-position and cleaves the glycosidic ester intermediate. The product is released with the retention of the anomeric carbon of the substrate (Figure 1.1 a).

1.4.2 Inverting mechanism

Glycosyl hydrolases that act with inversion of chirality at the anomeric carbon generally use a direct displacement mechanism through an oxocarbenium ion-like transition state. These enzymes also generally have two catalytic carboxyl groups, which are approximately 11 Å apart to accommodate the water molecule that directly attacks the anomeric carbon of the substrate (Figure 1.1 b). The reaction starts with the carboxyl group that acts as a general base extracting a proton to activate the nucleophilic water molecule to attack the anomeric carbon, while another carboxyl group acts as a general acid, protonating the departing oxygen atom in a concerted fashion as the bond is cleaved (Koshlan, 1953).

1.4.3 Configuration of the bound substrate, covalent-enzyme intermediate, and transition state

It was widely accepted that the configuration of covalent-enzyme intermediate in β-glucosidases is $^{4}H_{3}$ (half-chair). However, the study on several β-glucosidases revealed that the configurations of the noncovalent enzyme intermediate during hydrolysis are not $^{4}C_{1}$ and are different depending on the structures of pyranosides to appropriately present the anomeric carbon for nucleophilic attack and satisfy the stereoelectronic requirements for an incipient oxocarbenium ion intermediate (Davies et al., 2003). In glucoside hydrolysing β-glucosidases, the configuration of noncovalent-enzyme intermediate is a distorted $^{1}S_{3}$, which converts to $^{4}C_{1}$ after the leaving group departed (Davies et al., 1998). On the other hand, for GH 26 mannanase

and GH 11 xylanase, the configuration of covalent-enzyme intermediate is a distorted $^{2,5}B$, which converts to $^{2}S_0$ after the leaving group departed (Sidhu et al., 1999; Sabini et al., 1999).

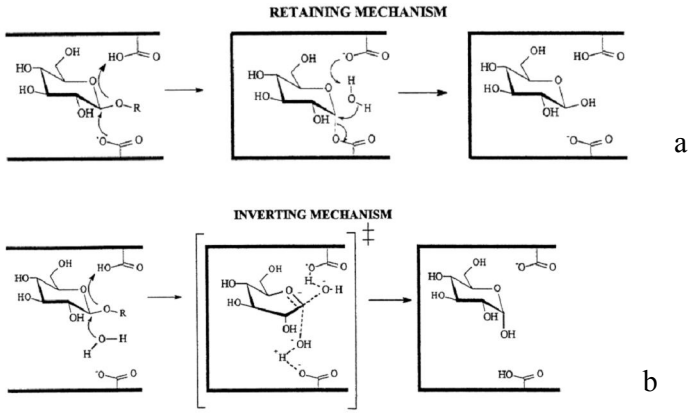

Figure 1.1 The retaining (a) and inverting (b) mechanisms of glycosyl hydrolases.

a) The retaining mechanism of glycosyl hydrolases is started by attack of the catalytic nucleophile on the anomeric carbon forming the oxocarbenium intermediate with retained configuration and the aglycone part of the substrate receives a proton from another carboxylic group which acts as a general acid/base. In the second step, the base catalyst removes a proton from an incoming water molecule, resulting in an activated water molecule, which attacks the oxocarbenium intermediate forming a second product containing the glycone part of the substrate. b) The inverting mechanism, which occurs via single step, starts with the activation of a water molecule by a carboxylate group, followed by the attack of the activated water molecule on the anomeric carbon to form the oxocarbenium intermediate. The acid catalyst protonates the oxygen atom of the aglycone portion, forming a product containing the aglycone part of the substrate, while the catalytic base withdraws a proton from activated water molecule forming a product containing the glycone part with inverted configuration.

1.5 Transglycosylation reaction

Like other glycosidase enzymes, some β-glucosidases can also be used for glycoside and oligosaccharide synthesis by reverse hydrolysis or transglycosylation. Synthesis of oligosaccharides and alkyl glucosides occurs by transfer of the glycosyl group from glycosides or short oligosaccharides onto sugars or alcohols. Reverse hydrolysis, a thermodynamically controlled reaction, comprises a reaction of a monosaccharide with a nucleophile, such as an alcohol, to give the corresponding glycoside and water until the equilibrium is reached as shown in equation 1 (Rantwijk et al., 1999).

$$\text{Glycosyl-OH} + R^1\text{-OH} \rightleftharpoons \text{Glycosyl-O}R^1 + H_2O \quad (1)$$

Glycoside synthesis by transglycosylation is based on monopolization of the catalyst by a reactive glycosyl donor, under which condition it is possible to overdrive the equilibrium conversion of reactant into product as shown in equation 2.

$$\text{Glycosyl-O}R^1 + R^2\text{OH} \rightleftharpoons \text{glycosyl-O}R^2 + R^1\text{OH} \quad (2)$$

As the reactant is consumed the concentration of the product will peak when its rates of synthesis and dealkylation become equal (Rantwijk et al., 1999). Therefore, the yield of glycoside is determined by a delicate balance between the rates of donor synthesis or hydrolysis, on the one hand, and product hydrolysis on the other (Figure 1.2).

In transglycosylation catalyzed by β-glucosidases, aryl-glucosides have been generated by transglycosylating monosaccharides and cellobiose or glucose, which are the products from hydrolysis of pNPGlc, onto primary, secondary, and tertiary alcohols generating glycosides and oligosaccharides (Svasti et al., 2003; Makropoulou et al., 1998).

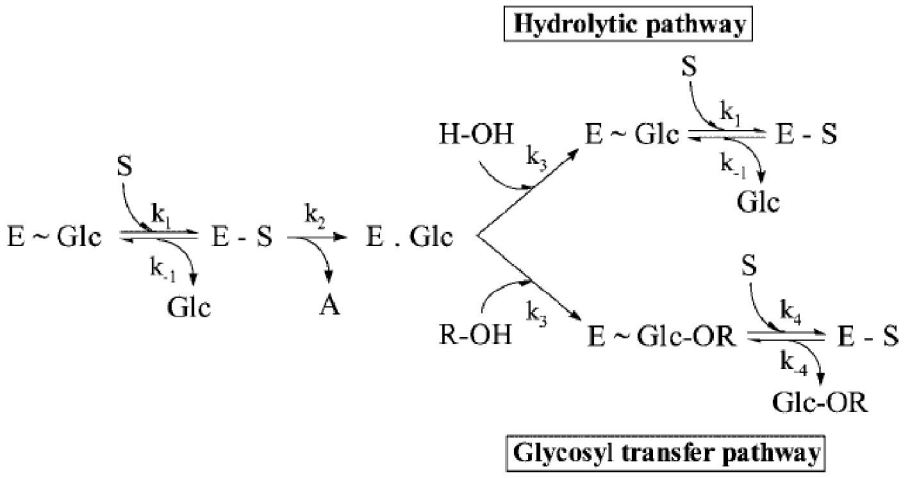

Figure 2 Kinetics of hydrolytic or glycosyl transfer reactions catalysed by a plant family 3 β-glucosidase. After an enzyme containing a noncovalently bound Glc product in the active site (E~Glc) binds the first molecule of substrate (S), the Michaelis complex (E - S) is formed (k_1), and the Glc product of the previous reaction is released from the active site. In the second step, the glycosidic bond is cleaved (k_2), and the glycone part of the substrate becomes covalently attached to the enzyme to produce a metastable covalent glycosyl-enzyme intermediate (E ~ Glc). At the same time, the aglycone part of the substrate (A) is released. In the third step, the covalent glycosyl-enzyme intermediate is subjected to cleavage (k_3) by a water molecule (H-OH), and a noncovalent E ~ Glc product complex is formed, which is ready to interact (k_1) with the second substrate molecule (S) to generate the next Michaelis complex (E - S), and again, the Glc molecule (Glc) is released from the active site. Alternatively, in the third step, the covalent glycosyl-enzyme intermediate (E ~ Glc) can be cleaved by an activated substrate molecule (R-OH), leading to a glycosyl rtansfer product (E ~ Glc-OR), which may remain noncovalently bound to the enzyme and is released (k_4) when a second substrate molecule approaches the active site and forms the next Michaelis complex (E - S). Figure obtained from Hrmova et al. (2002)

1.6 Mutagenesis approaches to identify the catalytic acid-base & nucleophile

Wang et al. (1995) studied residue E170, the possible acid/base residue, in *Agrobacterium faecalis*. By site-directed mutagenesis, the E170G mutant was constructed. The detailed pre-steady-state and steady state kinetic analyses of the mutant E170G suggested strongly that Glu170 is the acid/base catalyst. This is because the k_{cat} values were invariant over the pH range 5.0 - 9.0. Second, the rate of formation of the glycosyl-enzyme, calculated from k_{cat}/K_m and k_2, were similar to those of wildtype enzyme for the substrates not requiring protonic assistance but dramatically reduced for those needing acid catalysis. Third, addition of azide as a competitive nucleophile increased k_{cat} values 100-300 fold for substrates whose rate-limiting step is deglycosylation, yielding β-glycosyl azide, but had no effect on the wildtype enzyme. Lawson et al. (1997) determined the crucial roles of the acid/base catalyst in *Bacillus circulans* xylanase, a family 11 β-glycosidase with a retaining mechanism. Mutation of the E172, acid/base catalyst in *B. circulans*, to E172Q and E172C clearly showed the requirement of the carboxyl group in hydrolysis of substrates, because these two mutants could not hydrolyse xylan. However, E172D and idoacetate-reacted (IAA)-E172C could hydrolyse xylan with k_{cat} values reduced by only 25- and 400-fold, respectively, much less than that caused by complete removal of the carboxyl side chain in E172Q and E172C. This suggests that the carboxyl group is required as an acid/base catalyst in β-glycosidases, and its position can be changed slightly, though with a decrease in the catalytic rate. This suggested that acid/base catalysts need not be strictly conserved among β-glycosidases, as the catalytic nucleophile. Also, the presence of glutamine, which was found in place of

the acid/base catalyst in the TINQL motif in *Sinapis alba* myrosinase (Burmeister et al., 1997) also suggested that less conservation is required in the acid/base catalyst of β-glycosidases, and a noncovalently bound ascorbate molecule was found to play this role in myrosinase (Burmeister et al., 2000).

A study of *Agrobacterium faecalis* β-glucosidase, an exoglucanase in glycosyl hydrolase family 1, by trapping of a covalent glycosyl-enzyme intermediate identified E358 as the catalytic nucleophile (Withers and Street, 1988; Withers et al., 1990). The site-directed mutagenesis of this residue to N, Q, S, and H drastically decreased activity, thereby reaffirming the importance of this residue to catalysis. In a continued study, E358Q and E358N mutants showed low residual activities, which were approximately 10^6-fold lower than wildtype (Withers et al., 1992). In another case, Lawson et al. (1996) studied the effects of shorter and longer nucleophile catalysts in *B. circulans* xylanase. Two mutations, E78D and E78C, showed different results. The E78D mutant had a 1600-5000 fold decrease in the glycosylation step, while E78C had no measureable activity. This confirms the importance of precise positioning of the catalytic nucleophile at the active site of the enzyme.

1.7 Roles of β-mannosidases

β-mannosidases (EC 3.2.1.25) are enzymes that hydrolyse of terminal, non-reducing β-D-mannosyl residues in β-D-mannosides and oligosaccharides. β-mannosidases have been characterized in bacteria (Duffaud et al., 1996), fungi (Elbein et al., 1977), plants (Mo and Bewley, 2002), and animals (Chen et al., 1995). β-D-mannopyranosyl residues, the substrates of a β-mannosidase are building blocks of mannan, which is a homopolymer of β-(1,4)-D-mannopyranosyl residues in plant cell

walls and in the N-glycan decorations of mammalian proteins. In mammals, the deficiency of lysosomal β-mannosidase, an exoglycosidase that cleaves the single β-linked mannose residue from the nonreducing end of all *N*-linked glycoprotein oligosaccharides, causes the inability to stand, facial dysmorphism, intention tremors, and pastern joint hyperextension (Bryan et al., 1990; Jolly et al., 1990).

In a proposed structure and architecture of the primary cell wall models (Carpita and Gibeaut, 1993; McCann and Robert, 1994; Ha et al., 1997), cellulose and hemicelluloses are main constituents, which account for more than 50% of the dry weight, while pectin and structural glycoproteins are 25-40%, and 1-10% dry weight, respectively. Hemicelluloses are wall polysaccharides that are branched and are structurally homologous to cellulose in their backbones, which are composed of β-1,4-linked pyranosyl residues, such as D-glucose, D-mannose, and D-xylose. The mannose containing hemicelluloses, including galacto-mannans and galacto-glucomannans, are found in a variety of plant species as carbohydrate reserves. The galacto-mannans have a β-1,4-inked D-mannosyl (Man) residue backbone that is substituted at the O6 of certain Man residues (Stephen, 1982). Glucomannans are abundant in the secondary cell walls of woody species; they have a backbone that contains both β-1,4-linked Man and β-1,4-linked Glc residues. Galactoglucomannans are particularly abundant in the primary cell walls of Solanaceous species (O'Neil and York, 2003). They have a similar backbone as the glucomannans, but some of the backbone Man residues bear single-unit galactosyl residue side chains at the O6 position (Stephen, 1982). Three enzymes are responsible for hydrolysis of galactomannans, endo β-mannanase, α-galactosidase, and β-mannosidase. Mo and Bewley (2002) reported the increase of β-mannosidase expression in lateral and

mycropylar cell walls of germinating tomato seed. After 48 h of germination, the increase in expression of β-mannosidase and β-mannanase were reported, suggesting the cooperation of these two enzymes in degradation of endosperm cell wall galactomannan. Hrmova et al. (2006) also reported the cooperation of barley HvMan1 (β-mannanase) and HvβMANNOSE1 (β-mannosidase) in hydrolysis of galactomannan. In *A. thailiana*, the BGLU44 was reported to hydrolyse *p*NPMan twice as fast than *p*NPGlc (Xu et al., 2004).

1.8 Relation between structure and substrate specificities of plant β-glycosidases

In plants, several β-glucosidases show broad substrate specificities, while the rest are more substrate-specific β-glucosidases. This is due to differences in the shapes of their active sites. Therefore, there is a strong relationship between structure and substrate specificity of plant β-glucosidases.

Davies and Henrissat (1995) described the different structures among glycosyl hydrolases. First, a pocket or crater -like active site, this type of active site is found in glycosyl hydrolases that act on glycosides and short oligosaccharide chains, such as β-glucosidase and β-galactosidase. Second, the cleft-like active site allows random binding of several sugar units in polymeric substrates and is commonly found in endo-acting polysaccharides, which include β-1,3-1,4-glucanases and β-1,3-glucanases. Third, the tunnel-like active site is found in cellobiohydrolases enabling chains of polysaccharides to move through. The three different types of active sites found in glycosyl hydrolases are shown in Figure 1.3.

Barrett et al. (1995) determined the structure of the first plant β-glucosidase of white clover, a cyanogenic β-glucosidase (linamarase) which is a $(\beta/\alpha)_8$ barrel with its two catalytic glutamates, E183 and E397, located on β-strands 4 and 7, respectively. The catalytic glutamates E187 and E397 are found in the sequence motifs TFNEP and I(V)TENG, respectively, which are highly conserved among family 1 glycosyl hydrolases. The β/α_8 barrel is a conserved structure in all glycosyl hydrolase family 1 members. A list of plant glycosyl hydrolase family 1 crystal structures is provided in Table 1.1.

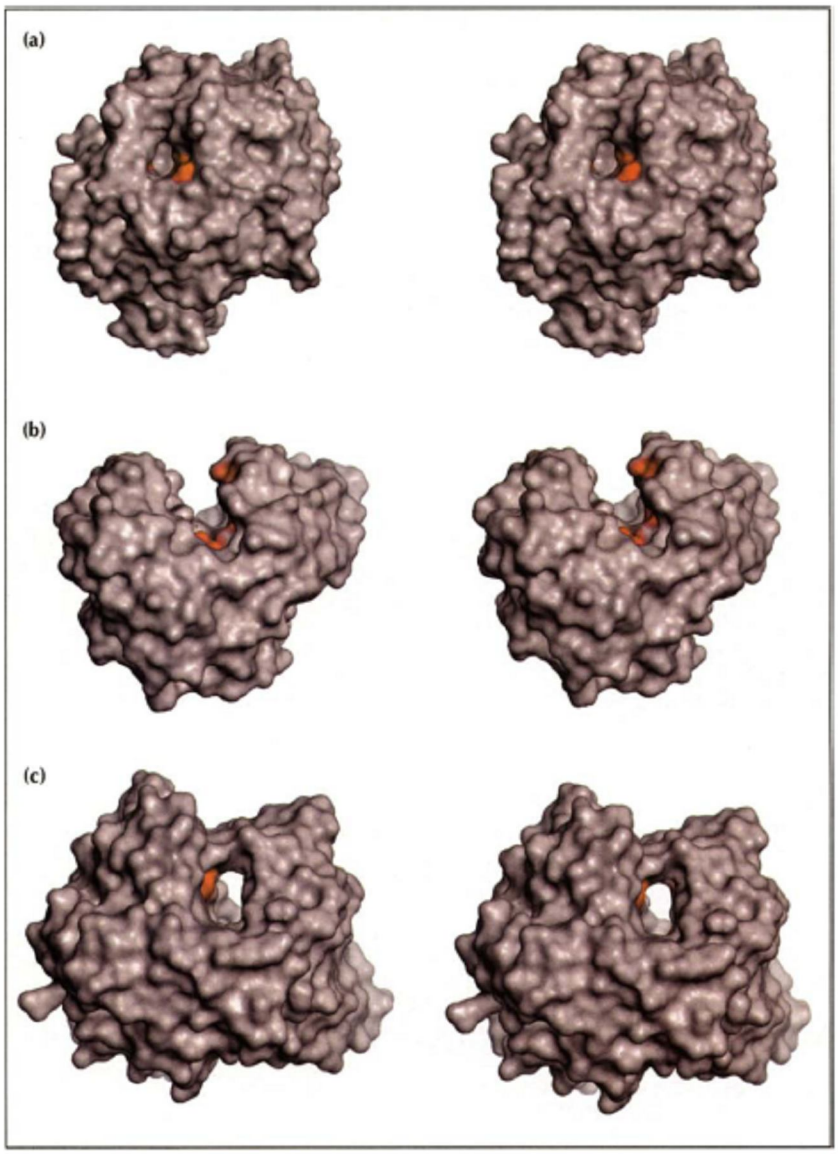

Figure 1.3 The three types of active site found in glycosyl hydrolases. (a) The pocket (glucoamylase from *A. awamori*). (b) The cleft (endoglucanase E2 from *T. fusca*). (c) The tunnel (cellobiohydrolase II from *T. reesei*). The figure is obtained from Davies, G. and Henrissat, B. (1995).

Table 1.1 Crystal structures of plant β-glucosidase that were previously reported

Organism	Activity	PDB	Sequence	Reference
Trifolium repens	cyanogenic β-glucoside	1CBG	CAA40057.1	(Barrett et al., 1995)
Sinalpis alba	myrosinase	1DWA 1DWF 1DWG 1DWH 1DWI 1DWJ 1E4M 1E6Q 1E6S 1E6X 1E70 1E71 1E72 1E73 1MYR 1W9B 1W9D 2MYR	Q7SIB0	(Burmeister et al., 1997; Burmeister et al., 2000; Bourderioux et al., 2005)
Zea mays	β-glucosidase 1	1E1E 1E1F 1E4L 1E4N 1E55 1E56 1H49 1V08	AAA65946.1	(Czjzek et al., 2000; Czjzek et al., 2001; Verdoucq et al., 2004)
Zea mays	β-glucosidase 60.1	1HXJ	CAA52293.1	(Zouhar et al., 2001)
Sorghum bicolor	cyanogenic β-glucoside	1V02 1V03	Q41290	(Verdoucq et al., 2004)
Triticum aestivum	β-glucosidase	2DGA	BAE92259.1	(Sue et al., 2006)
Rauvolfia serpentina	strictosidine β-glucosidase	2JF6	CAC83098.1	(Barleben et al., 2007)
Oryza sativa	β-glucosidase	2RGL 2RGM	U28047	(Chuenchor et al., 2008)
Rauvolfia serpentina	raucaffricine β-glucosidase	Crystal	AAF03675.1	(Warzecha et al., 2000)

Maize β-glucosidase (ZmGlu1) and sorghum dhurrinase (SbDhr1) share 72% sequence identity, but ZmGlu1 shows broad substrate specificity, which includes its natural substrate, DIMBOA-Glc, but not dhurrin. SbDhr1, on the other hand, is exclusively specific to dhurrin. Swapping of the C-terminal domain between ZmGlu1 and SbDhr1 gave rise to a chimeric ZmGlu1 with dhurrinase activity. Amino acid sequence comparison and homology modeling of ZmGlu1 and SbDhr1 revealed three amino acids, S462, S463, and F469, at the C-terminal of SbDhr1 which are involved in dhurrinase specificity (Czjzek et al., 2001). Later, comparison of the crystal structures of ZmGlu1 and SbDhr1 showed that these two β-glucosidases are different in their active site (Verdoucq et al., 2004). The active site of ZmGlu1 appears to be a flattened crater or slot, while the active site of SbDhr1 is wider and smaller. In ZmGlu1, aromatic sidechains of amino acids forming the aglycone binding site, W378, F198, F205, and F466, are responsible for binding to DIMBOA or other aromatic aglycones by aromatic stacking and π-interactions, (Czjzek et al., 2000). This is different from SbDhr1, in which N259, F261, and S462 are crucial for aglycone recognition and binding via hydrophobic interactions, hydrogen bonding and π-interactions. This suggests that interactions with the aglycone in plant GH1 family β-glucosidases is dominated by aromatic interactions with a help of hydrogen bonding in some cases.

In another case, the amino acid residues which are important in aglycone binding in the highly similar wheat (TaGlu) and rye (ScGlu) β-glucosidases were determined based on the TaGlu crystal structure (Sue et al., 2006). Wheat predominately hydrolyses DIMBOA-Glc, while DIBOA-Glc is more efficiently hydrolysed in rye. The changes of amino acids in ScGlu to the corresponding amino

acids in TaGlu, G464S, S465L, and F471Y, showed increased DIMBOA-Glc relative activity, while the relative activity toward DIBOA-Glc decreased. However, the counter mutations in ScGlu showed decreased relative activities to both DIMBOA-Glc and DIBOA-Glc. The changes of Y378, which is conserved in the two enzymes identified it as a crucial amino acid in rye, because the Y378A mutant showed decreased activity toward DIMBOA-Glc and DIBOA-Glc. In ScGlu, the Y378A mutant showed increased activity to DIMBOA-Glc by 4-5 fold. Therefore, the results suggest that amino acids with aromatic sidechains, and polar amino acids are required in substrate binding in TaGlu and ScGlu, like other plant β-glucosidases, but the amino acids determining substrate specificity of two closely related enzymes may be located in different locations.

1.9 Study of Barley β-glucosidases

Leah et al. (1995) purified and characterized a β-glucosidase (BGQ60) from mature barley seed. It hydrolysed cellobiose slightly faster than 4-nitrophenyl β-D-mannopyranoside (*p*NPMan) and 4-nitrophenyl β-D-glucopyranoside (*p*NPGlc), to which its activities were 55% and 47%, respectively, relative to cellobiose. It also slightly hydrolysed β-salicylic acid with 2.2% relative activity. BGQ60 hydrolysed (1-2)-, (1-3)-, and (1-4)-, but not (1-6)-β-linked oligosaccharides. BGQ60 activity increased as the degree of polymerization (DP) of cellooligosaccharides increased from 3 to 5, but was higher for cellobiose (DP 2). Simos et al. (1994) reported a barley β-glucosidase which is expressed for 2 weeks before germination and stored in the endosperm of barley seed. The determined N-terminal sequence and other peptide sequences of this enzyme exactly matched to that of BGQ60 suggesting that they are

the same enzyme. A barley β-D-glucosidase isozyme designated βII (Hv βII) was also purified from endosperm of germinated barley (*H. vulgare* L., cv. Clipper) seed, the NH_2-terminal amino acid sequence of which was nearly identical to BGQ60 (Hrmova et al., 1996). Hv βII also had the same substrate specificity as BGQ60, with preference of *p*NPMan to *p*NPGlc. Hv βII could also hydrolyse short oligosaccharides with (1-2)-, (1-3)-, and (1-4)-β-linked moieties with the same hydrolysis patterns toward cellooligosaccharides as BGQ60, suggesting that BGQ60 and βII may be orthologous isoenzymes in the two cultivars. Apart from Hv βII, three enzymes, β-glucan exohydrolase designated ExoI and ExoII and barley β-glucosidase isozyme βI, were also purified. The ExoI and ExoII hydrolysed substrates with (1,2)-, (1,3)-, (1,4)-, and (1,6)-β-linkages suggesting that they are not linkage specific. This is different from β-glucosidase isozyme βI because it is specific to (1,4)-β-linkage only. Recently, Hv βII was found to hydrolyse *p*NPMan nearly 3 times better than *p*NPGlc, so it was considered to be a β-D-mannosidase, and was renamed HvMANNOS1 (Hrmova et al., 2006). It was also found to efficiently hydrolyse oligosaccharides released from locust bean galactomannan by barley HvMAN1 β-D-mannanase, which suggested it may play a similar role in the breakdown of barley endosperm cell wall β-D-mannans during seed germination and seedling growth.

Homology modeling confirmed that Hv βII has a $(\beta/\alpha)_8$ barrel shape, like other plant family 1 β-glucosidases and the result from subsite-mapping that it has 6 subsites to bind β-1,4-linked glucosyl residues (Hrmova et al., 1998). The active site of Hv βII contains two amino acids with aromatic sidechains Y320 and W438, three amino acids with polar sidechains, H135, N180 and N318, two amino acids with charged sidechains, E445 and R91 at the -1 subsite. It is highly possible that aromatic

sidechains in the active site are largely responsible for substrate binding in Hv βII, as in maize, wheat, and rye β-glucosidases (Verdoucq et al., 2003; Sue et al., 2006).

1.10 Study of rice β-glucosidases

In rice (*Oryza sativa* L.), forty glycosyl hydrolase family GH1 genes were identified, 34 of which at least are likely to encode functional rice *β*-D-glucosidases (Opassiri et al., 2006). From this number of genes, it is possible that rice *β*-D-glucosidases have a range of substrate specificities. Several *β*-D-glucosidases have been characterized from rice seedlings (Schlieman, 1984; Akiyama et al., 1998; Opassiri et al., 2003). A cell wall-associated *β*-D-glucosidase that hydrolysed glucose disaccharides and oligosaccharides, but not polysaccharides, was described (Akiyama et al., 1998). It was specific to cellooligosaccharides and laminarioligosaccharides, and preferred disaccharides to higher oligosaccharides. Rice BGlu1 (Os3BGlu7) is another rice *β*-D-glucosidase, which is highly expressed in germinating seed, shoot, and flower, and showed broad substrate specificity towards natural and synthetic substrates (Opassiri et al., 2003). Towards disaccharides, Os3BGlu7 hydrolysed laminaritriose best, as indicating by low K_m and high k_{cat} parameters, while cellobiose, sophorose and gentiobose are not good substrates, as indicated by high K_m and low k_{cat} parameters (Opassiri et al., 2004). In hydrolysis of cellooligosaccharides, the k_{cat} increased while the K_m decreased as the DP increased from 2-6. In determining the catalytic efficiency, the k_{cat}/K_m value of cellohexaose is 3000-fold higher than that of cellobiose. This is different in hydrolysis of laminarioligosaccharides with DP 2-5, in which laminaribiose showed slightly higher k_{cat} and k_{cat}/K_m values compared to laminaritriose, while laminaritetraose and laminaripentaose are not hydrolysed. This

indicates that Os3BGlu7 is specific to β-(1-4)-D-linkage for longer oligosaccharides, but prefers short oligosaccharides with β-(1-3) linkages, Os3BGlu7 hydrolysed *p*NPGlc and 4-nitrophenyl β-D-fucopyranoside (*p*NPFuc) with much higher k_{cat}/K_m than 4-nitrophenyl β-D-galactopyranoside (*p*NPGal), *p*NPMan, 4-nitrophenyl β-D-xylopyranoside, 4-nitrophenyl β-D-arabinopyranoside, *p*NP-β-D cellobioside, and *p*NP-α-L-arabinoside. In hydrolysis of natural glucosides, Os3BGlu7 hydrolysed pyridoxine-5'-O-β-D-glucoside best with K_m value of 0.71 mM and k_{cat} of 1.64 s^{-1}, while it showed low activity toward cyanogenic glucosides, including prunasin, amygdalin, and dhurrin. However, Os3BGlu7 did not hydrolyse two cyanogenic glucosides (laminarin and DIMBOA), phenolic glucosides (phenyl-β-D-glucoside, arbutin, and salicin), a thioglucoside (sinigrin), and a hydroxyl coumarin glucoside (esculin). In transglycosylation, Os3BGlu7 catalyzed the transfer of glucose residue from *p*NPGlc to pyridoxine generating pyridoxine-5'-β-D-glucoside and four additional products which are *p*NP-cellobiose, *p*NP-cellotriose, cellobiose, and cellotriose.

Chuenchor et al. (2008) determined the crystal structure of Os3BGlu7 β-glucosidase alone and in a covalent complex with 2-deoxy-fluoroglucoside. The active site of Os3BGlu7 is a deep, narrow and straight binding cleft. The -1 subsite of Os3Bglu7 is formed by Q29, H130, Y131, E175, E176, Y315, E386, W433, E440, W441, and W433. Os3BGlu7 has a $(\beta/\alpha)_8$ structure like other family 1 β-glucosidases.

Amino acid sequence alignment of Os3BGlu7 and barley BGQ60 showed that these proteins share 64% identity, but these two *β*-D-glucosidases have different substrate specificities. Like barley BGQ60/*β*II *β*-D-glucosidase, Os3BGlu7 activity toward cellooligosaccharides increases with their degree of polymerization (DP) but

cellotriose is preferred to cellobiose by the barley enzyme. Os3BGlu7 also hydrolyses *p*NPGlc at a 10-fold higher rate than *p*NPMan. To change the activity of Os3BGlu7 to be more like BGQ60, improve the ratio of k_{cat}/K_m of cellobiose to cellotriose and decrease rate of *p*NPGlc hydrolysis, site directed mutagenesis was performed by changing the amino acids which bind to the substrate at subsites +1 (I179, N190, and L442) and +2 (N245) in Os3BGlu7 to the corresponding amino acids in BGQ60. The attempt to improve the cellobiase activity of Os3BGlu7 to that of BGQ60 failed as no mutant showed a comparable cellobiose:cellotriose k_{cat}/K_m ratio to that of BGQ60. The N190H mutant had a slightly improved k_{cat}/K_m ratio (0.15) compared to wildtype Os3BGlu7, which has a cellobiose:cellotriose k_{cat}/K_m ratio of 0.05 $s^{-1}mM^{-1}$. In cellotriose hydrolysis, N245V showed lowest k_{cat}/K_m value of 0.71 $s^{-1}mM^{-1}$ followed by I179V with a k_{cat}/K_m value of 3.06 $s^{-1}mM^{-1}$, which was 15- and 3.5-fold lower than the k_{cat}/K_m value of wildtype Os3BGlu7 (10.7 $s^{-1}mM^{-1}$). In comparison, BGQ60 had a k_{cat}/K_m of 2.01 $s^{-1}mM^{-1}$ in cellotriose hydrolysis, so the I179V mutation succeeded in decreasing the k_{cat}/K_m ratio to 0.71, which was 2.8-fold lower than that of BGQ60. However, L442R and N190H showed increased cellotriose k_{cat}/K_m values of 11.2 and 19.1 which were 1.1- and 1.8-fold higher than that of wildtype Os3BGlu7. In *p*NPGlc hydrolysis, L442R mutant showed similar kinetic parameters (k_{cat}, K_m, and k_{cat}/K_m) to wildtype Os3BGlu7, while N190H showed an increased K_m compared to 0.95 mM of 23.3 mM in wildtype Os3BGlu7, however N190H had a higher k_{cat} of 48.6 s^{-1}, which is 2.1-fold higher than wildtype Os3BGlu7. The N245V and I179V were promising in decreasing *p*NPGlc hydrolysis rate, because they showed increases in the K_m to 2.10 and 0.95 mM and lower k_{cat}/K_m ratios (2.24 and 6.40 $s^{-1}mM^{-1}$) than wildtype Os3BGlu7.

Opassiri et al. (2006) found that Os3BGlu7 and three other rice *β*-D-glucosidase isozymes (Os1BGlu1, Os3BGlu8, and Os7BGlu26) were grouped in the same phylogenetic cluster with barley BGQ60 and *Arabidopsis* (Xu et al., 2004) and tomato *β*-D-mannosidases (Mo and Bewley, 2002) (Figure 1). Within this cluster Os3BGlu8 was grouped with Os3BGlu7, suggesting that it would have higher activity to *p*NPGlc than *p*NPMan. Another two isozymes, Os1BGlu1, and Os7BGlu26, were grouped with barley BGQ60. This suggested that Os1BGlu1, and Os7BGlu26 should be more active toward *p*NPMan than *p*NPGlc.

1.11 Research objectives

The Objectives of this research thesis were as follows

1. To express active rice Os1BGlu1 and Os3BGlu8 β-glucosidases that are closely related to rice Os3BGlu7 β-glucosidase.

2. To close and express barley rHv βII and study the catalytic properties of rHv βII.

3. To determine the Os1BGlu1 and Os3BGlu8 β-glucosidases substrate specificities including activitities toward *p*NP-glycosides and oligosaccharides, and compare these with Os3BGlu7.

4. To determine the amino acids which are responsible for substrate binding and recognition in rHv βII, Os1BGlu1, Os3Glu7, and Os3BGlu8 and which amino acids differences make their substrate specificities different.

5. To construct structural models of rHv βII, Os1BGlu1, Os3BGlu8 by homology modeling based on the crystal structure of a Os3BGlu7 β-glucosidase in order to study the structural determinants of substrate-specificity.

CHAPTER II

MATERIALS AND METHODS

2.1 Materials

2.1.1 Plant materials

The barley (*Hordeum vulgare*) cultivar Clipper seeds were obtained from Assoc. Prof. Maria Hrmova of the Australian Centre for Plant Functional Genomics (ACPFG), Waite Campus, University of Adelaide, Glen Osmond, SA, Australia.

2.1.2 Plasmid and bacterial strains

The plasmid constructs containing full-length cDNA encoding rice β-glucosidase isozymes were acquired from the Rice Genome Resource Center, Tsukuba, Japan (http://www.rgrc.dna.affrc.go.jp/) (Kikuchi et al., 2003). The cloning vectors used in this study were pBluescript II SK (+) (Stratagene, La Jolla, CA, USA) and pENTR/D-TOPO (Invitrogen, Carlsbad, USA). The pBluscript II SK (+) was used in cloning of the cDNA encoding the rHv βII and Os3BGlu8 β-glucosidases, while pENTR/D-TOPO (Invitrogen) was used in cloning of the cDNA encoding the Os1BGlu1 β-glucosidase. The expression vectors used in this study were pET32a(+) (Novagen, EMB, Merck, Madison, WI, USA) and pET32a(+)/DEST (Opassiri et al., 2006).

Table 2.1 Plasmids used for this experiment

Recombinant Plasmid DNA	Antibiotic resistance	Total size (kb)
pBluescript II SK(+)	Ampicillin (50 μg/ml)	~3.0
pENTR/D-TOPO	Kanamycin (50 μg/ml)	~2.6
pET32a(+)	Ampicillin (50 μg/ml)	~6.0
pET32a/DEST	Ampicillin (50 μg/ml)	~6.0

2.1.3 Oligonucleotides and mutagenic primers

All oligonucleotides and mutagenic primers used in cloning and mutation of rHv βII were ordered from Genset-Proligo Singapore Pty Ltd. (Singapore) and are described in Table 2.3. The internal sequencing primers for rHv βII were ordered from GeneWorks (Sydney, Australia) and are described in Table 2.4. The primers used in cloning and sequencing of rice β-glucosidases Os1BGlu1 and Os3BGlu8 were ordered from Genset-Proligo and are described in Table 2.5.

Table 2.2 Bacterial strains

Bacterial strain	***Antibiotic Resistance***	***Genotype***	**Features**
DH5α	None	F^-, φ80d*lacZ*ΔM15, Δ(*lacZYA-argF*)U169, *deoR*, *recA*1, *endA*1, *hsdR*17(rk^-, mk^+), *phoA*, *supE*44, λ^-, *thi*-1, *gyrA*96, *relA*1	Convenient host for initial cloning of target DNA, High transformation efficiencies, good plasmid yields
One Shot® TOP10	Steptomycin Kanamycin (<50 μg/ml)	F- mcrA Δ(mrr-hsdRMS-mcrBC) φ80lacZΔM15 ΔlacX74 nupG recA1 araD139 Δ(ara-leu)7697 galE15 galK16 rpsL(Str^R) endA1 λ^-	Competent cells perfect for routine cloning and are included in many TOPO® cloning and expression kits
XL10-Blue	Tetracyclin (<40 μg/ml)	endA1 gyrA96(nal^R) thi-1 recA1 relA1 lac glnV44 F'[::Tn10 $proAB^+$ $lacI^q$ Δ(lacZ)M15] hsdR17(r_K^- m_K^+)	Ideal for cloning methylated DNA High efficiency electroporation-competent cells
Origami (DE3)	Kanamycin (30 μg/ml), Tetracyclin (12.5 μg/ml)	Δ(ara-leu)7697 ΔlacX74 Δ phoA PvuII phoR araD139 ahpC galE galK rpsL F′[lac^+ $lacI^q$ pro] (DE3) gor522::Tn10 trxB pLacI (Cam^R, Kan^R, Str^R, Ter^R)	Enhances the formation of disulfide bonds in the cytoplasm for greater yield of active protein

Table 2.3 Oligonucleotide primers used in cloning and mutation of the full-length and mature rHv βII cDNA

Primer name	Sequence	Length (bp)	T_m (ºC)
BGQ60_Ntermf	5'-GGACACGAGGATGAGGTCCTC-3'	21	54.7
BGQ60_Ctermr	5'-CCGGATCCTGTTTGCGATCCTAG-3'	23	60.6
BGQ60MatNcoIf	5'-CACCATGGACGGGCCGAACCCGAAC-3'	23	60.6
BGQ60CtermXho1	5'-CTCGAGCTAGCTCCTCTTCTTTTCGGAGAG-3'	30	72.4
BGQ60 V184I F	5'-CGAGCCAAGGATCGTCGCCGCTCTGGGGTAC-3'	31	77.1
BGQ60 V184I R	5'-GTACCCCAGAGCGGCGACGATCCTTGGCTCG-3'	31	77.1
BGQ60 A187L_F	5'-CCAAGGGTCGTCGCCCTTCTGGGGTACGACAATG-3'	34	77.3
BGQ60 A187L_R	5'- CATTGTCGTACCCCAGAAGGGCGACGACCCTTGG-3'	34	77.3
BGQ60 L246V_F	5'- GATTGGGATTGTATTGGATTTCG-3'	23	54.2
BGQ60 L246V_R	5'- CGAAATCCAATACAATCCCAATC-3'	23	54.2
BGQ60 V250N_F	5'-CTCTTGGATTTCAACTGGTACGAACC-3'	26	58.2
BGQ60 V250N_R	5' -GGTTCGTACCAGTTGAAATCCAAGAG-3'	26	58.2
BGQ60 E391G_F	5' -CCTACGATGATACTTTCTGGAAATGGAATGGACCAGCC-3'	38	72.3
BGQ60 E391G_R	5'-GGCTGGTCCATTCCATTTCCAGAAAGTATCATCGTAGG-3'	38	72.3
BGQ60 Q339S_F	5'-ACGCCGGTCAGTTACTCTGATGATTGGCATGTT-3'	33	70.8
BGQ60 Q339S_R	5'-AACATGCCAATCATCAGAGTAACTGACCGGCGT-3'	33	70.8
BGQ60W346P_F	5'-GATTGGCATGTTGGGCCAGTCTATGAACGAAAT-3'	33	70.1
BGQ60W346P_R	5'-ATTTCGTTCATAGACAGGCCCAACATGCCAATC-3'	33	70.1

Table 2.4 Primers for internal sequencing of the cDNA encoding the mature rHv βII protein.

Primer name	Sequence	Length (bp)	T_m
BGQ60_401_700F	5'-ACCACTATGACCTCCCGCTGG-3'	21	57.6
BGQ60_401_700R	5'-TCTCCCGGTATCGTTGCACC-3'	20	57.0
BGQ60_1001_1300_F	5'-CGCCGGTCAGTTACCAGGATGA-3'	22	60.2
BGQ60_1001_1300_R	5'-CAGCCACTCGGGCGCCATTG-3'	20	65.2

Table 2.5 Primers used in amplification of the cDNAs encoding mature rice β-glucosidases

Primer name	β-glucosidase isozyme	Sequence	Length (bp)	T_m
AK069177ConstR52Qf	Os1BGlu1	5'-CACCATGGTGAGCCGGCAGAGCTTCC-3'	26	70.6
AK069177Stopr	Os1BGlu1	5'-CCTCGAGTCAGTTTTTGCTGCTG-3'	23	57.9
AK120790NcoIFwd	Os3BGlu8	5'-CCATGGCCGCGTTCCCCAAGGGG-3'	23	72.5
AK120790stopXhoIr	Os3BGlu8	5'-TAACTCGAGCTAAATTGCTACTTCTACAG-3'	29	54.9

2.2 General methods

2.2.1 Transformation and selection

For transformation, an aliquot of frozen competent cells were thawed 5 min on ice. The ligation reaction or plasmid (10-200 ng) was added to fresh or thawed competent cells, mixed by tapping and incubated on ice for 30 min. The plasmid was transformed by heat shocking the cells at 42ºC for 90 s and quickly chilling on ice for 2 min. The 0.8 ml of LB broth was added to the transformed competent cells and they were incubated at 37ºC with shaking at 200 rpm for 1 h. The cells were collected by centrifugation at 12,000 rpm for 1 min, and the cell pellets were resuspended with 200 µl of LB broth. For antibiotic resistant selection of recombinant pET32a(+) clones, the transformed Origami(DE3) cells were spread on LB plates containing 15 µg/ml kanamycin, 12.5 µg/ml tetracycline and 50 µg/ml ampicillin.

2.2.2 Plasmid purification by the alkaline lysis method

Five milliliters of overnight transformed E. coli culture was collected by centrifugation at 4500xg, 5 min. The LB-media was removed and the cells were resuspended in 100 µl of alkaline lysis solution I (50 mM glucose, 10 mM EDTA, 25 mM Tris-Cl, pH 8.0) by mixing vigorously until the cell pellet was totally disrupted. Then, 200 µl of freshly prepared alkaline lysis buffer II (0.2 N NaOH, 1% (w/v) SDS) was added and the tube was mixed by inverting the tube 4-6 times. After that, 150 µl of ice-cold alkaline lysis buffer III (3 M potassium acetate, pH 4.8) was added and the tube was mixed by inverting 4-6 times. The alkaline lysis reaction was incubated on ice for 5 min and the clear solution containing the plasmids was separated from the cell debris by centrifugation at 13,000xg, 15 min, 4ºC. The clear supernatant was

transferred to a new tube and DNA were precipitated with 600 µl of absolute ethanol for 10 min at 4ºC. The precipitated DNA was collected by centrifugation at 13,000xg for 15 min at 4ºC and the supernatant was removed. The left over absolute ethanol was removed by inverting the tube on clean tissue paper. Then, the DNA pellet was washed with 1 ml of 70% ethanol, which was added and mixed by inverting the tube 4-6 times. The solution was removed and the DNA dried by inverting the tube on tissue paper for 10 min. The dried DNA pellet was redissolved in 100 µl TE buffer containing 20 µg/ml RNase A and incubated at 37ºC 10 min. At this step, the purified plasmids were clean enough for transformation and to check by digestion with restriction enzymes.

To purify the plasmids for DNA sequence determination, the RNase A treated plasmids were further purified by adding 70 µl of ice-cold precipitation solution (20% PEG 6000, 2.5 M NaCl) and chilled on ice for 1 h. The precipitated DNA was collected by centrifugation at 13,000xg, 15 min at 4ºC. The supernatant was removed. The pellet was washed by adding 1 ml of 70% ethanol and inverting the tube twice, and the ethanol solution was removed. The pellet was dried by inverting the tube on tissue paper for 10 min, and the DNA was redissolved in 50 µl of TE buffer, pH 8.0.

2.2.3 Agarose gel electrophoresis for DNA

The DNA samples, purified plasmids and PCR products, were checked by agarose gel electrophoresis. The agarose concentrations were 0.8% for purified plasmids and 1% for PCR products. The agarose gel was prepared by boiling the agarose in 1X TAE buffer (0.04 M Tris-HCl, pH 8.0, 0.04 M acetic acid, 0.001 M EDTA, pH 8.0) to melt and pouring it to set according to Sambrook et al. (1989). The DNA samples were mixed 5:1 with 6X loading dye (0.025% (w/v) bromophenol blue,

0.025% (w/v) xylene cyanol, 30% sterilized glycerol). Agarose gel electrophoresis was performed using a Pharmacia GNA-100 Gel Electophoresis Apparatus (GE Healthcare, Buckinghamshire, UK) at a constant voltage at 110 volt for 45 min. The DNA bands on the agarose gel were detected by staining with ethidium bromide (0.1 µg/ml) 30 s and destained in distilled water for 10 min. The DNA bands were visualized by UV light transillumination with a Fluoro-STM MultiImager (Bio-Rad, Hercules, CA, USA). The sizes of the DNA bands were estimated by comparing their migration with those of molecular markers, either 1 kb ladder or 2-log ladder (New England Biolabs, MA, USA), or GeneRulerTM 1 kb DNA ladder (Fermentas, Burlington, ON, Canada)

2.2.4 Purification of DNA bands from gels

The desired DNA band that had been separated on agarose gel electrophoresis was purified with a Perfectprep® gel cleanup kit (Eppendorf, Hamburg, Germany). The agarose gel containing the target DNA band was excised with a sharp razor blade, transferred to a microtube, and weighed. The agarose gel was dissolved in 3 µl of binding buffer for every 1 µg of wet gel weight. The tube was incubated at 50ºC for 5 to 10 min with vortexing every 2 min until the gel completely dissolved. One volume of isopropanol was added to the gel solution and mixed by inverting the tube 2-3 times. The solution was transferred, 800 µl at a time, to a spin column with a 2 ml collection tube. The spin column was centrifuged at 13,000xg 1 min and the solution in the collection tube was discarded. The spin column was washed with 750 µl of diluted wash buffer and centrifuged at 13,000xg for 1 min. The solution in the collection tube was discarded and the spin column was centrifuged for a further minute to remove residual wash buffer. The spin column was placed in a new

microtube, 30 µl of sterilized distilled water was added to the center of the membrane, the column as left to stand for 1 minute, and the spin column was centrifuged at 13,000xg for 1 min. The spin column was discarded and the tube containing the purified DNA solution was collected.

2.2.5 SDS-PAGE electrophoresis

Proteins were separated by sodium dodecyl sulfate–polyacrylamide gel electrophoresis (SDS-PAGE) with a method modified from that of Laemmli (1970) using a discontinuous buffer system. The 12% separating gel was prepared from these ingredients: 1.6 ml of distilled water, 1.3 ml of 1.5 M Tris-HCl, pH 8.8, 2.0 ml of acrylamide:bisacrylamide (30% T, 2.6% C), 100 µl of 10% (w/v) SDS, 100 µl of 10% (w/v) ammonium persulfate, and 10 µl TEMED. The stacking gel with 5% acrylamide was prepared with these ingredients: 2.7 ml of distilled water, 0.5 ml of 1.5 M Tris-HCl, pH 8.8, 0.67 ml of acrylamide:bisacrylamide (30% T, 2.6% C), 100 µl of 10% (w/v) SDS, 100 µl of 10% (w/v) ammonium persulfate, and 10 µl of TEMED. The protein samples were denatured by mixing with 5X SDS-PAGE loading buffer (60 mM Tris-HCl, pH 6.8, 25% glycerol, 2% (w/v) SDS, 14.4 mM 2-mercaptoethanol, 0.1% bromophenol blue) and boiling for 5 min. The insoluble proteins were separated from the soluble fraction by centrifugation at 13,000xg 5 min. Proteins were separated by SDS-PAGE on an SE260 Mini-Vertical electrophoresis unit (GE Healthcare), with the top and bottom reservoirs filled with 1x SDS-PAGE running buffer (25 mM Tris base, 192 mM glycine, 0.1% SDS, pH 7.5). Electrophoresis was performed at 150 volts constant voltage until the dye front reached the bottom of the gel. Separated protein bands were detected by staining in Coomassie brilliant Blue R-250 staining solution (0.1% Coomassie brilliant Blue R-

250, 45% (v/v) methanol, 45% (v/v) distilled water, 10% (v/v) glacial acetic acid) for 1 h. The excess dye was removed by soaking the gel in destaining solution (45% (v/v) methanol, 45% (v/v) distilled water, 10% (v/v) glacial acetic acid) and changing the destaining solution periodically until the background was clear. The protein sizes were estimated by comparing the proteins' migrations to those of the low molecular weight calibration kit for electrophoresis standards (GE Healthcare).

2.2.6 Bio-Rad assay

The Bio-Rad assay, based on the method of Bradford (1976), was performed to determine the concentration of protein. Standards were bovine serum albumin (BSA) ranging from 1-5 µg in 800 µl. Two hundred microlitres of dye reagent was added to each tube and mixed vigorously. The reaction was incubated at room temperature for 10 min. The absorbance at 595 nm was measured with a Genesys 10 UV spectrophotometer (Spectronic Instruments, Rochester, NY, USA) and the standard curve of the absorbance versus protein concentration was plotted.

2.3 Molecular cloning, and expression of barley and rice β-D-glycosidases.

2.3.1 Germination of the barley seeds, and purification of total mRNA from the germinated barley seeds

The barley cv. Clipper seeds were washed with 5% chlorox for 20 min, washed with distilled water twice, and soaked in distilled water overnight. The barley seeds were spread onto a polystyrene box which had a wet tissue paper at the bottom, and covered with wet tissue paper. The barley seeds were watered daily. After 42 h on

wet tissue paper, the germinated seed was separated from root and shoot, and the seed coat was removed. One hundred milligrams of germinated barley seeds were used in total RNA purification.

Barley seeds were ground to a power in a pre-chilled mortar in the presence of liquid nitrogen. Barley seed powder was transferred to a 1.5-ml microcentrifuge-tube, 1 ml TRIzol® reagent (Invitrogen, Carlsbad, CA, USA) was added, and the tube was mixed by vortexing for 1 minute. The solution was centrifuged at 13,000xg in a bench-top centrifuge 15 min to remove excess protein and fat, which were in the top layer, and the clear solution, which contained the RNA, was transferred to a new microcentrifuge tube and incubated at room temperature for 30 min. The solution was mixed with 0.2 ml chloroform, vortexed for 2 min and incubated at room temperature for 2 min. The solution was separated by centrifugation at 13,000xg for 10 min and the aqueous phase was transferred to a new microcentrifuge tube. Total RNA was precipitated by adding 0.5 ml isopropanol, mixing by inverting the tube twice and incubating the mixture at room temperature for 10 minute. The precipitated total RNA was collected by centrifugation at 13,000xg 10 min at 4ºC. The RNA pellet was washed with 70% ethanol twice and the pellet dried on tissue paper for 10 min. The RNA pellet was dissolved in 50 µl of DEPC-treated water and the A260/A280 ratio was determined.

Oligonucleotide primers to amplify full-length and mature cDNA encoding rHv βII were designed from the BGQ60 cDNA sequence (accession number L41869), and are listed in Table 2.3.

Total cDNA was reverse transcribed from the total RNA template from the Qt primer (5'-CCAGTGAGCAGAGTGACGAGGACTCGAGCTCAAGCT17-3') and

Superscript II reverse transcriptase (Invitrogen). In a 12 µl 1st cDNA strand synthesis pre-reaction, there were 1 µl of Qt primer (500 µg/µl), 1 µl (508 µg/µl) of total RNA purified from germinated barley seeds, and 10 µl of RNase free sterilized double distilled water. The reaction was incubated at 70ºC for 10 min and the tube was immediately transferred to ice. The reaction was mixed with 4 µl of 5X 1st strand synthesis buffer, 2 µl of DTT, and 1 µl of of 10 mM dNTP mix by pipetting, and incubated at 42ºC 2 min. Superscript II reverse transcriptase (1 µl) was added to the reaction and it was incubated at 42ºC for 50 min. The reaction was stopped by incubating it at 70ºC 15 min. The mRNA was hydrolyzed by adding RNase-H (Invitrogen) and further incubating it at 37ºC for 20 min.

2.3.2 Amplification and cloning of cDNAs encoding the mature rice Os1BGlu1 and Os3BGlu8 β-glucosidases

The cDNA encoding the mature rice Os1BGlu1 and Os3BGlu8 β-glucosidases were amplified with specific primers designed based on cDNA sequences in the Genbank database at NCBI, AK069177 for Os1BGlu1 and AK120790 for Os3BGlu8, the predicted protein products from which were submitted to Signal P (Bendtsen et al., 2004) to predict the signal peptide and start of the mature proteins. The four extra nucleotide overhang (CACC) was added at the 5' end of the Os1BGlu1 forward primer and *Nco*I and *Xho*I sites on the Os3BGlu8 forward and reverse primers, respectively. The primers and their T_m values are listed in Table 2.4. The reactions to amplify mature cDNA were performed with *Pfu* DNA polymerase (Promega, Madison, WI, USA).

2.3.2.1 Cloning the cDNA encoding the mature Os1BGlu1 β-glucosidase into pET32a/DEST

The amplified mature cDNA encoding the predicted mature Os1BGlu1 β-glucosidase was recombined with pENTR-D-TOPO using a pENTR™ Directional TOPO® Cloning Kit (Invitrogen). To set-up the TOPO® cloning reaction, 4 µl of fresh PCR product was mixed with the provided salt solution, 5 µl of sterilized distilled water, and 1 µl of pENTR/D-TOPO® vector. The reaction was mixed gently and incubated for 30 min at room temperature. Then, 2 µl of the TOPO® reaction was added to 25 µl of thawed One Shot® TOP10 competent cells and the cells and plasmid were mixed by tapping and incubated on ice for 30 min. The One Shot® TOP10 competent cells were heat shocked at 42ºC for 30 s and the reaction was immediately transferred to ice. The reaction was mixed with 250 µl S.O.C. medium at room temperature and incubated at 37ºC, with shaking at 220 rpm, 30 min. The transformed One-Shot® TOP10 competent cells were collected by centrifugation at 4000 rpm 5 min and 150 µl of the S.O.C. medium was removed. The collected One-Shot® TOP10 competent cells were resuspended in the remaining media and spread onto an LB plate containing 50 µl/ml kanamycin, which was then incubated at 37ºC overnight. The colonies that had grown overnight were picked, and checked by digestion with *Eco*RI and *Bam*HI, and their cDNA insert sequences were determined by automated DNA sequencing at Macrogen (Seoul, South Korea).

The recombinant pENTR-D-TOPO plasmids containing the cDNA encoding the mature Os1BGlu1 were transferred to pET32a/DEST (Opassiri et al., 2006) a Novagen pET32a(+) vector containing a Gateway® cloning cassette frame A) by an LR clonase recombination reaction (Invitrogen). The LR reaction was set-up in

an ice- chilled 1.5 ml tube by adding 150 µg of recombinant pENTR-D-TOPO Os1BGlu1 entry clone plasmid, 1 µl of 150 ng/µl of pET32a/DEST and TE buffer, pH 8.0, to adjust the volume to 4 µl. Then, 1 µl of LR ClonaseTM II enzyme was added to the reaction and it was further incubated at 25ºC overnight. Then, 1 µl of the provided 20 µg/µl Proteinase K solution was added to the LR recombination reaction and it was incubated at 37ºC 1 h. Then, 4 µl of the LR recombination reaction, was transformed into One-Shot® TOP10 competent cells by the heat shock method described above, the cells were spread onto LB-agar containing 50 µg/ml ampicillin, and the plate was incubated at 37ºC overnight. The colonies that grew overnight were picked and inoculated into LB media containing 50 µg/ml ampicillin and incubated at 37ºC overnight. The cultures were extracted for recombinant plasmids as described in section 2.2.2.

2.3.2.2 Cloning of Os3BGlu8 β-glucosidase

The amplified cDNA encoding Os1BGlu1 was blunt-ended ligated into pBluescript II SK (+) at the Sma I site. The ligation reaction was set-up with a 3:1 molar ratio of insert:vector. The ligation reaction was transformed into chemically prepared competent DH5α E. coli cells. The recombinant pBluescript II SK (+) plasmid was purified and digested with EcoRI and PstI to check for insert. The cDNA insert encoding O3BGlu8 β-glucosidase was cut from the pBluescript II SK (+) plasmids with the Nco I and Xho I restriction enzymes and ligated into pET32a(+) at the corresponding restriction sites. The ligation products were transformed into E. coli strain DH5α, as described in section 2.2.1 and plasmids prepared from ampicillin-resistant clones, as described in section 2.2.2. The recombinant pET32a(+) plasmids were digested with PstI to check for insert.

2.3.3 Mutagenesis of rHv βII

Mutagenesis of rHv βII was performed with the QuikChange® Site-Directed Mutagenesis Kit (Stratagene, La Jolla, CA, USA). The mutagenic primers of rHv βII were designed based on the sequence of the cDNA encoding mature BGQ60 according to the manufacturer's directions, which indicated that the primers should be 25-45 nucleotides long and contain 40% or higher G+C, and the mutated nucleotides in the middle should be flanked by 10-15 nucleotides on both ends. The Tm of the primers should be at least 78ºC or higher. The Tm of the primers were calculated using equation 2.1 below. Primers for generating mutations of rHv βII are listed in Table 2.3. The cycling parameters for the QuikChange mutagenesis method are described in Table 2.6.

Equation 2.1 $T_m = 81.5 + 0.41\ (\%GC) - 675/N - \%mismatch$

- N is the primer length in bases
- Values for %GC and %mismatch are whole numbers

Table 2.6 Cycling parameters for the QuikChange site-directed mutagenesis method

Segment	Cycles	Temperature	Time
1	1	95ºC	30 sec
2	12	95ºC	30 sec
		55ºC	1 min
		68ºC	1min

After the DNA synthesis cycles completed, the reaction was mixed with 1 µl of *Dpn* I and further incubated at 37ºC for 1 h. Then, 1 µl of the *Dpn* I treated reaction was transformed into XL1-Blue competent cells by heat shock. The transformed XL1-Blue competent cells were spread on LB agar containing 50 µg/ml ampicillin and the plate was incubated overnight at 37ºC. Transformed colonies that had grown overnight were picked into LB media containing 50 µg/ml ampicillin and incubated with shaking at 220 rpm, at 37ºC, overnight. The mutated plasmids were purified by the alkaline lysis method (section 2.2.2) and the DNA sequences were determined with the primers described in Table 2.4 at Macrogen.

2.3.4 Recombinant protein expression

Protein expression was carried out by transforming the pET32a expression constructs into *E. coli* Origami (DE3) cells (Novagen, Madison, WI, USA) by the $CaCl_2$ method (Sambrook et al., 2001). The colonies containing pET32a expression constructs were selected on LB broth containing 50 µg/ml ampicillin, 15 µg/ml kanamycin, and 12.5 µg/ml tetracycline. The selected clones were picked into LB media containing the same antibiotics to make a starter culture. To express recombinant β-glucosidases, 1% final concentration of starter culture was added into the same type of media and cultured at 37°C with rotary shaking at 220 rpm. Protein expression was induced when the OD_{600} of the culture reached 0.6-0.8. The optimum expression conditions were determined by varying the expression time from 3 to 16 h, the final concentration of IPTG at 0.2, 0.4 and 0.6 mM, and the temperature at 20°C and 25°C. The cell pellets were collected by centrifugation at 4800xg 15 min at 4°C. The cell pellets were kept at -80°C before use.

2.4 Recombinant rHv βII extraction and purification

Cell pellets were thawed on ice and resuspended in freshly prepared lysis buffer (20 mM Tris-Cl pH 8.0, 0.1 mg/ml soy bean trypsin inhibitor, 200 µg/ml lysozyme, 1% Triton-X 100, and 40 µg/ml DNase I) for 30 min with brief shaking at room temperature. The supernatant was separated by centrifugation at 17,200xg, 15 min, at 4°C.

The supernatant fraction containing recombinant rHv βII was loaded onto a pre-equilibrated immobilized metal ion affinity chromatography (IMAC) column (GE Healthcare, Buckinghamshire, United Kingdom) charged with Co2+. After loading the cell extract supernatant, the IMAC column was washed twice with 10 column volumes (CV) of equilibration/wash buffer (50 mM Tris-HCl, pH 7.2, 100 mM NaCl) to remove unbound protein. Bound rHv βII was eluted using 2 CV of elution buffer (50 mM Tris-HCl, pH 7.2, containing 150 mM imidazole). The eluted fractions were checked for hydrolysis of pNPGlc before dialysis in 20 mM Tris-HCl, pH 7.2, overnight.

The N-terminal thioredoxin and histidine tags were removed by digestion with 2 ng of enterokinase (New England Biolabs) per 1 mg of total protein, according to supplier's protocol. The released fusion tag was removed by adsorption to a second IMAC column. The unbound and low-stringency wash fractions from IMAC were checked for pNPGlc hydrolysis activity and those with activity were pooled and dialysed in 50 mM sodium acetate, pH 5.0, overnight. The dialysed rHv βII was purified by CM-sepharose (Takara, Tokyo, Japan) chromatography with elution by a gradient of 0-0.5 M NaCl in 50 mM NaOAc, pH 5.0. The rHv βII eluted at 0.15 mM NaCl.

2.4.1 Purification of rice Os1BGlu1 and Os3BGlu8 β-glucosidases

The rice Os1BGlu1 and Os3BGlu8 β-glucosidases were first extracted from expression cell pellets and purified on IMAC resin (GE Healthcare) charged with Co^{2+}, as with rHv βII. The Os1Bglu1 and Os3Bglu8 proteins were then purified by Q-sepharose chromatography (GE Healthcare) in 50 mM sodium acetate, pH 5.0, with elution by a gradient from 0 - 0.5 M NaCl in 50 mM sodium acetate, pH 5.0.

The NaCl concentration of the Os1BGlu1 and Os3BGlu8 β-glucosidase solutions was adjusted to 3 M with solid NaCl and each was loaded on a phenyl sepharose column, which had been pre-equilibrated with 3 M NaCl, 50 mM sodium acetate, pH 5.0. The proteins were eluted by decreasing the NaCl concentration from 3 M to 0 M NaCl in a smooth gradient over 50 CV. The Os1BGlu1 and Os3BGlu8 β-glucosidases eluted at 0.2 and 0.22 M NaCl, respectively. The fractions exhibiting pNPGlc hydrolysis activity were pooled and dialysed in 20 mM Tris-HCl, pH 7.2, overnight.

The N-terminal thiorexodin and histidine tag of the Os1BGlu1 protein was removed by enterokinase digestion and the released fusion tag was removed by adsorption to IMAC resin, as with rHv βII.

2.4.2 Tryptic mapping and N-terminal sequencing of rHv βII and Os3BGlu7

Tryptic mapping by MALDI TOF/TOF mass spectrometry (MS) of expressed rHv *β*II and Os3BGlu7 proceeded as follows. The two proteins (about 1 µg of protein) were digested with 10 ng of sequencing grade trypsin (Promega). The digest was reduced with 1 µl of 1 M DTT and acidified with the addition of 2 µl of 20% (v/v) acetic acid. The digest was desalted using a C18 ZipTip (Millipore) and eluted in 5 µl

of 60% (v/v) acetonitrile/1% (v/v) TFA and 1 µl of the sample was applied to a 600 µm AnchorChip (Bruker Daltonik GmbH, Bremen, Germany) according to the α-cyano-4-hydroxycinnamic acid (HCCA, Bruker Daltonik) thin-layer method. MALDI TOF mass spectra were acquired on a Bruker Ultraflex II MALDI TOF/TOF mass spectrometer (Bruker Daltonik GmbH) operating in reflectron mode under the control of FlexControl software (Version 3.0, Bruker Daltonik GmbH). External calibration was performed using peptide standards (Bruker Daltonik GmbH) that were analysed under the same conditions. Spectra were obtained at random locations over the surface of the matrix spot at an intensity determined by the operator. MS spectra were subjected to smoothing, background subtraction and peak detection using FlexAnalysis (Version 3.1, Bruker Daltonik GmbH). The spectra and mass lists were exported to BioTools (Version 3.1, Bruker Daltonik GmbH). Here, the MS and corresponding MS/MS spectra were combined and submitted to the in-house Mascot database-searching engine (http://www.matrixscience.com). The specifications were: Taxonomy - viridiplantae, Database - NCBI non-redundant 20071013, enzyme - trypsin, fixed modifications - carbamidomethyl (C), variable modifications - oxidation (M), mass tolerance MS - 50 ppm, MS/MS tolerance - 0.5 Da, missed cleavages - 1. Automated NH_2-terminal amino acid sequence analysis of the expressed rHv *β*II and Os3BGlu7, based on Edman degradation chemistry, proceeded as described previously (Hrmova et al., 2006).

2.4.3 Enzyme assay and determination of optimal pH and temperatures

Reactions to test for enzyme activity were set-up with 1 mM *p*NPGlc in 50 mM sodium acetate, pH 5.0, at 30ºC for 10-30 min, depending on the isozyme.

Reactions determining kinetic parameters of *p*NPGlc and *p*NPMan were stopped with two volumes of 2 M Na_2CO_3 and the 405 nm absorbance was measured. The amount of released *p*NP was determined by comparison to a *p*NP standard curve. For cellooligosaccharides and laminarioligosaccharides, the reactions were stopped by heating at 95ºC for 5 min. The amount of glucose released was determined by peroxidase/glucose oxidase coupled reactions (PGO assay, Sigma Aldrich, St. Louis, MO, USA) by comparison to a glucose standard curve.

The optimum temperature was determined over the range from 0 to 90°C in 10°C increments by incubating 4 nmol of enzyme at the temperatures for 15 min then adding 1 mM pNPG and incubating a further 30 min. The reactions were stopped by adding two reaction volumes of 2 M Na2CO3 and the absorbance at 405 nm was measured, and compared to a pNP standard curve prepared under the same buffer conditions.

The optimum pH was determined by incubating 4 nmol of enzyme with 1 mM pNPGlc in McIlvain buffers with pH ranging from 3.0-8.0 for 20 min at 30°C, stopping the reactions and measuring the absorbance as described above.

2.4.4 Determination of substrate specificity

The substrate specificity of rHv βII toward natural and synthetic substrates was evaluated by incubating 4 nmol of enzyme in 100 µl reactions with 3 mM final concentration of substrates at 30°C for 1 to 16 h in 50 mM NaOAc buffer, pH 4.0. Hydrolysis of *p*NP-linked substrates was detected by stopping the reactions with 2 volumes of 2 M Na_2CO_3 then measuring the absorbance at 405 nm. For cellooligosaccharides, laminarioligosaccharides, and other natural glucosides, 4 nmol of rHv βII was incubated with 1 mM final concentration of substrates in 100 µl

reactions at 30°C for 1 to 16 h in 50 mM NaOAc buffer, pH 4.0. The reactions were stopped by boiling for 5 min and the amount of glucose released was determined as described in section 2.3.4.

2.5 Determination of kinetic parameters

To determine the kinetic parameters of rHv βII toward *p*NPGlc, *p*NPMan, cellooligosaccharides DP 2-6, and laminarioligosaccharides DP 2-3, first, the optimum time point, at which the velocity of rHv βII hydrolysis gave a first order rate constant, was determined. In this step, 4 pmol of rHv βII was incubated with three different substrate concentrations at 0.5 K_m, K_m, and 2 K_m, based on the K_m of barley β-glucosidase isozyme βII purified determined by Hrmova et al. (1998), and the reaction was stopped at four different time points within 60 min to generate a plot between the hydrolysis rate and time. The time point at which the velocity of the β-glucosidase followed a first order rate constant was chosen and used in determination of the rHv βII kinetic parameters. In kinetic reactions, 2-4 pmol of rHv βII was incubated with $0.2K_m$-$3K_m$ at the chosen time point. For kinetic parameters toward *p*NPMan, the rHv βII was incubated with 0.2-3 times of the K_m of *p*NPGlc, on the assumption that kinetic parameters of natural and recombinant barley β-glucosidase should be similar. Kinetic parameters were calculated by fitting the rate of product formation and substrate concentrations in nonlinear regression of the Michaelis-Menten curves with Grafit 5.0 (Erithacus Software, Horley, Surrey, U.K.). The k_{cat} constant was calculated by dividing the V_{max} with total amount of enzyme in the reaction (2-6 pmol).

The kinetic parameters of Os1BGlu1 and Os3BGlu8 were determined according to the method determining rHv βII kinetic parameters by varying the substrate concentrations around the Km of Os3BGlu7. The minimum concentration of the substrate showing saturation of the product formation rate was the predicted 2Km. Then, the substrate concentrations from 0.2Km-3Km, using the new predicted Km, were used in determination of Os1BGlu1 and Os3BGlu8 kinetic parameters.

Subsite affinities of β-glucosidase enzymes were determined by calculating the differences in affinities from the Michaelis constants (Km) and catalytic rate constants (kcat) from the hydrolysis of (1,4)-β-oligosaccharides of DP 2-6 using the equation $An = RT[\ln (kcat/Km)n+1 - \ln (kcat/Km)n]$ and the method derived from Hrmova et al. (1998) and Hiromi (1973) described by Opassiri et al. (2004). The affinities at subsites -1 and +1 were determined by using values estimated from kcat and Km of cellooligosaccharides with DP 2-6 using the equation $A-1,+1 = RT\ln\{1/(0.018)Km\}n- \Sigma Ai$ for $1 < i < n$ and $1< j < 7$, where i is the subsite number and Kn,j is the binding constant for oligosaccharide of length n starting from subsite j.

The Ki constant of pNP-thioglucoside in inhibition of pNPGlc was determined. The reactions were set-up by incubating 0.4 pmol of rHv βII with pNPGlc from 0.083-1.5 mM (0.0830, 0.125, 0.250, 0.500, 1.00, and 1.50 mM) in the presence of 100, 200 and 400 μM pNP-thioglucoside in 100 μl reactions, at 30ºC, 40 min. Concentrations of pNPMan ranging from 0.0420 – 0.75 mM were used (0.042, 0.063, 0.115, 0.250, 0.500, and 0.750 mM) in the presence of 200 and 400 μM of pNP-thiomannoside.

The reactions were stopped with 2M Na2CO3 and the absorbance at 405 nm was measured. The Ki values for pNP-thioglucoside and pNP-thiomannoside were calculated with the competitive inhibition template of Grafit 5.0.

2.6 Transglycosylation assay

Transglycosylation reactions were carried out by incubating 0.45 nmole enzyme with 20 mM final concentration of substrates (pNPGlc, pNPMan, cellobiose, or mannobiose) in 10 mM sodium acetate buffer, pH 4.0, at 30ºC. Fractions were collected at 10 min, 8 h, and 16 h. The reactions in the collected aliquots were stopped by boiling for five minutes and the solutions dried using a DNA110 SpeedVac® (Savant Instruments, Holbrook, NY, USA). Dried products were re-dissolved in water and spotted onto Kieselgel 60 thin-layer plates (Merck, Darmstadt, Germany). Transglycosylated products were separated using a mobile phase containing ethyl acetate, acetic acid and water in the ratio 3:2:1. After separation was complete, the TLC plate was dried with a hair-dryer. The fluorescent products were detected under UV light. Sugar-containing products from the transglycosylation reactions were detected by spraying the TLC plate with 1% orcinol in 10% w/w sulfuric acid, then baking the plate at 150ºC for 20 s or until the signals were visualized.

2.7 Determination of relative β-mannosidase activity

2.7.1 Mannooligosaccharides standard

The standard for mannooligosaccharides hydrolysis standard was prepared as a 50 µl mannooligosaccharide solution containing mannose and β-1-4-linked

mannooligosaccharides with DP from 2-6 together at 2, 5, 10, 20, 30, and 40 nmole, respectively. Then 150 µl of acetonitrile was added to make 75% (v/v) acetonitrile. The mannooligosaccharides standard solution (200 µl) was separated on an Alltech Prevail carbohydrate ES column (Grace, Deerfield, IL, USA) connected to a model 1090 liquid chromatography system (Agilent Technology, Palo Alto, CA. USA) at a flow rate 0.4 ml/min. The mannooligosaccharides were vaporized and detected with an Alltech® 800 evaporative light scattering detector. The integrated area of a known mannose peak was used to calculate the amount of mannose.

2.7.2 Determining relative mannooligosaccharides hydrolysis rates

Relative mannooligosaccharide hydrolysis rates were determined for rHv βII and Os3BGlu7. For rHv βII, the reaction contained 0.45 nM enzyme and 0.8 mM (final concentration) mannobiose, and the reaction volume was adjusted to 200 µl with 10 mM sodium acetate buffer, pH 4.0. The reaction was incubated at 30ºC, 20 min, stopped by boiling 5 min, and dried by speedvacuum. Dried reactions were redissolved in 75% acetonitrile. The released mannose was separated using the same method as the mannooligosaccharides standards. The area under the mannose peak was measured and used to determine the amount of mannose released by fitting the area under mannose peak to the standard curve.

For Os3BGlu7, the method to determine the relative mannooligosaccharide hydrolysis rate was the same as rHv βII, but 10 mM sodium acetate, pH 5.0, was used in the reaction.

2.8 Protein homology modeling

The rice BGlu1 (Os3BGlu7) β-glucosidase structure (Protein databank accession number 2RGL), which is the known structure with the sequence most similar to rHv βII and the rice β-glucosidase isozymes, was obtained from Chuenchor et al. (2008) and used as template for homology modelling. A protein sequence alignment between the rice β-glucosidase template and each β-glucosidase was made with ClustalW (Thompson et al., 1994). The three-dimensional models of the β-glucosidase enzymes were generated with Modeller9v2 (Sali and Blundell, 1993) by satisfaction of spatial restraints and statistical analysis of the known secondary structures in the Modeller database. The five from 20 models generated by Modeller9v2 which showed the lowest objective function values were selected. The choices of best models were further refined with Procheck (Laskowski et al., 1993) by checking the stereochemical quality of the models and Prosa2003 (Guntert et al., 1992), which determines if the model has a correct fold by energy comparison between the template and model structures (Z-scores) that specify these folds.

CHAPTER III

RESULTS

3.1 Cloning and expression of plant β-glucosidases

3.1.1 Cloning and expression of barley rHv βII

The cDNA encoding mature barley rHv βII was amplified by RT-PCR with primers based on BGQ60 (Genebank accession L41869) with total mRNA of 3-day germinated barley (*H. vulgare* cv. Clipper) seeds as template. In the first amplification, a trace amount of cDNA encoding full-length rHv βII precursor was amplified (Figure 3.1). In the second PCR reaction, PCR products from the first amplification were used as template to amplify a cDNA encoding the mature rHv βII (Figure 3.2). The cDNA encoding the mature rHv βII was cloned into pENTR-D-TOPO and its sequence was determined and found to match the BGQ60 full-length cDNA sequence in the National Center for Biotechnology Information (NCBI) Genbank database (L41869) at 1551 out of 1557 bases resulting in four amino acid differences between rHv βII and BGQ60 (Figure 3.3). The cDNA encoding the mature rHv βII was translated to protein sequence, which was aligned with the mature BGQ60 protein and the N-terminal sequence from barley β-glucosidase isozymes βII (Figure 3.4).

3.1.2 Cloning and expression of rice β-glucosidases

The cDNAs encoding the predicted mature rice Os1BGlu1 and Os3BGlu8 β-glucosidases were PCR amplified from full-length cDNA clones encoding the

corresponding isozymes, obtained from the Rice Genome Resource Center, Tsukuba, Japan (http://www.rgrc.dna.affrc.go.jp/) (Kikuchi et al., 2003) to give products of 1605 and 1448 bp, respectively (Figure 3.5). The cDNA encoding Os1BGlu1 and Os3BGlu8 were cloned into pENTR-D-TOPO® and sequenced. The determined sequences of the cDNA encoding the predicted mature Os1BGlu1 and Os3BGlu8 rice β-glucosidases matched the cDNAs sequences of the corresponding entries in the NCBI and Knowledge-based Oryza Molecular Biological Encyclopedia (KOME, http://cdna01.dna.affrc.go.jp/cDNA/) databases, Genebank accessions AK69177 and AK120790, respectively.

3.1.3 Expression of recombinant β-glucosidases

The optimum conditions for expression of barley rHv βII and rice β-glucosidases (Os1BGlu1 and Os3Bglu8) as thioredoxin fusion proteins from pET32a/DEST in Origami (DE3) E. coli were determined. Of the conditions tested, the optimum expression condition for rHv βII, rice Os1Bglu1 and Os3BGlu8 β-glucosidases is induction with 0.6 mM IPTG at 20ºC, overnight (Table 3.1).

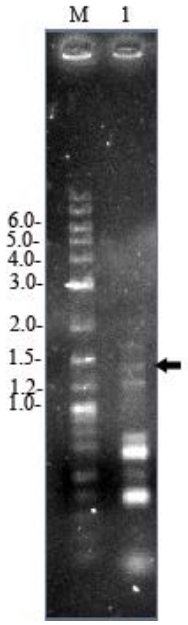

Figure 3.1 First amplification of a cDNA encoding full-length barley rHv βII precursor protein using the single stranded cDNA pool reversed-transcribed from germinated barley seed RNA as template. The PCR products were separated on 1% agarose gel electrophoresis and stained with ethidium bromide.

Lane M, 2-log DNA ladder (New England Biolabs)

Lane 1, PCR product from first round PCR amplification of a cDNA encoding full-length rHv βII

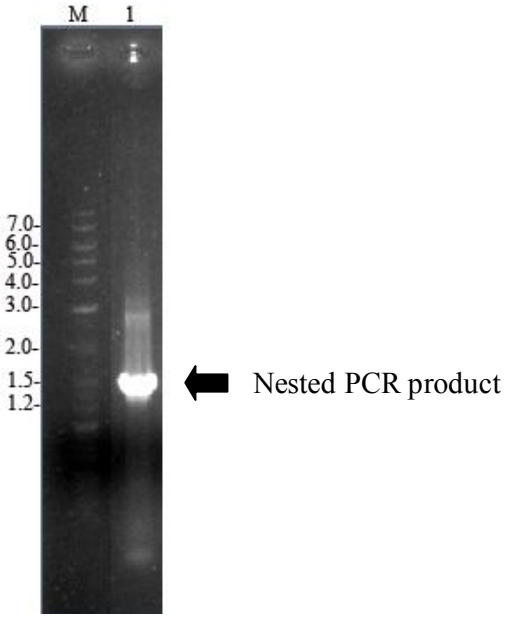

Figure 3.2 Nested PCR product of cDNA encoding mature rHv βII. The PCR products were separated on 1% agarose electrophoresis and stained with ethidium bromide.

Lane M, 2-log DNA ladder (New England Biolab)

Lane 1, Nested PCR products amplified using the first round rHv βII PCR amplification product as template with the BGQ60MatNcoIf and BGQ60CtermXho1 primers

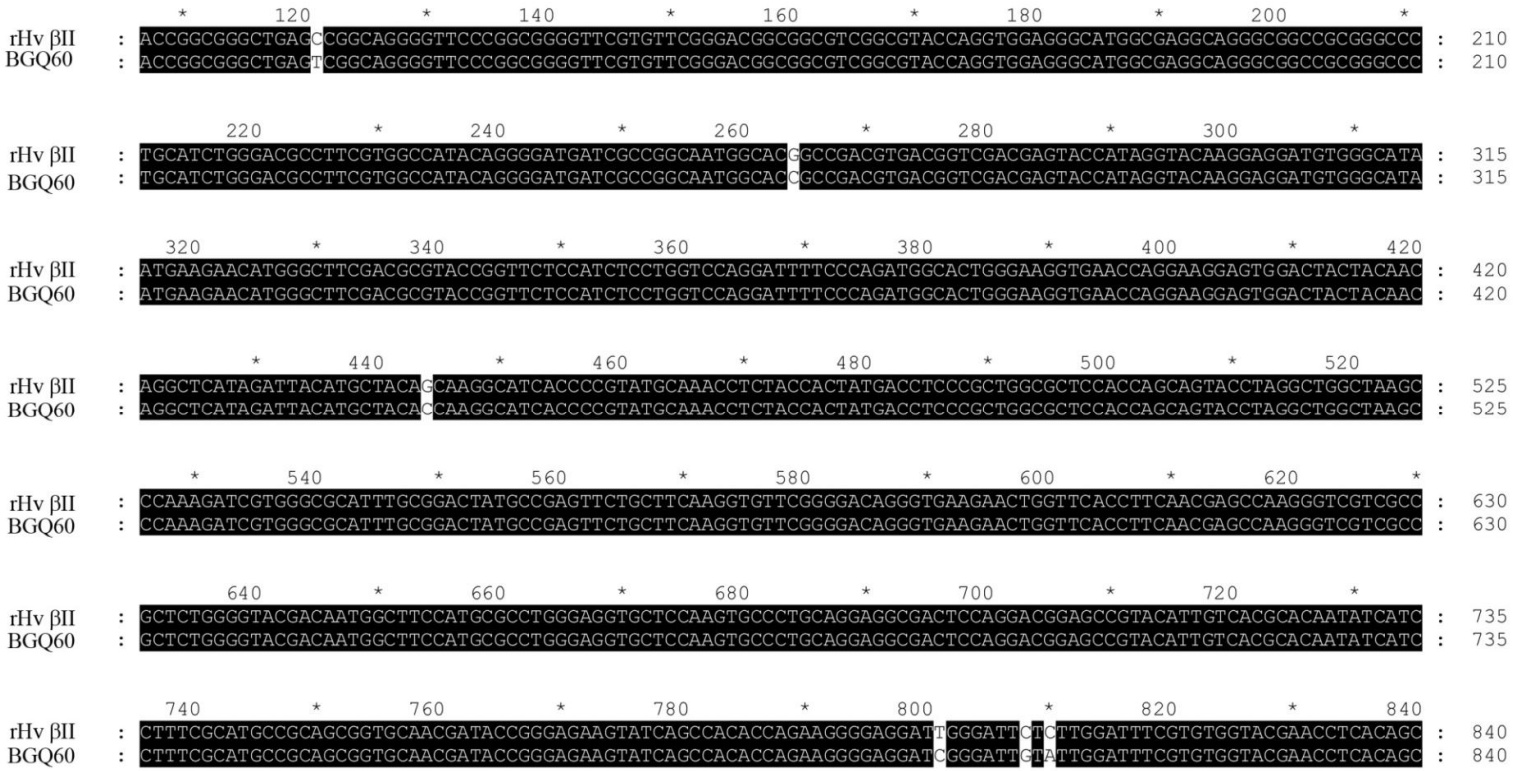

Figure 3.3 Alignment of cDNA encoding full-length BGQ60 (Leah et al., 1995) and rHv βII showing the 100-840 bp region, in which they are different by 6 nucleotides

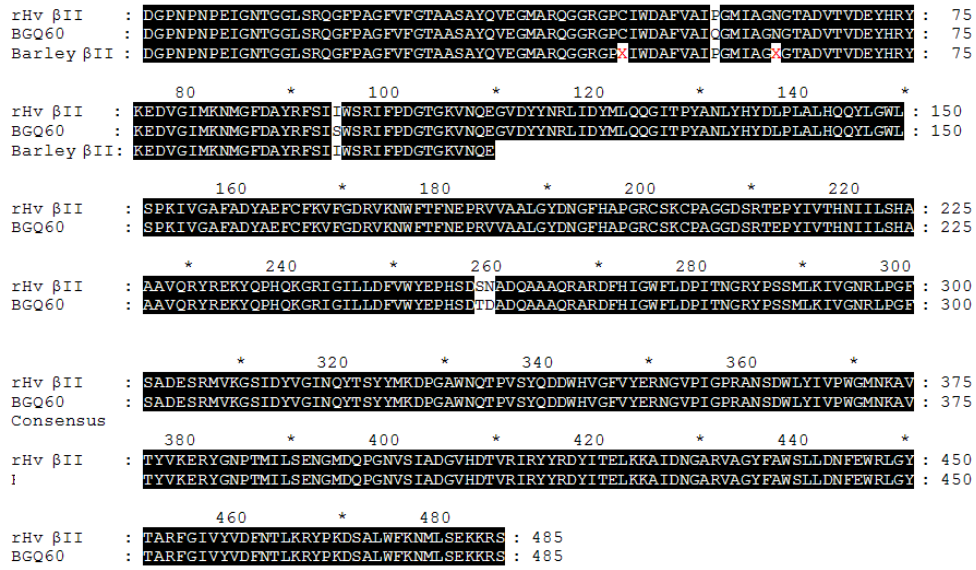

Figure 3.4 Alignment of mature protein sequences of rHv βII, and BGQ60 and barley β-glucosidase isozymes βII (Barley βII) showing four different amino acid differences between rHv βII and BGQ60.

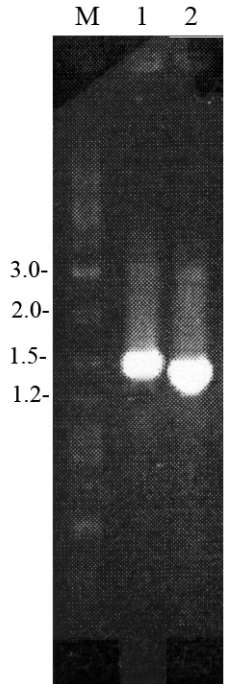

Figure 3.5 Amplification of cDNA encoding mature Os1BGlu1 and Os3BGlu8. The PCR products were separated by electrophoresis on a 1% agarose gel and stained with ethidium bromide.

Lane M, 2-log DNA ladder (New England Biolabs)

Lane 1, PCR product from amplification of the cDNA encoding Os1BGlu1 with the AK069177ConstrtF2 and AK69177Stopr primers

Lane 2, PCR product from amplification of the cDNA encoding Os3BGlu8 with the AK120790NcoIFwd and AK120790stopXhoIr

Table 3.1 Determination of the optimal expression conditions for rHv βII, Os1BGlu1, and Os3BGlu8. Ten micrograms of total protein was assayed for activity towards 1 mM pNPGlc in 50 mM NaOAc, pH 5.0. The reactions were incubated at 30°C 15 min and stopped by adding 2 M Na2CO3 and the absorbance at 405 nm was measured. The bold print indicates the expression condition which gives highest activity in pNPGlc hydrolysis.

Expression conditions	**Specific activity (nmol pNP/μg/min)**		
[IPTG] mM/Temperature (°C)/Time (h)	Os1BGlu1	Os3BGlu8	rHv βII
0.2/25/16	0.27	0.45	0.38
0.4/25/16	0.74	0.68	0.81
0.6/25/16	0.95	1.09	1.14
0.2/20/16	0.70	0.83	0.76
0.4/20/16	0.95	1.01	1.06
0.6/20/16	1.16	1.24	1.19

3.2 Purification of β-glucosidases

3.2.1 Purification of barley β-glucosidase (rHv βII)

The barley fusion protein (rHv βII) was purified by IMAC on resin charged with Co2+. The eluted fractions which hydrolysed pNPGlc were collected. The N-terminal tag was cleaved from rHv βII by enterokinase digestion. The rHv βII was separated from the N-terminal tag by reloading the digestion products on IMAC resin charged with Co2+. The rHv βII ran through the column while the N-terminal tag, which contained a hexahistidine tag, was bound to the IMAC column. The rHv βII from the various purification steps was analysed by SDS-PAGe in Figure 3.6.

3.2.2 Purification of rice Os1BGlu1 and Os3BGlu8 β-glucosidases

The active recombinant rice Os3BGlu8 was first purified by IMAC on resin charged with Co2+, as was used in purification of recombinant rHv βII, and it was

separated from most of the proteins in E. coli (Figure 3.7). However, the fusion protein containing the thioredoxin and hexahistidine tags, which gave bands at 18-21 kDa on SDS-PAGE, co-eluted with Os3BGlu8. The Os3BGlu8 purified from the Co2+ IMAC column was subjected to purification using Q-sepharose (GE Healthcare), and was eluted at 0.18 mM NaCl. Still, the fusion protein containing hexahistidine tag co-eluted with Os3BGlu8 (Figure 3.8). Therefore, Os3BGlu8 was further purified by phenyl sepharose (GE Healthcare) and it eluted at 0.22 mM NaCl (Figure 3.9).

The Os1BGlu1 protein was purified with the same methods used in Os3BGlu8 purification, Co2+ IMAC column, Q-sepharose, and phenyl sepharose. Os1BGlu1 was purified from most of the E. coli proteins by Co2+ IMAC (Figure 3.10), followed by purification using Q-sepharose, in which Os1BGlu1 eluted at 0.2 mM NaCl (Figure 3.11), and phenyl sepharose chromatography, in which Os1BGlu1 eluted at 0.2 mM NaCl (Figure 3.12). In the final step, Os1BGlu1 was purified by digestion with enterokinase to cleave off the N-terminal fusion tag containing the hexahistidine tag and Os1BGlu1 was purified from the fusion tag protein by Co2+ IMAC (Figure 3.13).

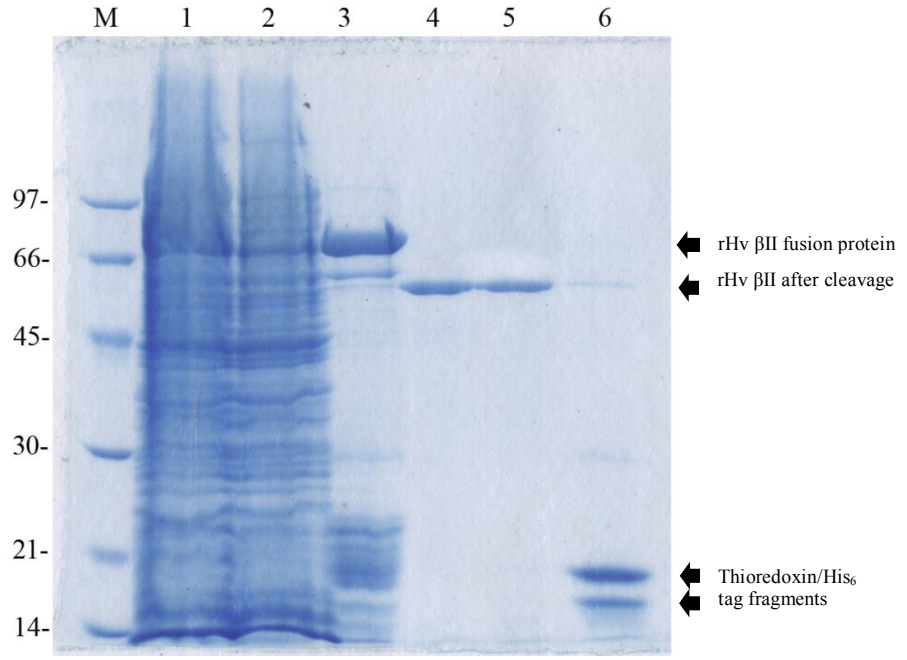

Figure 3.6 SDS-PAGE electrophoresis showing barley rHv βII at different purification steps.

Lane M, LMW-SDS marker kit

Lane 1, Crude proteins after cell lysis (whole cell lysate)

Lane 2, Soluble protein fraction

Lane 3, IMAC purified rHv βII

Lane 4, Flow-through fraction from the second IMAC purification of rHv βII after enterokinase digest.

Lane 5, Wash fraction from second IMAC purification of rHv βII after enterokinase digest.

Lane 6, Eluted fraction from second IMAC purification of rHv βII after enterokinase digest.

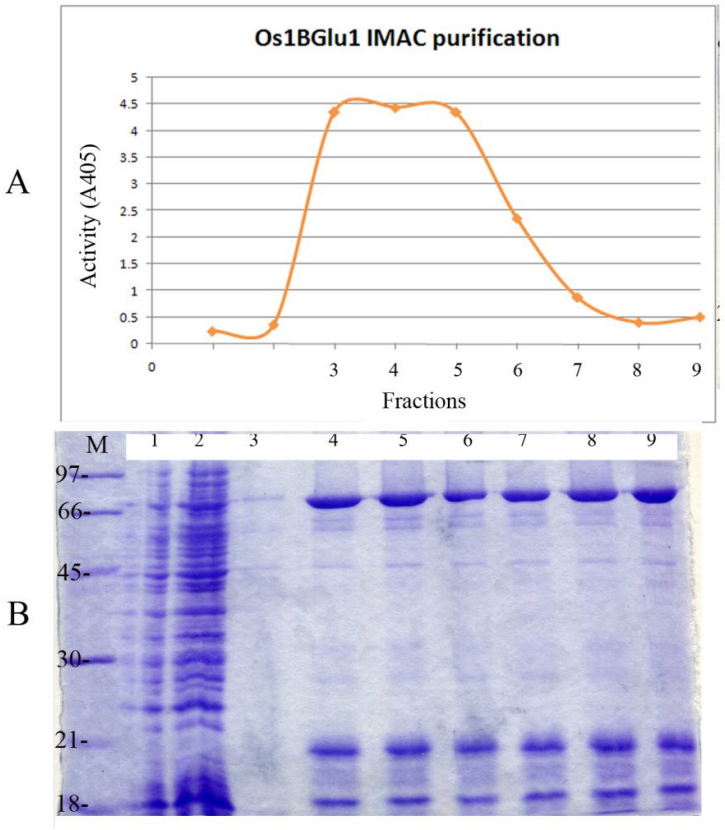

Figure 3.7 Purification of Os3BGlu8 β-glucosidase with Co2+ IMAC.

The Os3BGlu8 was first purified over a Co^{2+} IMAC column. Six fractions of eluted Os3BGlu8 were collected with 1.5 ml per fraction. The activity toward *p*NPGlc of Os3BGlu8 in each fraction was determined by incubating 10 µl of each fraction with 1 mM *p*NPGlc, in 50 mM NaOAc, pH 5.0, at 30ºC for 15 min. The OD_{405} was determined and plotted versus the fractions. The SDS-PAGE lanes in B are:

Lane M, LMW-SDS marker kit

Lane 1, Crude proteins after cell lysis (whole cell lysate)

Lane 2, Soluble protein fraction

Lane 3, Flow-through fraction from IMAC purification

Lane 4-9, IMAC elution fractions which had *p*NPGlc hydrolysis activity

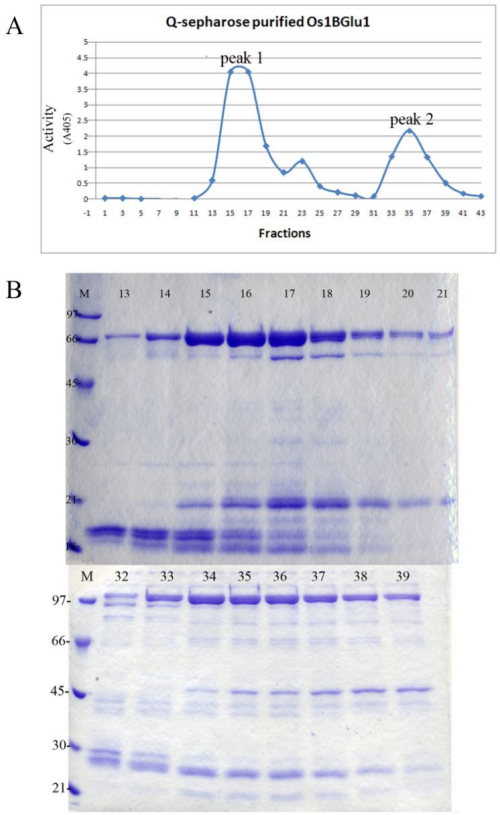

Figure 3.8 Purification of Os3BGlu8 β-glucosidase by Q-sepharose chromatography

A. The Os3BGlu8 β-glucosidase was purified by Q-sepharose chromatography with an increasing gradient of NaCl from 0-0.5 mM in 50 mM NaOAc, pH 5.0. Os3BGlu8 eluted at 0.18 mM NaCl. The activity toward *p*NPGlc of Os1BGlu1 in each fraction was determined by incubating 10 µl of each fraction with 1 mM *p*NPGlc, in 50 mM NaOAc, pH 5.0, at 30ºC, for 30 min. The OD_{405} was determined and plotted versus the fractions.

B. SDS-PAGE of the purification fractions with lanes as follows:

Lane M, LMW-SDS marker kit

Lanes 13-21, Peak 1 fractions 13-21 containing purified Os1BGlu1 from Q-sepharose chromatography

Lanes 32-39, Peak 2 fractions 32-39 containing Os1BGlu1 purified from Q-sepharose chromatography

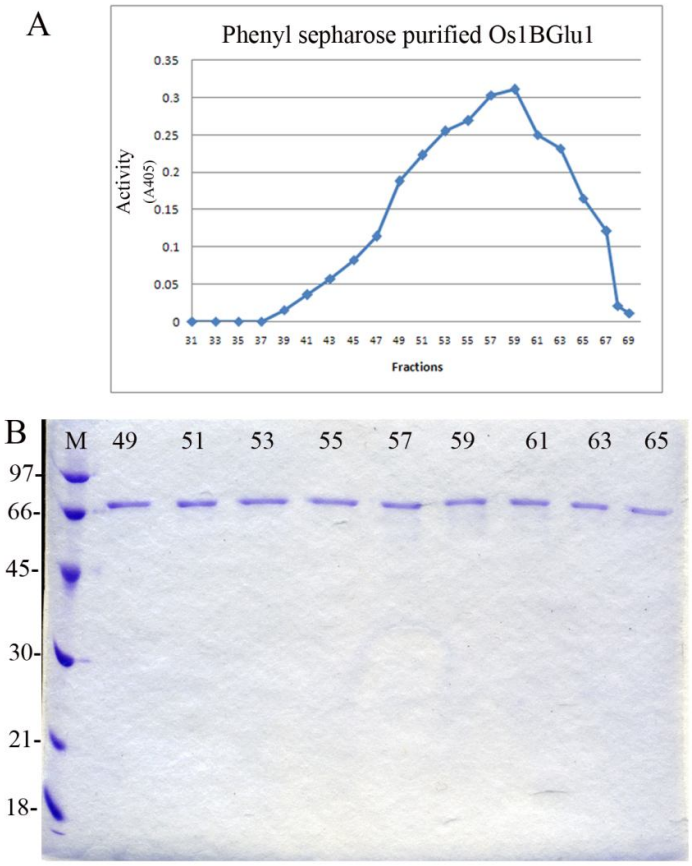

Figure 3.9 Purification of Os3BGlu8 β-glucosidase using phenyl sepharose.

The Os3BGlu8 β-glucosidase was purified by phenyl sepharose chromatography with a decreasing gradient of NaCl from 3.0-0 mM in 50 mM NaOAc, pH 5.0. Os3BGlu8 eluted at 0.22 mM NaCl. The activity toward *p*NPGlc in each fraction was determined by incubating 20 µl of each fraction with 1 mM *p*NPGlc in 80 µl of 50 mM NaOAc, pH 5.0, at 30ºC for 1 h. The OD_{405} was determined and plotted versus the fractions in A.

B. SDS-PAGE of fractions from theb-glucosidase activity peak.

Lane M, LMW-SDS marker kit

Lanes 49-65, fractions of Os3BGlu8 purified with phenyl sepharose, with numbers corresponding to the chromatography fractions.

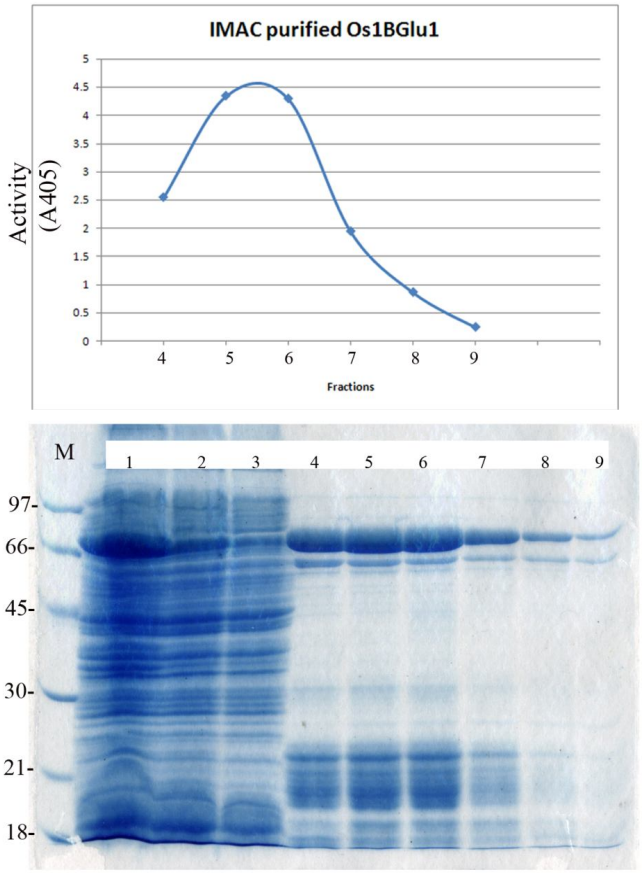

Figure 3.10 Purification of Os1BGlu1 β-glucosidase by Co2+ IMAC.

The Os1BGlu1 was purified using a Co^{2+} IMAC column. Six fractions of eluted Os1BGlu1 were collected with 1.5 ml per fraction. The activity of Os1BGlu1 in each fraction toward *p*NPGlc was determined by incubating 10 µl of each fraction with 1 mM *p*NPGlc, in 80 µl of 50 mM NaOAc, pH 5.0, at 30ºC, for 15 min. The OD_{405} was measured and plotted versus the fractions numbers.

Lane M, LMW-SDS marker kit

Lane 1, Crude proteins after cell lysis (whole cell lysate)

Lane 2, Soluble protein fraction

Lane 3, Flow-through fractions from IMAC purification

Lane 4-9, IMAC elution fractions with *p*NPGlc hydrolysis activity

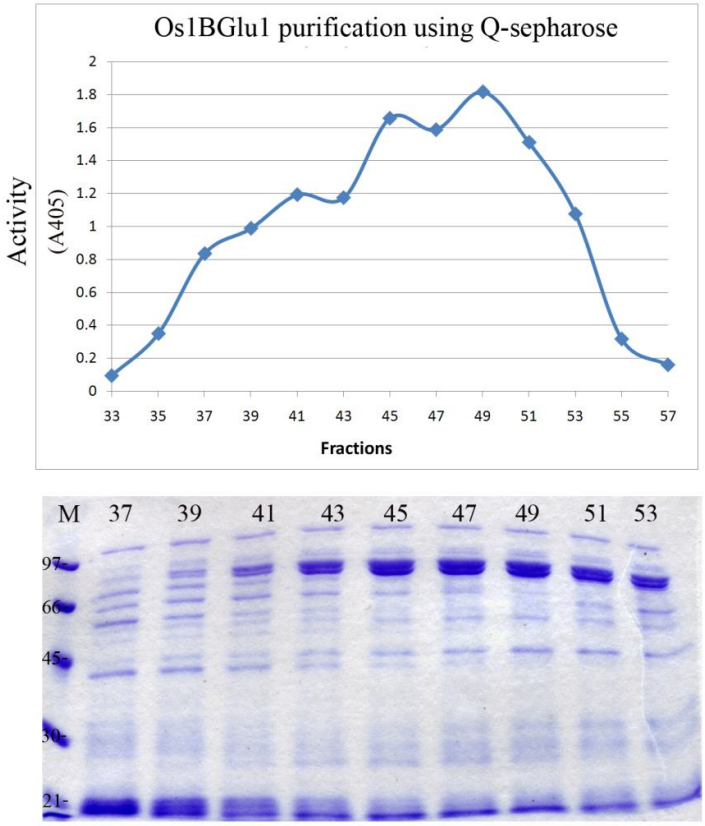

Figure 3.11 Purification of Os1BGlu1 β-glucosidase with Q-sepharose.

The Os1BGlu1 β-glucosidase was purified using Q-sepharose chromatography with elution by an increasing gradient of NaCl from 0-0.5 mM in 50 mM NaOAc, pH 5.0. Os3BGlu8 eluted at 0.18 mM NaCl. The activity of Os1BGlu1 in each fraction toward *p*NPGlc was determined by incubating 10 µl of each fraction with 1 mM *p*NPGlc, in 50 mM NaOAc, pH 5.0, at 30ºC, for 1 h. The OD_{405} was determined and plotted versus the fraction numbers.

Lane M, LMW-SDS marker kit

Lanes 35-53, Os1BGlu1-containing fractions from Q-sepharose chromatography

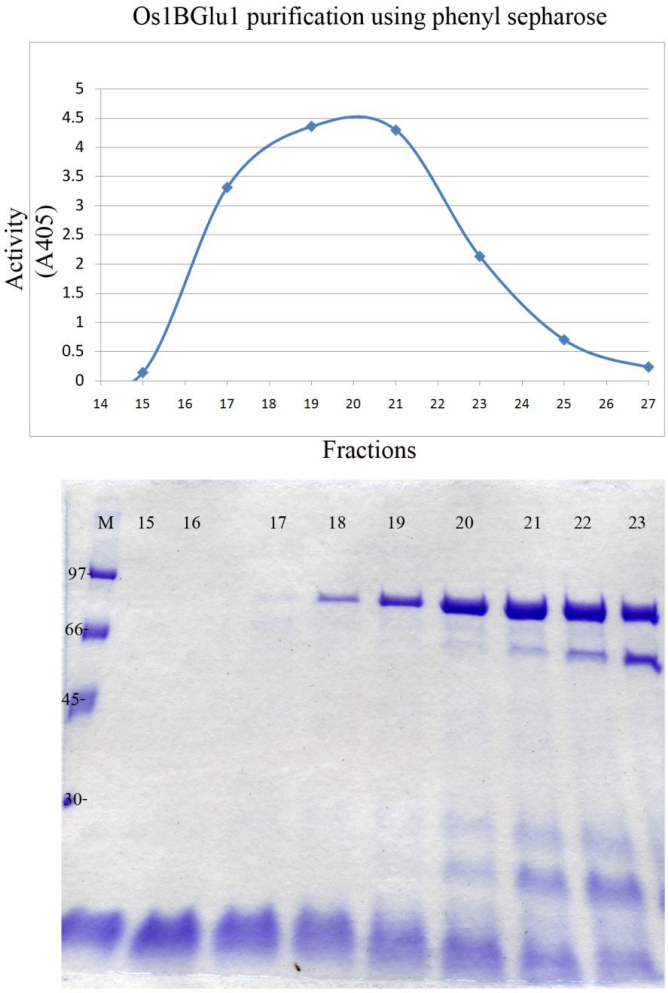

Figure 3.12 Purification of Os1BGlu1 β-glucosidase on phenyl sepharose.

The Os1BGlu1 β-glucosidase was purified by phenyl sepharose chromatography with a decreasing gradient of NaCl from 3.0-0 mM in 50 mM NaOAc, pH 5.0. Os3BGlu8 eluted at 0.22 mM NaCl. The pNPGlc hydrolysis activity of Os1BGlu1 in each fraction was determined by incubating 20 µl of each fraction with 1 mM pNPGlc, in 50 mM NaOAc, pH 5.0, at 30ºC, for 1 h. The OD405 was determined and plotted versus the fraction numbers (A). B SDS-PAGE gel of the fractions:

Lane M, LMW-SDS marker kit

Lane 16-25, Os1BGlu1 fractions 16-25 from the phenyl sepharose column

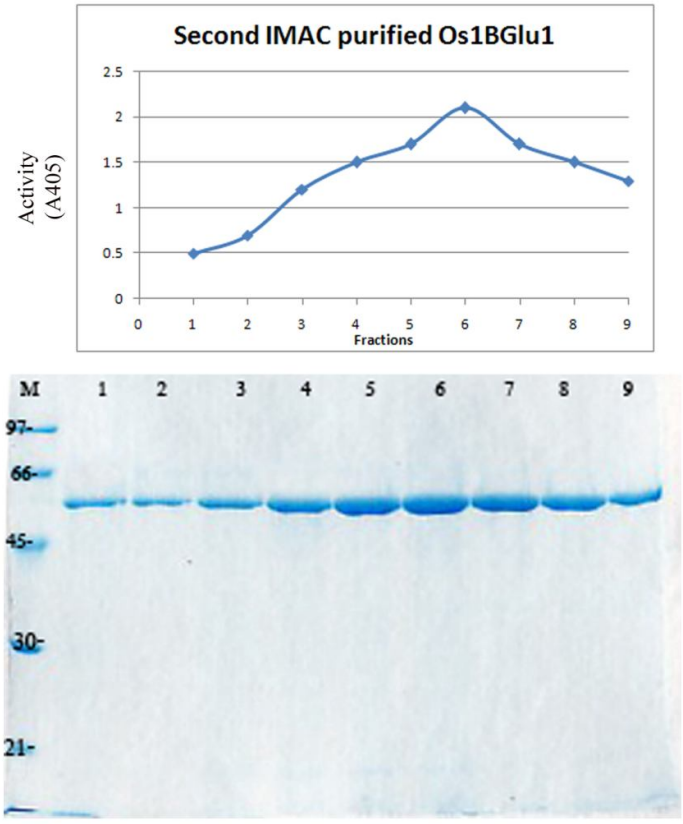

Figure 3.13 Fractions of enterokinase digested Os1BGlu1 β-glucosidase from the Co2+ IMAC.

The Os1BGlu1 was digested with enterokinase to cleave off the N-terminal fusion tag containing thioredoxin and a hexahistidine tag. The N-terminal tag was removed by loading the enterokinase digested Os1BGlu1 onto a Co2+ IMAC, the unbound and washed fractions were collected.

Lane M, LMW-SDS marker kit

Lanes 1-4, Unbound fractions from the Co2+ IMAC column

Lanes 5-9, Wash fractions from the Co2+ IMAC column

3.3 Characterization of plant β-glucosidases

3.3.1 Optimum conditions of β-glucosidases

The optimum conditions of the rHv βII, rice Os1BGlu1 and Os3BGlu8 β-glucosidases were determined by varying the pH and temperature. The rHv βII enzyme showed highest activity in 50 mM NaOAc buffer, pH 4.0, at 30ºC, as shown in Figures 3.14 and 3.15. The rHv βII enzyme showed half maximal activity at pH 3.0 and 6.5. The optimum conditions for rice Os1BGlu1 are pH 5.5 and 40ºC (Figures 3.16 and 3.17, respectively). The Os1BGlu1 showed half maximal activity at pH 3.75 and 7.2, respectively. The optimum conditions for Os3BGlu8 are pH 5.0 and 30ºC, (Figures 3.18 and 3.19 respectively). The Os3BGlu8 showed half maximal activity at pH 3.75 and 6.9, respectively.

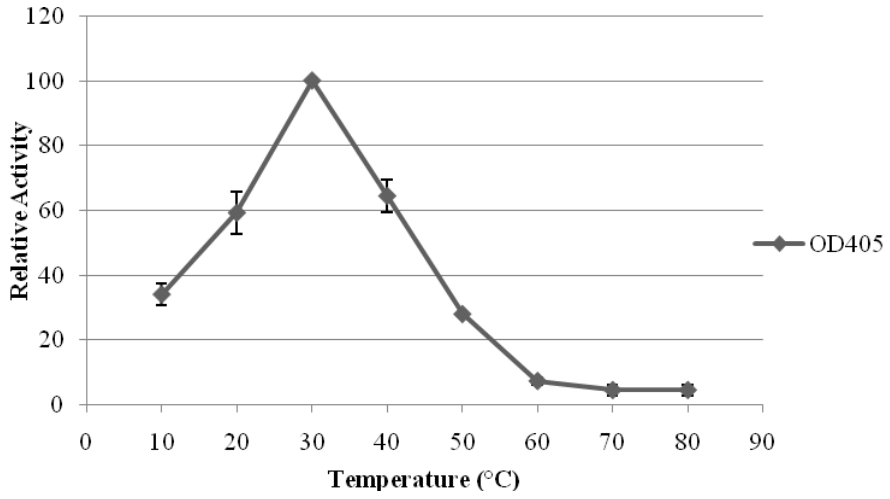

Figure 3.14 Activity profile of rHv βII at temperatures ranging from 10 to 80°C. The enzyme was assayed with 1 mM *p*NPGlc in 50 mM NaOAc, pH 4.0, for 20 min.

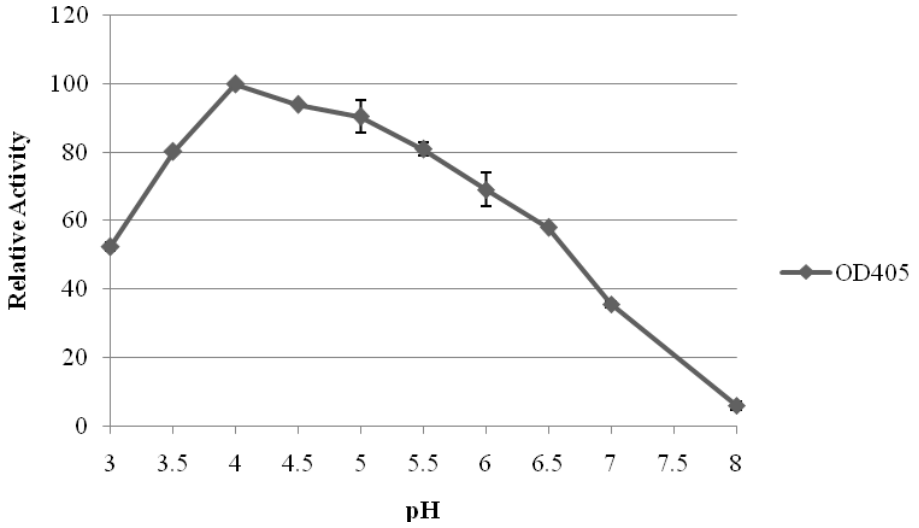

Figure 3.15 Activity profile of rHv βII at pH values ranging from 3.0 to 8.0 assayed with 1 mM pNPGlc in 50 mM NaOAc, pH 5.0, for 20 min.

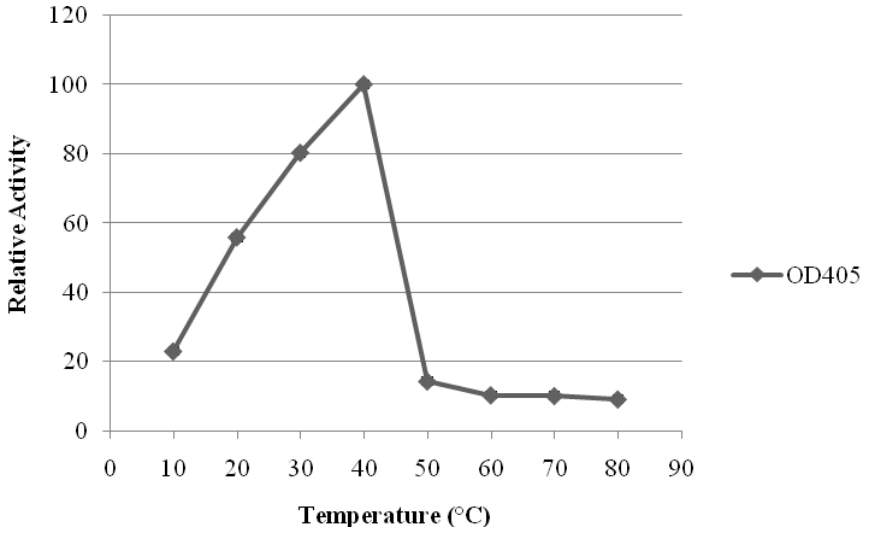

Figure 3.16 Activity profile of Os1BGlu1 at temperatures ranging from 10-80°C. The enzyme was assayed with 1 mM pNPGlc in 50 mM NaOAc, pH 5.5, for 20 min.

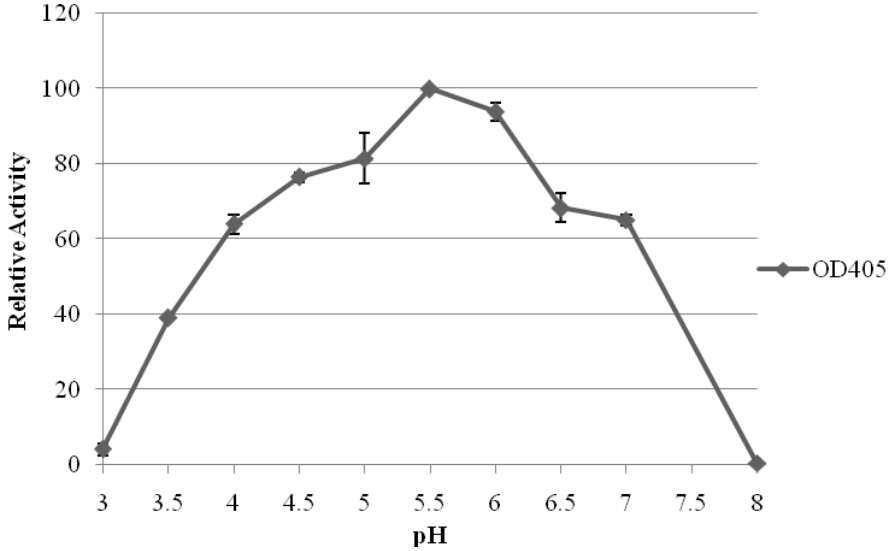

Figure 3.17 Activity profile of Os1BGlu1 at pH values ranging from 3.0 to 9.5 The activity was assayed with 1 mM pNPGlc in McIlvain buffers with pH ranging from 3.0-8.0, for 20 min.

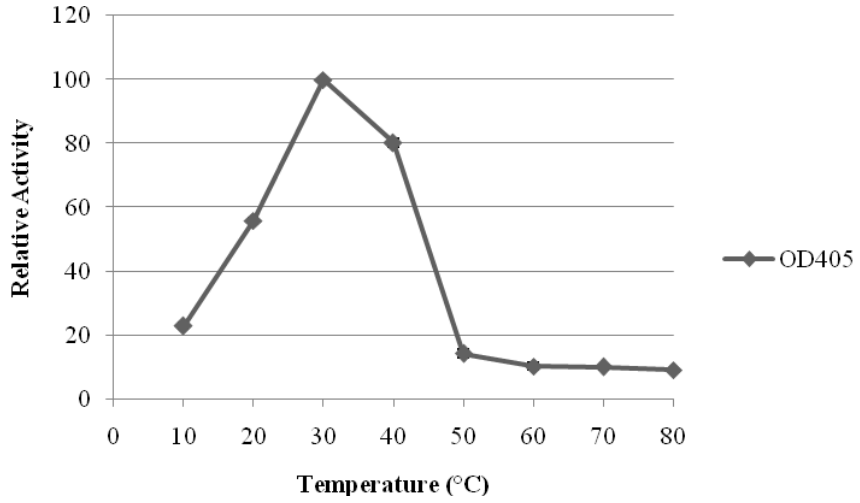

Figure 3.18 Activity profile of Os3BGlu8 at temperatures ranging from 10-80°C. The activity was assayed with 1 mM pNPGlc in 50 mM NaOAc, pH 5.0, for 20 min.

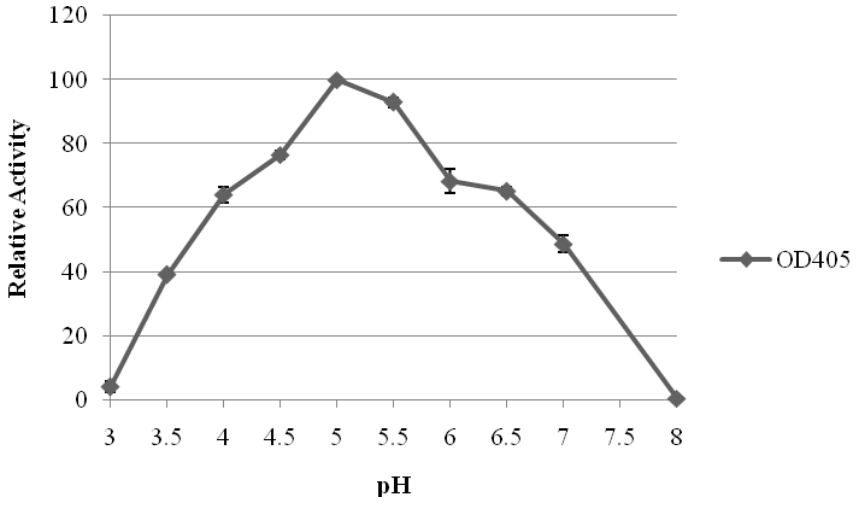

Figure 3.19 Activity profile of Os3BGlu8 at pH values ranging from 3.0 to 8.0. The activity was assayed with 1 mM pNPGlc in McIlvain buffers with pH ranging from 3.0-8.0, for 20 min**.**

3.3.2 Substrate specificity of β-glucosidases

The rHv βII was tested for activity toward natural and synthetic substrates and the results are shown in Table 3.2. The structures of natural glycosides tested are shown in Figure 3.20. rHv βII was able to hydrolyze gluco-oligosaccharides with (1-2)-, (1-3)-, and (1-4)-β-linkages, and several glucosides, including alcohol glucoside (salicin), cyanogenic glucosides (D-amygdalin, esculin, epiheterodendrin, dhurrin, prunasin, sambunigrin, and tetraphyllin), isoflavonoid glucosides (diazin, genistin, and glycitin), lignin precursors (coniferin and *p*-coumaryl alcohol glucoside), a phytohormone glucoside (trans-zeatin glucoside), and a vitamin glucoside (pyridoxine glucoside).

3.3.3 Tryptic mapping and N-terminal sequencing of rHv βII and Os3BGlu7

The protein sequence of the expressed rHv βII was in excellent agreement with its theoretical sequence, as confirmed by MALDI-TOF/TOF spectrometry. The MS sequence coverage was found to be approximately 50% (Figure 3.21). The list of monoisotopic masses of rHv βII tryptic peptides are shown in Table 3.3. The identity of rHv βII was also confirmed by automated NH2-terminal amino acid sequencing of a homogenous rHv βII, which showed that the enzyme was properly processed at its NH2-terminus. The sequence of Os3BGlu7, expressed for activity comparison, was also confirmed with MALDI-TOF/TOF mass spectrometry (MS). Peptide masses were matched to approximately 40% of the spectra and with 33% of the total intensity of ions matching the sequence (Figure 3.22). The list of monoisotopic masses of Os3BGlu7 peptides are shown in Table 3.4. In addition, NH2-terminal amino acid sequencing showed that Os3BGlu7 was accurately processed at its NH2-terminus.

Table 3.2 Ability of barley rHv βII to hydrolyze natural and synthetic substrates. The substrate specificity of rHv βII toward natural and synthetic substrates was evaluated by incubating 4 nmol of enzyme in 100 µl reactions with 3 mM final concentration of substrates at 30°C for 1 to 16 h in 50 mM NaOAc buffer, pH 4.0. Hydrolysis of *p*NP-linked substrates was measured as described in section 2.4.4. For TLC detection, 4 nmol of rHv βII was incubated with 2 mM of substrates for 4 h. The products were detected as described in section 2.6. For cellooligosaccharides, laminarioligosaccharides, and other natural glucosides, 4 nmol of rHv βII was incubated with 1 mM final concentration of substrates in 100 µl reactions at 30°C for 1 to 16 h in 50 mM NaOAc buffer, pH 4.0. The reactions were stopped by boiling for 5 min and the amount of glucose released was determined as described in section 2.3.4.

Substrate	rHv βII	Substrate	rHv βII
*p*NP-*β*-D-glucopyranoside	+	Salicin	+
*p*NP-*β*-D-mannopyranoside	+	Esculin	+
*p*NP-*β*-D-galactopyranoside	+	Epiheterodendrin	+
*p*NP-*β*-D-xylopyranoside	-	Dhurrin	+
*p*NP-*β*-D-fucopyranoside	+	Linamarin	-
*p*NP-*β*-L-arabinopyranoside	+	D-amygdalin	+
4-methylumberlliferyl glucopyranoside	+	Sambunigrin	+
Sophorose (*β*-1-2 glucobiose)	+	DIMBOA	-
Laminaribiose (*β*-1-3)	+	Tetraphyllin	+
Laminaritriose	+	Neolinustatin	-
Laminaritetraose	+	Prunasin	+
Laminaripentose	-	Trans-Zeatin glucoside	+
Laminarihexose	-	Daidzin	+
Cellobiose (*β*-1-4 glucobiose)	+	Genistin	+
Cellotriose	+	Glycitin	+
Cellotetraose	+	Naringin	-
Cellopentose	+	Quercetin-3-glucoside	-
Cellohexose	+	*p*-coumaryl alcohol glucoside	+
Gentiobiose (*β*-1-6 glucobiose)	-	coniferin	+
Mannobiose (*β* 1-4 mannobiose)	+	Indoxyl-*β*-D glucoside	-
Mannotriose	+	Pyridoxine glucoside	+
Mannotetraose	+	Gibberellin A1-3-0-β-D-glucopyranoside	-
Mannopentose	+	Gibberellin A9-13-0-β-D-glucopyranoside	-
Mannohexose	+	n-heptyl-β-glucoside	-
		n-octyl-β-glucoside	-

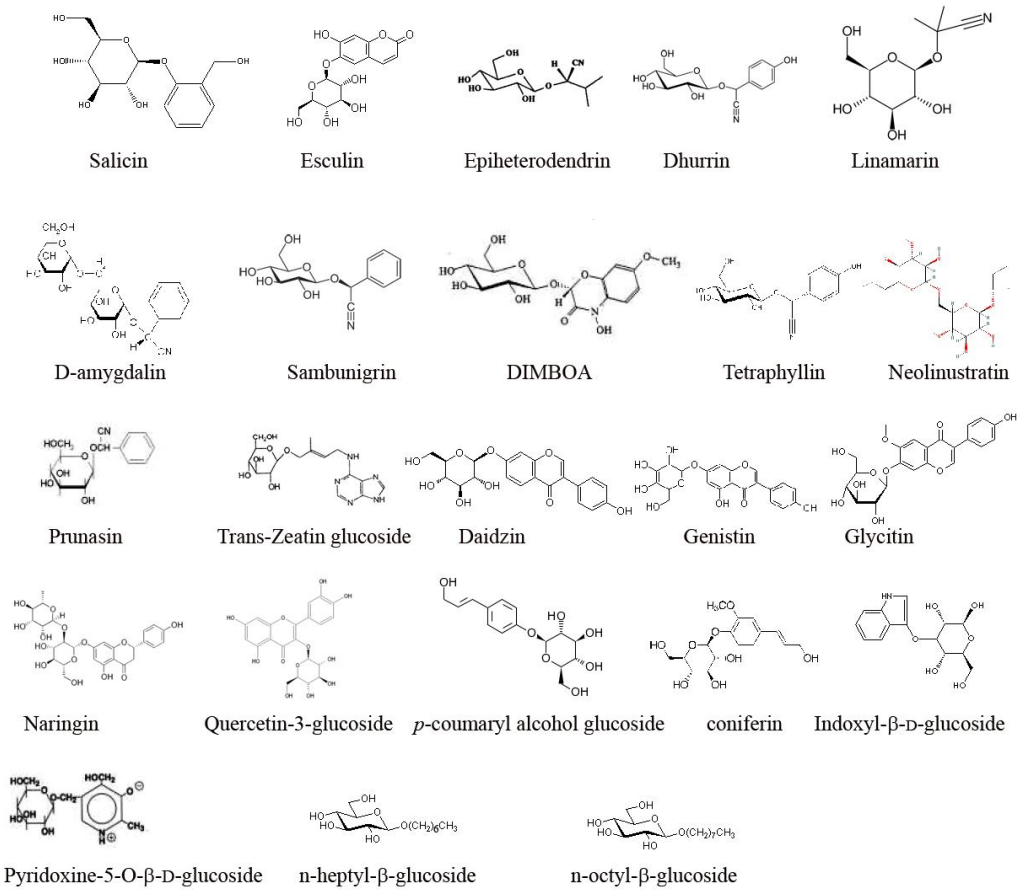

Figure 3.20 Structures of natural glycosides tested with rHv βII and Os3BGlu7

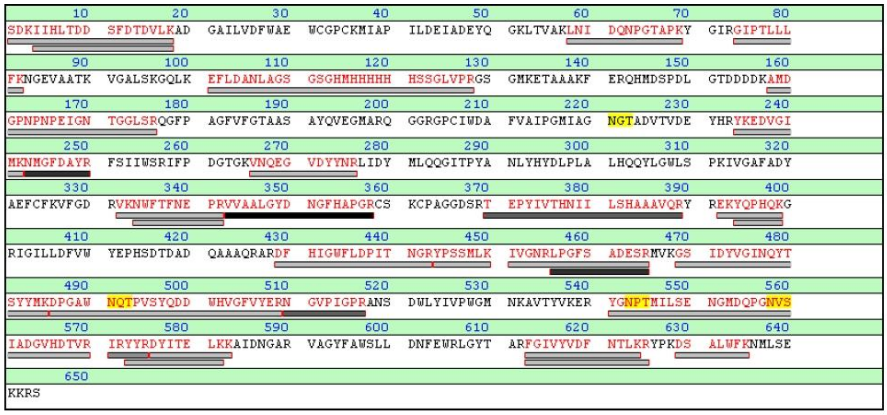

Figure 3.21 Comparison of the MS spectrum and with the sequence of mature rHv βII. The MS sequence was found to be 49.4% of the protein sequence of mature rHv βII. The bars indicates the regions over which the peptides masses matched those predicted from the rHv βII sequence.

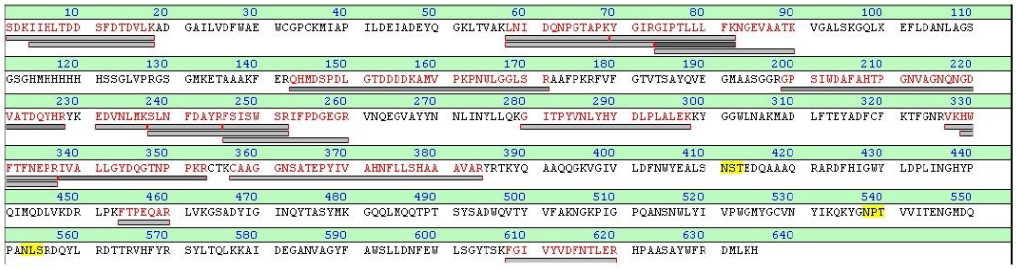

Figure 3.22 Comparison of the MS spectrum with the sequence of mature Os3BGlu7. The MS sequence was found to cover 40% of the protein sequence of mature Os3BGlu7. The bars indicates the regions over which the peptides masses matched those predicted from the Os3BGlu7 sequence.

Table 3.3 Table of monoisotopic masses of mature rHv βII peptides

m/z	Intensity	m/z	Intensity
500.920	91	1437.718	60
507.971	801	1482.714	17
515.009	198	1491.767	42
523.832	92	1513.726	13
558.045	111	1571.839	105
563.052	120	1617.820	123
567.849	242	1626.782	43
595.062	547	1643.818	1553
617.048	32	1665.801	101
621.805	36	1731.865	58
680.168	178	1787.876	63
770.411	486	1819.869	152
792.409	64	1841.844	28
800.390	364	1863.820	15
809.444	895	1873.984	22
822.376	119	1896.868	90
825.404	131	2001.909	38
831.422	76	2017.897	25
842.488	290	2023.890	28
866.417	127	2039.892	24
870.524	51	2052.041	7
882.430	1060	2061.983	11
904.416	73	2233.198	904
914.408	45	2255.172	57
973.409	1380	2306.109	39
989.396	77	2345.094	148
995.391	77	2361.086	317
1001.628	97	2378.118	41
1009.549	51	2383.048	28
1057.525	88	2442.372	29
1078.487	1490	2463.390	26
1082.541	293	2866.229	14
1100.457	120	2898.207	12
1104.517	70	2902.201	9
1210.551	243	2930.230	9
1267.655	44	3024.356	61
1289.626	44	3040.350	21
1292.730	51	3187.414	19
1356.603	200	3203.393	28
1363.664	13	3219.383	12
1415.735	37		

Table 3.4 Table of monoisotopic masses of mature Os3BGlu7 peptides

m/z	Intensity	m/z	Intensity
500.920	91	1482.714	17
507.971	801	1491.767	42
515.009	198	1513.726	13
523.832	92	1571.839	105
558.045	111	1617.820	123
563.052	120	1626.782	43
567.849	242	1643.818	1553
595.062	547	1665.801	101
617.048	32	1731.865	58
621.805	36	1787.876	63
680.168	178	1819.869	152
770.411	486	1841.844	28
792.409	64	1863.820	15
800.390	364	1873.984	22
809.444	895	1896.868	90
822.376	119	2001.909	38
825.404	131	2017.897	25
831.422	76	2023.890	28
842.488	290	2039.892	24
866.417	127	2052.041	7
870.524	51	2061.983	11
882.430	1060	2233.198	904
904.416	73	2255.172	57
914.408	45	2306.109	39
973.409	1380	2345.094	148
989.396	77	2361.086	317
995.391	77	2378.118	41
1001.628	97	2383.048	28
1009.549	51	2442.372	29
1057.525	88	2463.390	26
1078.487	1490	2866.229	14
1082.541	293	2898.207	12
1100.457	120	2902.201	9
1104.517	70	2930.230	9
1210.551	243	3024.356	61
1267.655	44	3040.350	21
1289.626	44	3187.414	19
1292.730	51	3203.393	28
1356.603	200	3219.383	12
1363.664	13		
1415.735	37		
1437.718	60		

3.3.4 Kinetic parameters of plant β-glucosidases toward oligosaccharides

Protein sequence-based phylogenetic analysis (Figure 3.23) showed two other rice *β*-D-glucosidase isozymes, Os1BGlu1 and Os3BGlu8, cluster together with Os3BGlu7, Os7BGlu26, barley *β*-D-glucosidase isozyme βII, and tomato (Mo and Bewley, 2002) and *Arabidposis β*-D-mannosidases (Xu et al., 2004). To test whether these two enzymes also act as *β*-D-mannosidases with exo-hydrolytic modes of action, they were also expressed in *E. coli*. The kinetics of hydrolysis of *p*NPGlc, *p*NPMan, cellooligosaccharides (DP 2-6) and laminaribiose and laminaritriose were determined for rHv βII, Os1BGlu1, and Os3BGlu8, as shown in Table 3.5. As expected, rHv βII hydrolysed *p*NPMan with higher k_{cat}/K_m values than *p*NPGlc, while Os3BGlu8 hydrolysed *p*NPGlc more efficiently than *p*NPMan, like Os3BGlu7, to which it is most similar. Surprisingly, Os1BGlu1, which is more similar to the *β*-D-mannosidases, e.g. rHv βII, could not hydrolyse *p*NPMan. All the recombinant enzymes hydrolysed laminaribiose more efficiently than laminaritriose, and hydrolysed cellooligosaccharides with higher efficiency as the DPs increased from 3 to 6. However, although rHv βII hydrolysed cellobiose better than cellotriose, all the rice isozymes hydrolysed cellobiose poorly, as does Os3BGlu7 (Opassiri et al., 2004).

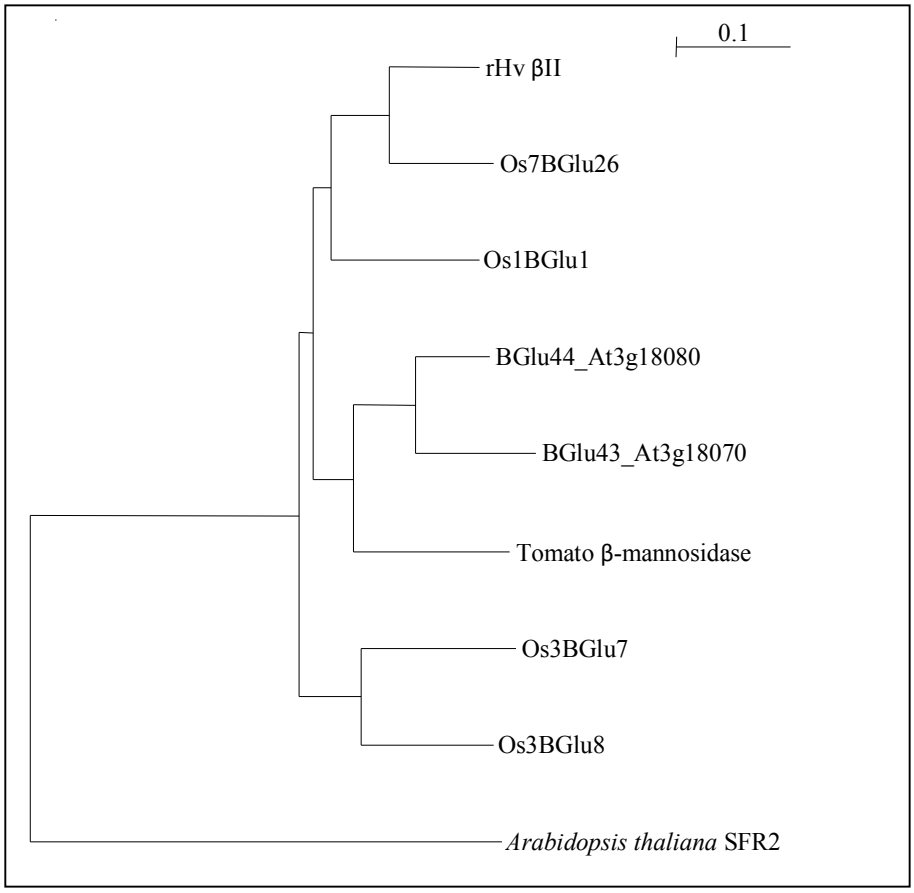

Figure 3.23 Phylogenetic tree of plant β-D-mannosidases with rHv βII (GenBank accession number EU807965), Os1BGlu1 (AC AK069177), Os3BGlu7 (AC U28047), Os3BGlu8 (AC AK120790), and Os7BGlu26 (AC AK068499) rice β-D-glucosidases. *Arabidopsis thaliana* SFR2 (AC At3g06510) is included as an outgroup. Plant β-D-mannosidases include *Arabidopsis* BGlu44 and its sister isozyme BGlu43 (Xu et al., 2004), and tomato β-D-mannosidase (AC AAL37714) (Mo and Bewley, 2002).

Table 3.5 Kinetic parameters of natural barley β-glucosidase isozyme βII (Hv βII), rHv βII, Os3BGlu7, Os1BGlu1, and Os3BGlu8 isozymes for hydrolysis of *p*NPGlc, *p*NPMan, cellooligosaccharides with the DP from 2-6, laminaribiose and laminarotriose.

[a] Kinetics constants from Hrmova et al. (1998).

[b] Kinetics constants from Opassiri et al. (2004)

Substrate	Kinetic parameters	Hv *β*II[a]	rHv *β*II	Os1BGlu1	Os3Bglu8	Os3BGlu7[b]
*p*NPG	K_m (mM)	0.50	0.50 ± 0.03	0.41 ± 0.01	0.27 ± 0.04	0.23 ± 0.02
	k_{cat} (s^{-1})	0.50	0.50 ± 0.07	12.52 ± 0.33	3.29 ± 0.37	7.93 ± 0.37
	k_{cat}/K_m (s^{-1} mM^{-1})	1.00	1.00 ± 0.05	30.53 ± 0.77	12.64 ± 3.10	34.70 ± 1.40
*p*NPM	K_m (mM)	N.D.	0.25 ± 0.01	No hydrolysis	1.55 ± 0.29	1.27 ± 0.10
	k_{cat} (s^{-1})	N.D.	3.06 ± 0.02	No hydrolysis	0.24 ± 0.03	1.32 ± 0.05
	k_{cat}/K_m (s^{-1} mM^{-1})	N.D.	12.67 ± 0.17	No hydrolysis	0.16 ± 0.1	1.01 ± 0.02
Cellobiose	K_m (mM)	2.67 ± 0.19	2.76 ± 0.10	13.21 ± 1.13	25.57 ± 2.34	31.50 ± 1.60
	k_{cat} (s^{-1})	11.58 ± 0.63	16.08 ± 0.15	1.55 ± 0.06	0.98 ± .08	1.52 ± 0.13
	k_{cat}/K_m (s^{-1} mM^{-1})	4.34 ± 0.07	5.84±0.23	0.12 ± 0.01	0.04 ± 0.01	0.05 ± 0.01
Cellotriose	K_m (mM)	0.97 ± 0.06	0.74 ± 0.06	0.38 ± 0.30	0.56 ± 0.01	0.72 ± 0.02
	k_{cat} (s^{-1})	1.95 ± 0.12	2.97 ± 0.39	32.90 ± 0.71	6.08 ± 0.08	18.13 ± 0.35
	k_{cat}/K_m (s^{-1} mM^{-1})	2.01 ± 0.01	3.45 ± 0.08	21.56 ± 0.56	10.95 ± 1.60	25.4 ± 0.04
Cellotetraose	K_m (mM)	0.89 ± 0.05	1.03 ± 0.02	0.53 ± 0.03	0.25 ± 0.01	0.28 ± 0.01
	k_{cat} (s^{-1})	8.88 ± 0.58	9.57 ± 0.40	32.35 ± 1.02	16.10 ± 0.08	17.34 ± 0.63
	k_{cat}/K_m (s^{-1} mM^{-1})	9.98 ± 0.08	9.34 ± 0.53	85.20 ± 9.22	64.45 ± 1.60	61.10 ± 0.40
Cellopentaose	K_m (mM)	0.41 ± 0.02	0.33 ± 0.02	0.53 ± 0.03	0.15 ± 0.01	0.24 ± 0.01
	k_{cat} (s^{-1})	11.66 ± 0.76	12.87 ± 0.35	50 ± 0.01	15.94 ± 0.14	16.90 ± 0.06
	k_{cat}/K_m (s^{-1} mM^{-1})	28.44 ± 0.44	40.20 ± 0.80	94.64 ± 5.40	108.8 ± 2.6	71.50 ± 2.20
Cellohexaose	K_m (mM)	0.29 ± 0.02	0.23 ± 0.01	0.4 ± 0.01	0.12 ± 0.01	0.22 ± 0.01
	k_{cat} (s^{-1})	11.80 ± 0.77	13.10 ± 0.08	53.04 ± 1.00	21.65 ± 1.46	16.93 ± 0.32
	k_{cat}/K_m (s^{-1} mM^{-1})	40.69 ± 0.14	54.24 ± 1.59	132.62 ± 0.39	175.3 ± 5.0	152.9 ± 0.50
Laminaribiose	K_m (mM)	5.37 ± 0.38	5.00 ± 0.00	0.84 ± 0.01	0.32 ± 0.07	2.05 ± 0.01
	k_{cat} (s^{-1})	14.14 ± 1.02	11.28 ± 0.03	25.68 ± 0.98	11.11 ± 0.26	31.90 ± 3.10
	k_{cat}/K_m (s^{-1} mM^{-1})	2.63 ± 0.01	2.30 ± 0.06	30.59 ± 1.42	36.14 ± 8.18	15.70 ± 1.90
Laminaritriose	K_m (mM)	2.77 ± 0.17	2.77 ± 0.17	6.92 ± 0.78	6.03 ± 0.62	1.92 ± 0.04
	k_{cat} (s^{-1})	1.44 ± 0.10	2.33 ± 0.17	23.43 ± 1.89	13.06 ± 1.44	21.20 ± 0.20
	k_{cat}/K_m (s^{-1} mM^{-1})	0.52 ± 0.01	0.84 ± 0.01	3.40 ± 0.12	2.18 ± 0.29	11.0 ± 0.2

3.3.5 Subsite mapping of β-glucosidases

To better understand the differences in oligosaccharide preferences between the barley and rice *β*-D-glucosidases, their subsite affinities for *β*-(1,4)-linked glucosyl residues were calculated. It is clear from Figure 3.24, that the main difference between rHv βII and the rice isozymes is the negative interaction at the +2 site in rHv βII (-1.33 $kJmol^{-1}$) and relatively high positive interaction of the rice isozymes at this site (13.1 $kJmol^{-1}$ for Os1BGlu1 and 13.83 kJ/mol^{-1} for Os3BGlu8). The Os1BGlu1 and Os3BGlu8 isozymes are more similar to Os3BGlu7 with stronger interaction at the +2 site, but still maintain relatively strong binding at the +1 site compared to Os3BGlu7.

3.3.6 Multiple protein sequence alignment and structure of β-glucosidases

To rationalize the differences between rHv βII and the rice isozymes in relative activity toward *p*NPGlc and *p*NPMan and *β*-1,4-linked D-glucosyl residue binding subsite affinities, the sequences were aligned (Figure 3.25) and molecular models of rHv βII and the rice isozymes were constructed based on the rice BGlu1 (Os3BGlu7) crystal structure (Chuenchor et al., 2008). Figure 3.26 shows a comparison of residues around the active site in the context of their electrostatic potentials mapped on the molecular surfaces. The residues creating specific subsites in the active site regions are marked in the alignment of Figure 3.25. As seen in the alignment, the differences in amino acid residues around the active sites generally followed phylogenetic relationships, rather than similarity in substrate specificity.

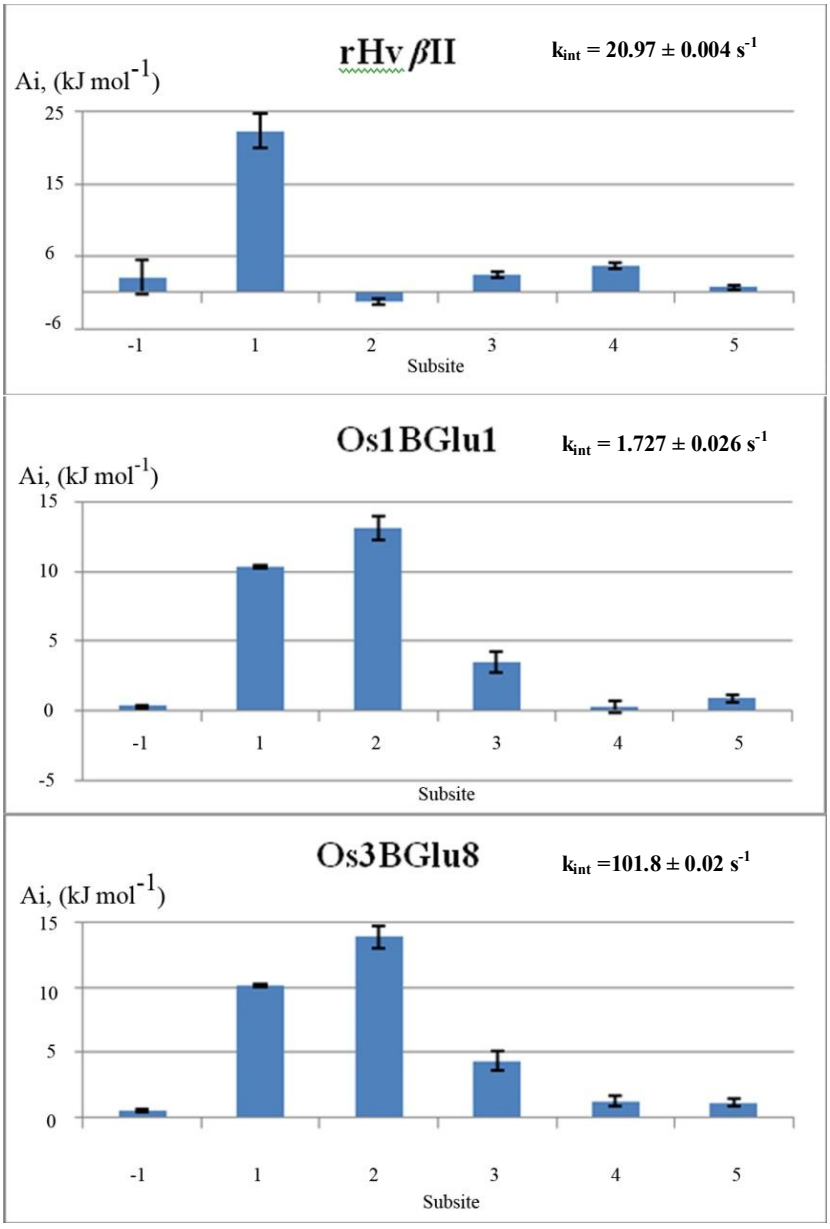

Figure 3.24 Subsite affinities of barley rHv βII, rice Os1BGlu1, and Os3BGlu8 for cellooligosaccharides. Subsite affinities were calculated from the kinetic data in Table 3.2. The intrinsic k_{cat} (k_{int}) for each isozyme is shown in the upper right hand corner of the graph with standard deviations (from calculations based on each (1,4)-β-D-linked oligosaccharide, cellobiose to cellohexaose). Subsite affinities and intrinsic rate constants were calculated as described by Opassiri et al. (2004).

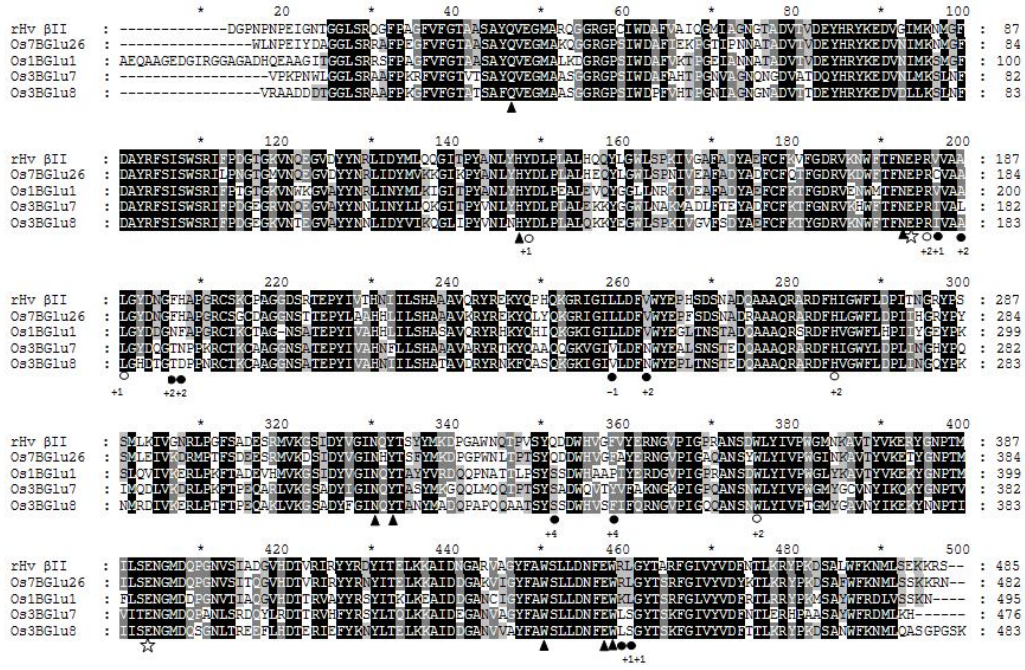

Figure 3.25 Amino acid sequence alignment between rHv βII, Os1BGlu1, Os3BGlu7, Os3BGlu8, and Os7BGlu26. Stars indicate the catalytic acid/base and nucleophilic residues, triangles represent amino acids contacting with glucosyl residue at the -1 subsite of Os3BGlu7. Open circles represent residues predicted to be at the +1, +2, +3, and +4 subsites of Os3BGlu7 that are conserved within these enzymes, while filled circles represent those that differ between the different *β*-glucosidases. The numbers beneath the circles are the main subsites at which the marked amino acids are predicted to contact a substrate glucosyl residue, based on the Os3BGlu7 structure. The alignment was generated with Clustal W (Thompson et al., 1994).

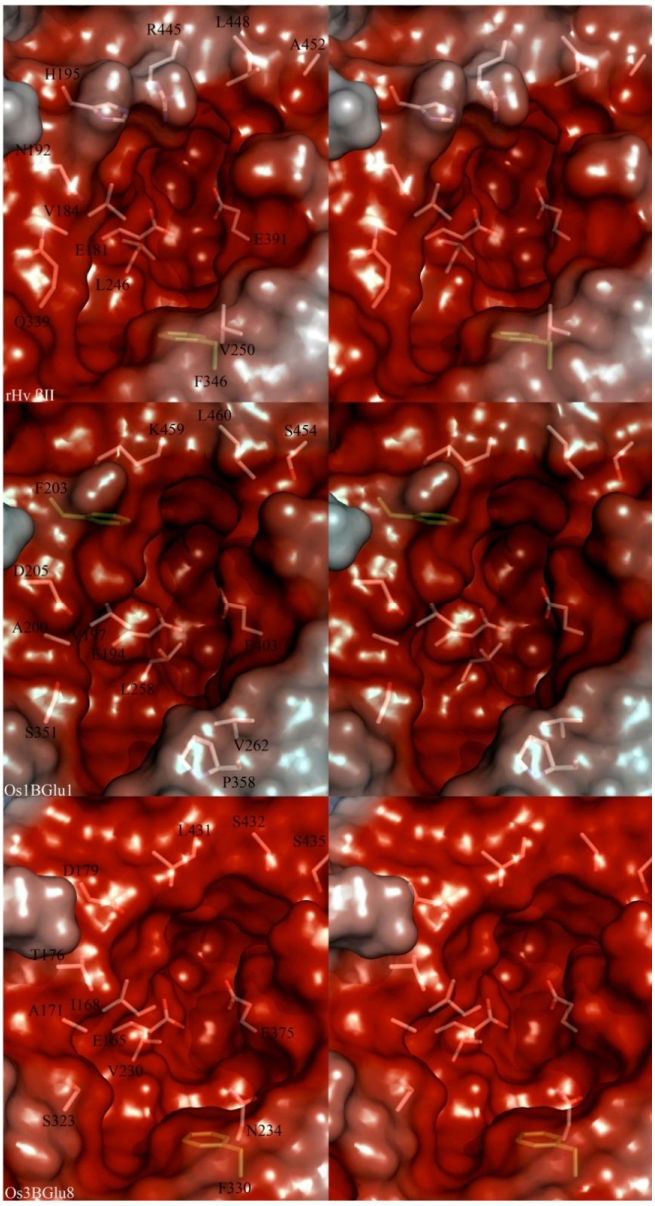

Figure 3.26 Stereo representations of molecular surface morphologies illustrating the catalytic sites of modeled barley rHv βII, rice Os1BGlu1, and Os3BGlu8 isozymes. The non-identical amino acid residues between these β-D-glucosidases are shown as sticks under the projected molecular surfaces. Catalytic residues (Glu) are also shown in all models. The surface electrostatic potentials were calculated using Adaptive Poisson-Boltzmann Solver (Baker et al., 2001). Blue and red areas indicate electropositive and electronegative regions, respectively, and are contoured at ± 5 kTe^{-1}.

3.3.7 Transglycosylation products of rHv βII and rice Os3BGlu7 β-glucosidase

Transglycosylase activities of rHv βII were analyzed with 20 mM *p*NPGlc, *p*NPMan, cellobiose, and mannobiose (Figure 3.27). Transglycosylation products of rice Os3BGlu7 are shown in Figure 3.28. It was identified that rHv βII and rice Os3BGlu7 can catalyse transglycosylation reactions by using either *p*NPGlc or cellobiose as the donors and acceptors. The transglycosylation products of rHv βII using *p*NPGlc as acceptor and donor were *p*NP-laminaribioside, *p*NP-cellobioside, and *p*NP-gentiobiose, while the products from transglycosylation using cellobiose was cellotriose. The rHv βII also generated laminaribiose, cellobiose, and gentiobiose using glucosyl residues from hydrolysis reaction as donor and acceptor. The products from transglycosylation reactions catalyzed by rice Os3BGlu7 were similar to products of rHv βII reactions (Figure 3.28).

This is different from attempted transglycosylation reactions using either *p*NPMan, or mannobiose, in which no transglycosylation products were obtained and *p*NPMan and mannobiose were hydrolysed into *p*NP and mannose, only.

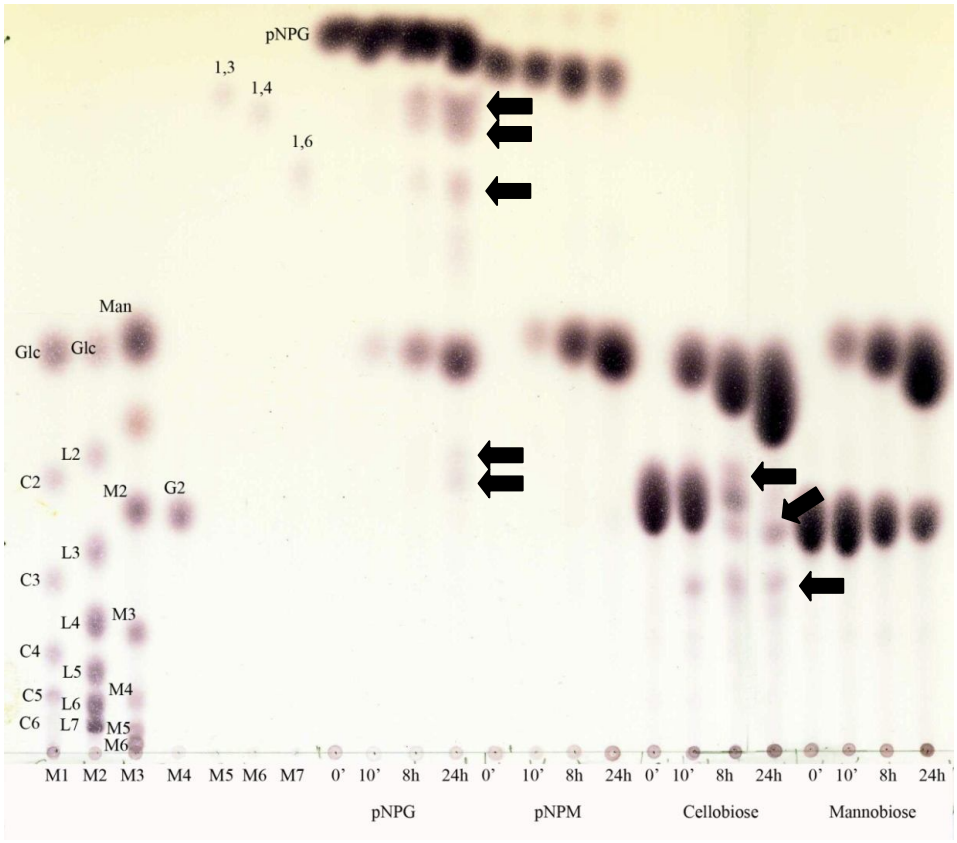

Figure 3.27 TLC chromatogram separating the transglycosylation products of rHv βII with *p*NPGlc, *p*NPMan, cellobiose, and mannobiose as substrates. The transglycosylation reaction was set-up with 0.45 nmole of rHv βII and 20 mM substrates, which were *p*NPGlc, *p*NPMan, cellobiose, and mannobiose, respectively, in 10 mM NaOAc, pH 4.0. Aliquots of the transglycosylation reactions were collected at 10 min, 8 h, and 24 h. The products were separated on a silica gel 60 F_{254} TLC plate with a mobile phase containing ethyl acetate, acetic acid and water at the ratio 3:2:1. Lane M1 contains cellooligosaccharide standards DP 2-6, lane M2 contains laminarioligosaccharide standards DP 2-7, lane M3 contains mannooligosaccharide standards DP 2-7, lane M4 contains gentiobiose, lane M5 contains *p*NP-laminaribioside (1,3-β-linked), lane M6 contains *p*NP-cellobioside (1,4-β-linked), lane M7 contains *p*NP-gentiobioside (1,6-β-linked).

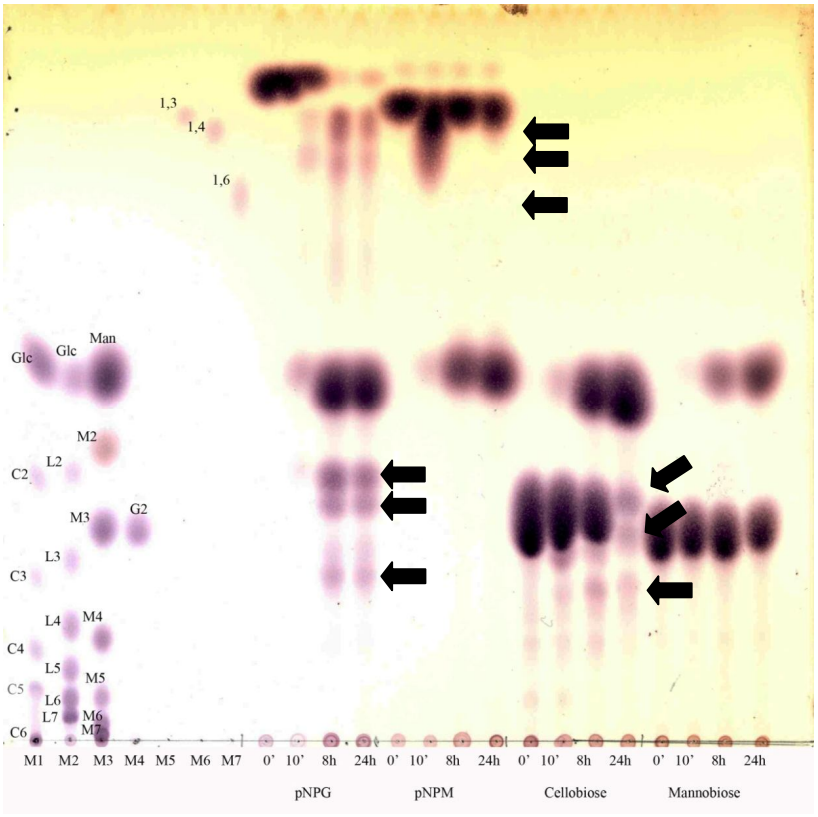

Figure 3.28 TLC chromatogram separating the transglycosylation products of Os3BGlu7 with *p*NPGlc, *p*NPMan, cellobiose, and mannobiose as substrates. The transglycosylation reaction was set-up with 0.45 nmole of rHv βII and 20 mM substrates, which were *p*NPGlc, *p*NPMan, cellobiose, and mannobiose, respectively, in 10 mM NaOAc, pH 4.0. Aliquots of the transglycosylation reactions were collected at 10 min, 8 h, and 24 h. The products were separated on a silica gel 60 F_{254} TLC plate with a mobile phase containing ethyl acetate, acetic acid and water at the ratio 3:2:1. Lane M1 contains cellooligosaccharide standards DP 2-6, lane M2 contains laminarioligosaccharide standards DP 2-7, lane M3 contains mannooligosaccharide standards DP 2-7, lane M4 contains gentiobiose, lane M5 contains *p*NP-laminaribioside (1,3-β-linked), lane M6 contains *p*NP-cellobioside (1,4-β-linked), lane M7 contains *p*NP-gentiobioside (1,6-β-linked).

3.3.8 Relative β-mannosidase activity of expressed β-glucosidases toward mannooligosaccharides

The relative β-mannosidase activities of rHv βII and rice Os3BGlu7 toward mannooligosaccharides with DP 2-6 were determined and the rates of mannose released from mannooligosaccharides are shown in Figure 3.29. The relative β-mannosidases activities of rHv βII and rice Os3BGlu7 increased with the increasing DP of mannooligosaccharides from 2 to 6. rHv βII showed higher relative β-mannosidase activity than rice Os3BGlu7. From Figure 3.29, it is clear that rHv βII hydrolysed mannooligosaccharides more efficiently than Os3BGlu7. This is identified by the higher specific activity of rHv βII toward mannooligosaccharides DP 2-6 compared to Os3BGlu7 by 0.49, 1.13, 1.89, 4.07, and 4.40 nmol mannose/min per nmol enzyme, respectively.

3.3.9 Inhibition of rHv βII

The inhibition of rHv βII by *p*NP-thiomannopyranoside and *p*NP-thiopyranoglucoside was studied. We found that *p*NP-thioglucoside inhibited *p*NPGlc and *p*NP-thiomannoside inhibited *p*NPMan hydrolysis by rHv βII. The inhibition constants (K_i) and K_m in the presence of *p*NP-thioglucoside and *p*NP-thiomannoside are shown in Table 3.6. The Michaelis-Menten and Eadie-Hofstee plots of *p*NP-thioglucoside and *p*NP-thiomannoside inhibitions are shown in Figures 3.30 and 3.31, respectively.

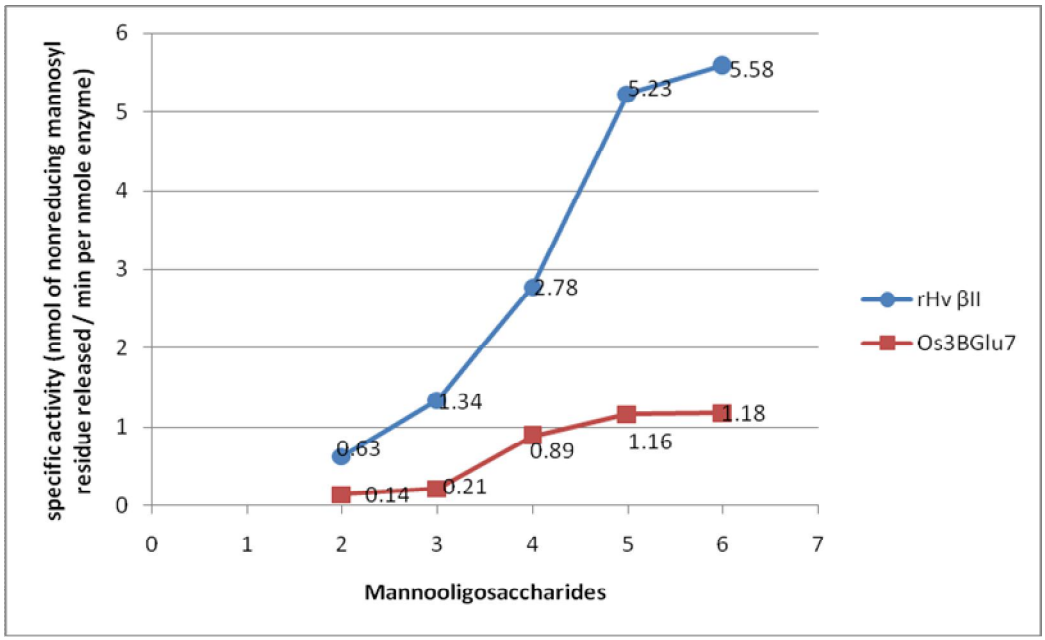

Figure 3.29 Specific β-mannosidase activities of rHv βII and rice Os3Bglu7. The specific β-mannosidase activities of both enzymes toward mannooligosaccharides DP 2-6 were determined by incubating 0.45 nmole of enzyme with 0.8 mM of mannooligosaccharides for 15 min. The reactions were stopped by boiling and dried. The dry products were redissolved in 75% acetonitrile and separated on an Alltech Prevail carbohydrate ES HPLC column at a flow rate 0.4 ml/min. The mannooligosaccharides were vaporized and detected with an Alltech® 800 evaporative light scattering detector. The integrated area of a known mannose peak was used to calculate the amount of mannose released by comparison to a mannose standard curve. The amount of mannose detected with mannobiose was divided by two to account for the release of both the reducing and nonreducing residues in a single cleavage.

Table 3.6 Determined kinetic constants for competitive inhibition of rHv βII by *p*NP-β-D-thioglucoside and *p*NP-β-D-thiomannoside compared to the reaction without inhibitor. The K_m of rHv βII increased from 0.5 mM at no inhibition to 0.95 mM in the presence of 170 μM *p*NP-thioglucoside. Using *p*NP-β-D-thiomannoside to inhibit *p*NPGlc hydrolysis, the K_m increased from 0.2, in no inhibition reaction, to 0.4 mM in the presence of 200 μM *p*NP-thiomannoside.

Substrate	Inhibitor	K_m (mM)	K_i (mM)
*p*NPGlc	-	0.5 ± 0.03	-
*p*NPGlc	thioGlc	0.95 ± 0.16	0.17 ± 0.01
*p*NPMan	-	0.25 ± 0.01	-
*p*NPMan	thioMan	0.4 ± 0.05	0.20 ± 0.06

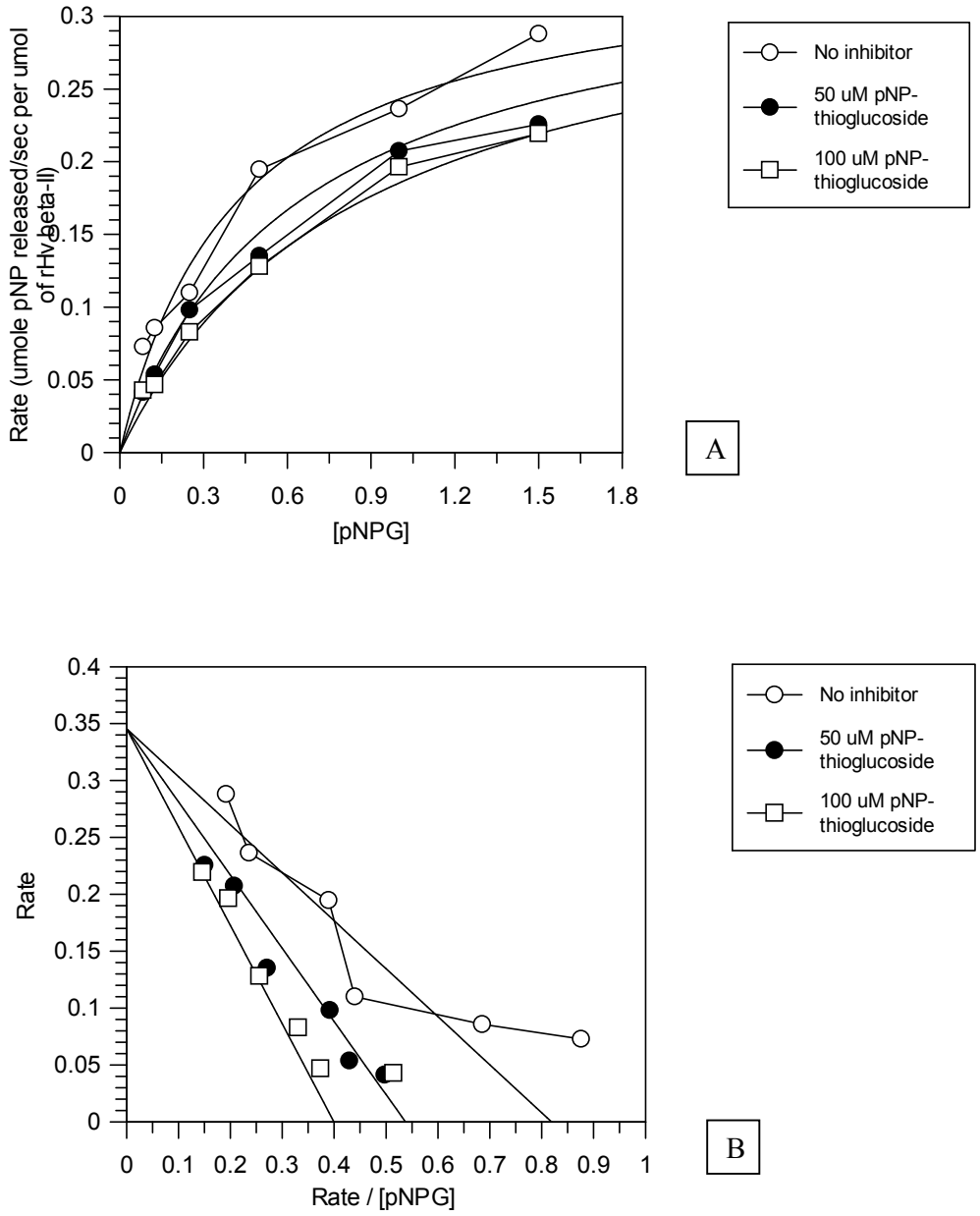

Figure 3.30 Michaelis-Menten (A) and Eadie-Hofstee (B) plots of inhibition of rHv βII hydrolysis of *p*NPGlc by *p*NP-β-D-thioglucoside. The figure was generated by Grafit 5 (Erithacus software).

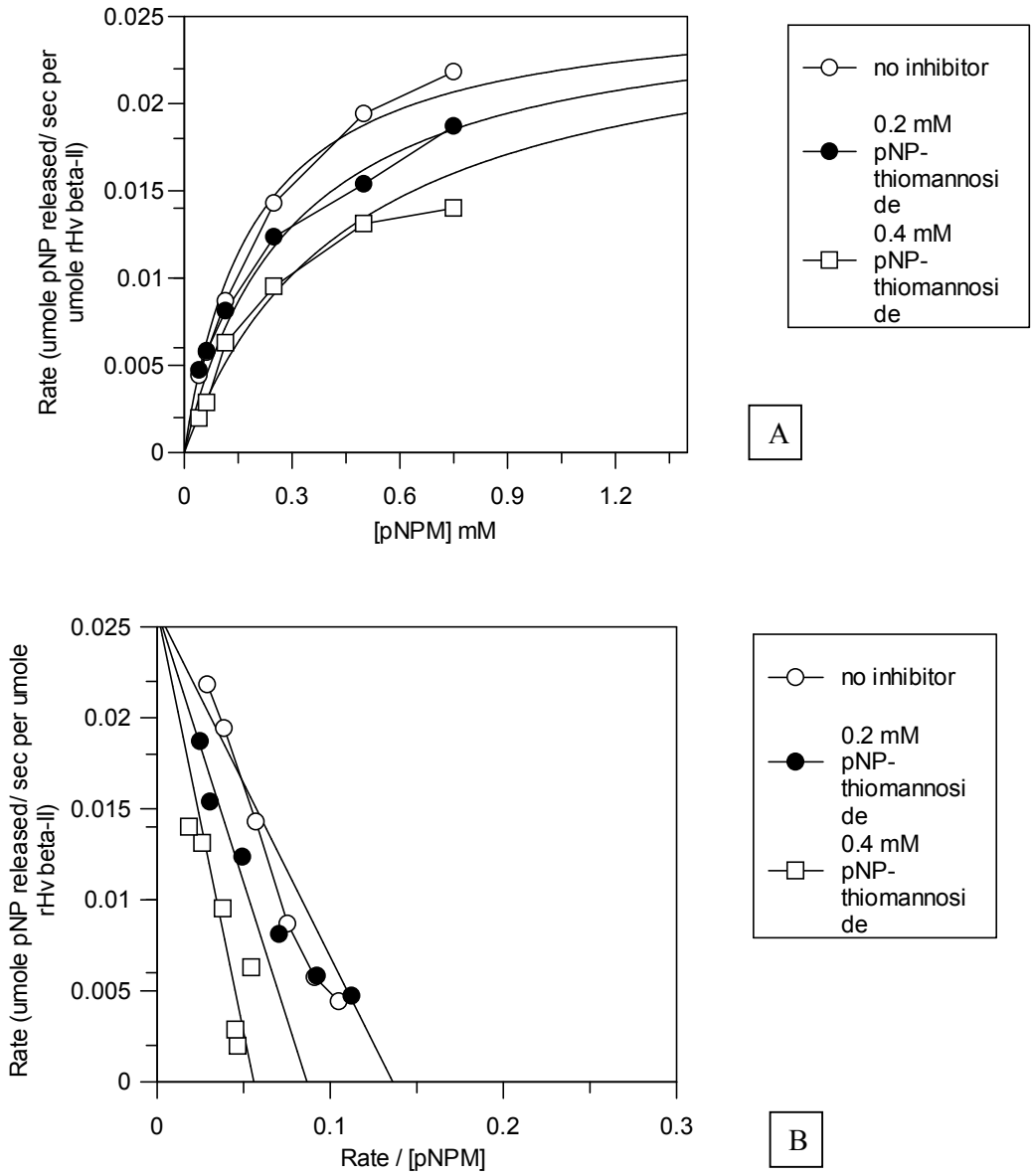

Figure 3.31 Michaelis-Menten (A) and Eadie-Hofstee (B) plots of inhibition of rHv βII hydrolysis of *p*NPMan by *p*NP-β-D-thiomannoside. The figure was generated by Grafit 5 (Erithacus software).

3.4 rHv βII mutation and characterization of mutant proteins

3.4.1 The rHv βII mutation

By comparing the ratios of specific activity for hydrolysis of *p*NPGlc and *p*NPMan between barley rHv βII and rice Os3BGlu7, it was found that the β-mannsidase/β-glucosidase ratio of barley rHv βII is 3.5 by incubating 2 μg of enzyme with 1 mM final concentration of *p*NPGlc and *p*NPMan at 30ºC, 30 min while that for Os3BGlu7 is 0.1. Therefore, it is interesting to determine if changes in residues in the active site of rHv βII to corresponding residues in Os3BGlu7 can convert rHv βII to have more β-glucosidase activity, like rice Os3BGlu7. The putative residues involved in determining the β-mannosidase activity of rHv βII were identified by multiple protein sequence analysis of rHv βII and four rice β-glucosidases, Os1BGlu1, Os3BGlu7, Os3BGlu8, and Os7BGlu26, superposition of an rHv βII homology model onto the Os3Bglu7 crystal structure (protein databank accession number 2RGL), and investigating those residues within 3 Å range of the cellopentaose which is bound in the Os3BGlu7 crystal structure. The putative amino acid residues involved in determination of β-mannosidase and β-glucosidase activities are shown in Table 3.7. From the phylogenetic relationships in Figure 3.23, it appeared that Os1BGlu1 and Os7BGlu26 should be primarily a β-mannosidases, like rHvβII, and Os3BGlu8 should be primarily β-glucosidase, like Os3BGlu7. Therefore, the conserved amino acids in rHv βII and Os7BGlu26 but not Os1BGlu1 may determine their relatively high β-mannosidase activity, while the corresponding amino acids which are conserved in Os3BGlu7 and Os3BGlu8, but different from the other three enzymes, may determine their relatively high β-glucosidase activity. First, V184I and A187L mutants were constructed because valine 184 is found at the +1 site in rHv βII, while the

corresponding residue is isoleucine in Os3BGlu7 and Os3BGlu8 and the difference of alanine at residue 187 in rHv βII and leucine at the corresponding residue of Os3BGlu7 might have resulted in the greater β-glucosidase activity of Os3BGlu7. Also, leucine 246 is conserved in rHv βII, Os3BGlu26 and Os1BGlu1, while the corresponding residue is valine in Os3BGlu7 and Os3BGlu8. Alanine 187 was changed to leucine, which is a corresponding amino acid in Os3BGlu7 because leucine may prevent the incoming *p*NPMan from binding at the productive position. The valine 250 in rHv βII is mutated to asparagine, which is the corresponding residue in Os3BGlu7 because asparagine at this position may help in selection of *p*NPGlc over *p*NPMan.

3.4.2 Characterization of rHv βII mutants

The β-mannosidase/β-glucosidase specific activity ratios of the rHv βII mutants were determined (Table 3.8). Among the rHv βII mutants, the L246V mutant showed a 44% decrease in its β-mannosidase/β-glucosidase activity ratio (1.95) compared to the wild type rHv βII, which has a β-mannosidase/β-glucosidase specific activity ratio of 3.5. The V250N showed a β-mannosidase/β-glucosidase specific activity ratio of 2.23. The V184I mutant showed a 2.3-fold increase in the β-mannosidase/β-glucosidase activity ratio to 8.02. The A187L and E391G mutants showed decreased β-mannosidase/β-glucosidase activity ratios of 1.34 and 1.14, respectively. However, the A187L mutant showed lower activity to *p*NPGlc (6-fold lower than wildtype) and *p*NPMan (16-fold lower). This suggests that A187 contributes to the hydrolysis of both *p*NPGlc and *p*NPMan by rHv βII.

3.4.3 Determination of rHv βII mutants kinetic constants

The kinetic constants of V184I and L246V mutants towards *p*NPG, *p*NPM, cellobiose and cellotriose were determined (Table 3.9).

Table 3.7 Putative substrate binding residues in active site of barley rHv βII, rice Os1BGlu1, Os3Bglu7, Os3Bglu8, and Os7Bglu26 β-glucosidases, which were identified by multiple protein sequence alignment and superposition of homology models of the barley rHv βII, rice Os1BGlu1, Os3Bglu7, and Os3Bglu8, Os7Bglu26 β-glucosidases onto the crystal structure of Os3Bglu7.

rHv βII	Os7BGlu26	Os1BGlu1	Os3Bglu7	Os3BGlu8
V184I	C181	V197	I179	I180
A187	A184	A200	L182	A187
E391	E388	E403	E386	E387
L246	L243	L258	V241	V242
V250	V247	V262	N245	N246

Table 3.8 Specific activity of barley rHv βII mutants toward *p*NPGlc and *p*NPMan. The specific activity of rHv βII toward *p*NPGlc and *p*NPMan was assayed by using 2 μg of enzyme incubating with 1 mM final concentration of *p*NPGlc and *p*NPMan at 30ºC 30 min.

Mutants	Specific activity toward *p*NPGlc (nmol *p*NPGlc/min per μg enzyme)	Specific activity toward *p*NPMan (nmol *p*NPMan/min per μg enzyme)	*p*NPMan/*p*NPGlc ratio
WT	3.66	13.0	3.50
V184I	5.50	44.1	8.02
A187L	0.59	0.79	1.34
L246V	1.56	3.04	1.95
V250N	0.62	1.38	2.23

Table 3.9 Kinetic constants of rHv βII L246V and V184I mutants toward *p*NPGlc, *p*NPMan, cellobiose, and cellotriose.

Substrates	Kinetic parameters	WT	L246V	V184I
***p*NPGlc**	K_m (mM)	0.50 ± 0.03	1.06 ± 0.06	0.245± 0.015
	k_{cat} (s^{-1})	0.50 ± 0.07	1.55 ± 0.04	0.29 ± 0.02
	k_{cat}/K_m (s^{-1} mM^{-1})	1.0 ± 0.1	1.46 ± 0.04	1.18 ± 0.01
***p*NPMan**	K_m (mM)	0.25 ± 0.01	2.32 ± 0.21	0.27 ± 0.02
	k_{cat} (s^{-1})	3.06 ± 0.02	9.03 ± 0.97	0.72 ± 0.02
	k_{cat}/K_m (s^{-1} mM^{-1})	12.67 ± 0.17	3.96 ± 0.78	2.67 ± 0.11
C2	K_m (mM)	2.8 ± 0.1	1.51± 0.05	2.3 ± 0.5
	k_{cat} (s^{-1})	16.08 ± 0.15	12.56 ± 0.19	0.18 ± 0.04
	k_{cat}/K_m (s^{-1} mM^{-1})	5.86 ± 0.23	8.32 ± 0.15	0.08 ± 0.02
C3	K_m (mM)	0.74 ± 0.06	1.06 ± 0.02	2.73 ± 0.77
	k_{cat} (s^{-1})	1.67 ± 0.39	2.86 ± 0.05	0.14± 0.01
	k_{cat}/K_m (s^{-1} mM^{-1})	3.45 ± 0.08	2.7 ± 0.1	0.05± 0.01

CHAPTER IV

DISCUSSION

4.1 Expression and purification of β-glucosidases

The rHv βII, Os1BGlu1, and Os3BGlu8 were expressed as fusion proteins with N-terminal thioredoxin and hexahistidine tags. Initially, the *Os1BGlu1* and *Os3BGlu8* cDNAs were amplified as cDNA encoding the mature proteins. However, the recombinant Os1BGlu1 and Os3BGlu8 did not bind to the cobalt IMAC column because the N-terminal fusion tag containing hexahistidine was cleaved off during the protein extraction. Therefore, the new construct without the predicted trypsin-like protease site at the N-terminus of Os3BGlu8 was made, which is 12 amino acids shorter (lacking N'-VRAADDDTGGLS-C'), but an N-terminally truncated construct of Os1BGlu1 could not be constructed. In the first purification step using Co^{2+} IMAC to separate recombinant rHv βII and Os3BGlu8 from total proteins (Figure 4.1), their proteolytic fragments co-purified with mature fusion proteins. This suggested that phenylmethylsulfonylfluoride (PMSF), the serine protease inhibitor in protein extraction buffer, could not inhibit the digestion of recombinant rHv βII and Os3BGlu8. To overcome the problem, soybean trypsin inhibitor was used instead of PMSF and it prevented the random digestion of rHv βII and Os3BGlu8. Soybean trypsin inhibitor also helped prevent the proteolytic digestion of Os1BGlu1 during protein extraction and purification, therefore, Os1BGlu1 could be separated from total proteins by Co^{2+} IMAC. In the second step of rHv βII purification, the fusion tags were

removed from rHv βII in order to determine the kinetic parameters of recombinant rHv βII and compare with the kinetic constants of natural Hv βII. The recombinant Hv βII with fusion tags is less stable than rHv βII with the fusion tag removed, in that it degraded to smaller rHv βII.

Os1BGlu1 and Os3BGlu8 were purified from total proteins by Q-sepharose (anion exchange) chromatography and phenyl sepharose (hydrophobic interaction) chromatography. However, the N-terminal tag containing thioredoxin and the hexahistidine sequence co-eluted with Os1BGlu1 including the fusion N-terminal tag. Therefore, the Os1BGlu1 was subjected to enterokinase digestion in order to purify it from the fusion tag. For Os3BGlu8, the enterokinase digestion gave rise to several protein bands, which suggested that enterokinase inappropriately digested Os3BGlu8 in multiple locations. In purification of a bZIP-like protein using enterokinase (New England Biolabs), the bZIP-like protein was digested into smaller fragments, which were not expected (Shahravan et al., 2008). They tried to overcome the nonspecific enterokinase cleavage by varying the digestion conditions including lowering the temperature from 37°C to 25°C, lowering the pH from 7.6 to 7.0, and lowering the enterokinase concentration in the reaction. However, the digestion pattern of enterokinase was not changed. They proposed that accessibility of the enterokinase digestion site was impeded by the aggregation of the protein via the hexahistidine tag. They showed that addition of urea 1-4 M could greatly improved enterokinase cleavage specificity at the canonical site and reduced adventitious cleavage. Therefore, it is believed that this enhancement in specificity is due to a more open protein structure, in which the now accessible canonical target can compete effectively with adventitious cleavage sites of related sequence.

N-terminal fusion tag does not likely affect the function of Os3BGlu8 because its substrate specificity and sequence are similar to Os3BGlu7, the activity of which was similar with and without the fusion tag (Opassiri et al., 2004).

1	VRAADDDTGG LSRAAFPKGF VFGTATSAFQ VEGMAASGGR GPSIWDPFVH
51	TPGNIAGNGN ADVTTDEYHR YKEDVDLLKS LNFDAYRFSI SWSRIFPDGE
101	GKVNTEGVAY YNNLIDYVIK QGLIPYVNIN HYDLPLALQK KYEGWLSPKI
151	VGVFSDYAEF CFKTYGDRVK NWFTFNEPRI VAALGHDTGT DPPNRCTKCA
201	AGGNSATEPY IVAHNIILSH ATAVDRYRNK FQASQKGKIG IVLDFNWYEP
251	LTNSTEDQAA AQRARDFHVG WFLDPLINGQ YPKNMRDIVK ERLPTFTPEQ
301	AKLVKGSADY FGINQYTANY MADQPAPQQA ATSYSSDWHV SFIFQRNGVP
351	IGQQANSNWL YIVPTGMYGA VNYIKEKYNN PTIIISENGM DQSGNLTREE
401	FLHDTERIEF YKNYLTELKK AIDDGANVVA YFAWSLLDNF EWLSGYTSKF
451	GIVYVDFTTL KRYPKDSANW FKNMLQASGP GSKSGSGTSD SQVGSATSAS
501	HPVGSAISSS HRLLLPLLVS LHFLFPSFFM FLSL

Figure 4.1 Mature Os3BGlu8 protein sequence

The predicted mature Os3BGlu8 protein sequence is shown here. The fifteen underlined amino acids were removed from the N-terminus in the truncated Os3BGlu8 construct to avoid predicted trypsin protease site between R_{13} and A_{14}.

4.2 Characterization of β-glucosidases

4.2.1 pH and temperature optima

The pH and temperature optima of rHv βII (pH 4.0, 30ºC) are slightly different from natural Hv βII, in which the pH and temperature optima are pH 5.0, and 37ºC (Hrmova et al., 1998). However, the small differences in pH and temperature optima of rHv βII do not change the substrate specificity of rHv βII, in that it still prefers *p*NPMan to *p*NPGlc and cellobiose to cellotriose, like the enzyme from barley seed. The products from the transglycosylation reaction with rHv βII, cellobiose, cellotriose and laminaribiose, matched the products from transglycosylation with Hv βII confirming that rHv βII is highly similar to natural Hv βII. The optimum

temperature for Os1BGlu1, 40ºC, is still lower than other plant β-glucosidases which have higher temperature optima than Os1BGlu1, including β-glucosidase from rice (Akiyama et al., 1998) and *Dalbergia nigrescens* Kurz (Chuankhayan et al., 2005) which have optimum temperatures of 50ºC and 65ºC, respectively. The optimum pH and temperature of Os3BGlu8 at pH 5.0, 30ºC are identical to Os3BGlu7 (Opassiri et al., 2004). The optimum pH of Os1BGlu1 at pH 5.5 is similar to other plant β-glucosidases (Hrmova et al., 1998; Esen, 1992; 1993).

The lower optimum temperatures of recombinant β-glucosidases expressed in prokaryotic hosts than recombinant β-glucosidases expressed in eukaryotic hosts could be explained by the lack of glycosylation. Solovicová et al. (1996) compared the α-glucoamylase which was expressed in *E. coli* and *Saccharomycopsis fibuligera*. They found that the α-glucoamylase expressed in E. coli had a lower optimum temperature of 42ºC, while the optimum temperature of α-glucoamylase expressed in S. *fibuligera* was 50ºC. Olsen et al. (1991) examined the relationship between stability and glycosylation with the two heavily glycosylated β-(1,3)- and β-(1,4)-glucanases. They found that the glycosylated enzymes expressed in *Saccharomyces cerevisia* were considerably more heat stable that their nonglycosylated counterparts which were expressed in *E. coli*.

4.3 Substrate specificity of β-glucosidases

4.3.1 Substrate specificity of rHv βII

rHv βII hydrolyzes a broad range of substrates, which include *p*NP-glucosides and natural substrates. Toward *p*NP substrates, rHv βII hydrolysed *p*NP-*β*-D-glucopyranoside, *p*NP-*β*-D-mannopyranoside, *p*NP-*β*-D-galactopyranoside, *p*NP-*β*-D-

fucopyranoside, *p*NP-*α*-L-arabinopyranoside. This is different from BGQ60, which hydrolyzed just *p*NP-*β*-D-glucopyranoside and *p*NP-*β*-D-mannopyranoside (Leah et al., 1995), but not *p*NP-*β*-D-galactopyranoside. Os3BGlu7 can also hydrolyze the same *p*NP-glycosides (Opassiri et al., 2003) which were hydrolysed by rHv βII. The rHv βII could hydrolyze various glucosides, which included alcohol glucosides (salicin and esculin), cyanogenic glucosides (epiheterodendrin, dhurrin, D-amygdalin, sambunigrin, and tetraphyllin), isoflavonoids (daidzin, genistin, and glycitin), lignin precursors (p-coumaryl alcohol glucoside and coniferin), and a vitamin glucoside (pyridoxine glucoside). For oligosaccharides, rHv βII can hydrolyse laminarioligosaccharides with DP of 2-3, cellooligosaccharides with DP of 2-6, and (1,4)-β-D-mannooligosaccharides with DP of 2-6. As noted previously, the specificity of rHv βII is almost identical to Hv βII in that they are more both active to *p*NPMan than *p*NPGlc, and they hydrolyse cellobiose better than cellotriose (Hrmova et al., 1998). However, the hydrolysis of laminaritetraose is not observed in rHv βII, while Hrmova et al. (1998) reported a low level in hydrolysis of laminaritriose in Hv βII.

4.3.2 Hydrolysis of synthetic glucosides by β-glucosidases

By comparing the k_{cat}/K_m of *p*NPGlc and *p*NPMan of rHv βII and rice Os1BGlu1 and Os3BGlu8 β-glucosidase, it is found that Os1BGlu1 displayed the highest *p*NPGlc hydrolysis efficiency (k_{cat}/K_m = 30.5 $mM^{-1}s^{-1}$) but it barely hydrolysed *p*NPMan, as it showed approximately 22,000 times less activity against *p*NPMan than *p*NPGlc, based on the absorbance of free *p*NP detected after extended period of hydrolysis (3 h) followed by colorimetric assay. Therefore, it is appropriate to described Os1BGlu1 as a rice β-glucosidase. However, the lack of β-mannosidase activity in Os1BGlu1 was not expected because Os1BGlu1 was the second most

similar to rHv βII after Os7BGlu26 (Figure 3.22). For Os3BGlu8, it is more specific to *p*NPGlc than *p*NPMan, as expected from the phylogenetic tree. The k_{cat}/K_m to *p*NPGlc of Os3BGlu8 12.6 $mM^{-1}s^{-1}$ which is second to Os1BGlu1. However, the k_{cat}/K_m towards *p*NPMan of Os3BGlu8 is 0.16 $mM^{-1}s^{-1}$, while it was not detectable for Os1BGlu1. rHv βII hydrolysed *p*NPMan best with a k_{cat}/K_m of 12.67 which is 79 times higher than the k_{cat}/K_m of Os3BGlu8 (0.16 $mM^{-1}s^{-1}$). For *p*NPGlc, rHv βII has the lowest k_{cat}/K_m (1.00 $mM^{-1}s^{-1}$), which is 30.5 times lower than Os1BGlu1, which is best in *p*NPGlc hydrolysis in this study.

4.3.3 Hydrolysis of oligosaccharides by β-glucosidases

The rHv βII, Os1BGlu1 and Os3BGlu8 β-glucosidases hydrolysed cellooligosaccharides with DP of 2-6, and laminarioligosaccharides with DP 2-3. Here, the k_{cat}/K_m parameters of the β-glucosidases toward oligosacchairdes are compared. The rHv βII hydrolysed cellobiose best with a k_{cat}/K_m of 5.84 $mM^{-1}s^{-1}$, while Os1BGlu1 and Os3BGlu8 barely hydrolysed cellobiose as shown by very low k_{cat}/K_m values, (0.12 $mM^{-1}s^{-1}$ and 0.04 $mM^{-1}s^{-1}$, respectively). The rHv βII hydrolysed cellotriose with much less efficiency with k_{cat}/K_m value of 3.45 $mM^{-1}s^{-1}$, compared to Os1BGlu1 and Os3BGlu8, which efficiently hydrolysed cellotriose with k_{cat}/K_m values of 21.6 $mM^{-1}s^{-1}$ and 10.95 $mM^{-1}s^{-1}$, respectively.

The difference in hydrolysis efficiency toward cellobiose and cellotriose of rHv βII, Os1BGlu1, and Os3BGlu8 can be explained by subsite affinities at the +1 and +2 sites. The subsite affinity of rHv βII is -1.33 $kJ{\cdot}mol^{-1}$ at subsite +2 but the subsite +1 has highest affinity (22.2 $kJ{\cdot}mol^{-1}$) toward a cellooligosaccharide glucosyl residue. This is different from Os1BGlu1 and Os3BGlu8, in which subsite +2 has

higher affinity (13.1 kJ·mol^{-1} and 13.0 kJ·mol^{-1}, respectively) than subsite +1 (10.3 kJ·mol^{-1} and 10.15 kJ·mol^{-1}, respectively). The negative affinity at the +2 subsite of rHv βII allows cellobiose to bind at the cleavage site which is located between the -1 and +1 subsites. This is different in Os1BGlu1 and Os3BGlu8, for which cellobiose molecules are predicted to bind best at the nonproductive position covering the +2 and +3 subsites, which have high affinities. For cellotriose, the high affinity at the +1 site of rHv βII may force cellotriose to bind at nonproductive site at subsite +1 to +3 or it could be the steric interactions at the +2 site which prevent cellotriose to bind well at the productive site. Rice Os1BGlu1 and Os3BGlu8 showed higher k_{cat}/K_m values compared to that of cellobiose hydrolysis, which is expected, since binding to the -1 to +2 sites is similar to binding to the +1 to +3 sites for these isozymes and more favourable for Os3BGlu7 (Opassiri et al., 2004). For cellooligosaccharides with DP 4-6, rHv βII and rice Os1BGlu1 and Os3BGlu8 showed higher k_{cat}/K_m values. The probability for cellooligosaccharides to bind at the productive positions increases as the number of subsites are filled during substrate binding (Hiromi et al., 1970). Therefore, the cellooligosaccharide hydrolysis efficiency (k_{cat}/K_m) of Os1BGlu1 and Os3BGlu8 increase as the DP increases. This is different from rHv βII which hydrolyses cellobiose better than cellotriose, but its hydrolysis efficiency for cellooligosaccharides with DP 3-6 increase as the DP increases.

In hydrolysis of laminarioligosaccharides, Os1BGlu1 and Os3BGlu8 hydrolysed laminaribiose with k_{cat}/K_m values of 30.6 mM^{-1}s^{-1} and 36.1 mM^{-1}s^{-1}, respectively, while the k_{cat}/K_m value of rHv βII is 2.30 mM^{-1}s^{-1}. This indicates that Os1BGlu1 and Os3BGlu8 hydrolysed laminaribiose more efficiently than rHv βII. rHv βII, Os1BGlu1 and Os3BGlu8 hydrolysed laminaritriose with k_{cat}/K_m values of

0.84, 3.40 and 2.18 $mM^{-1}s^{-1}$, respectively. Therefore, laminaritriose is a less preferred substrate of rHv βII, Os1BGlu1, and Os3BGlu8.

4.4 Transglycosylation by rHv βII and Os3BGlu7

The rHv βII and Os3BGlu7 enzymes can catalyze transglycosylation reactions by using the glucose residues from cellobiose and *p*NPGlc as donor and acceptor. The products from transglycosylation reactions catalyzed by rHv βII and Os3BGlu7 are *p*NP-laminaribioside, *p*NP-cellobioside, *p*NP-gentiobioside, cellobiose, laminaritriose, and gentiobiose. However, no transglycosylation product was detected in transglycosylation reactions using *p*NPMan and mannobiose. The β-mannosidase purified from *Rhizopus niveus* is the only β-mannosidase that has been reported to catalyze the transglycosylation of mannosyl residues onto other mannosyl residues acting as acceptor (Fujimoto et al., 1997). After 24 h incubation, mannooligosaccharides with DP of 2-5 were obtained. This suggests that β-mannosidases which catalyze transglycosylation reactions are rare. The lack of observed transglycosylation reactions using *p*NPMan or mannobiose as substrate in rHv βII could be explained by the opposite configuration of the hydroxyl group at carbon 2 between glucose and mannose. The mannosyl residue, which has axial hydroxyl group at this position, blocks the acceptor position in the active site of rHv βII and Os3BGlu7 in transglycosylation, while the glucosyl residue which has an equatorial 2-hydroxyl group allows an acceptor to fit well in the active site of rHv βII and Os3BGlu7 in transglycosylation. As a result, the transglycosylation reactions catalyzed by rHv βII and Os3BGlu7 are specific to transferring the glucose residue only. By comparing the lengths of glycosylation products, β-(1,4)-D-cellotriose was the longest product of rHv

βII and Os3BGlu7, indicating that rHv βII and Os3BGlu7 prefers to transfer glycosyl residue onto the acceptor in a β-(1,4)-D-linkage more than β-(1,2)- and β-(1,3)-D-linkages.

4.5 Relative β-mannosidase activity of rHv βII and Os3BGlu7

The relative β-mannosidase activity of rHv βII was compared to Os3BGlu7 because Os3BGlu7 represented the closely related plant β-glucosidase with relatively little β-D-mannosidase activity, while rHv βII has more β-D-mannosidase activity than β-D-glucosidase activity. The hydrolysis rate of Os3BGlu7 toward mannooligosaccharides increased as the DP increased from 2-6, which is the same as the pattern seen for its hydrolysis of cellooligosaccharides. For rHv βII, the hydrolysis rate toward mannooligosaccharides increased as the DP increased from 2-6. This is different from cellooligosaccharide hydrolysis by rHv βII, in which the hydrolysis rate dropped at cellotriose and rose up again at cellotetraose. The β-mannosidase hydrolysis rates of rHv βII toward mannooligosaccharides DP 2-6 are 0.63, 1.34, 2.78, 5.23 and 5.58 nmol mannose/min per nmol enzyme, respectively, while that of Os3BGlu7 are 0.14, 0.21, 0.89, 1.16, and 1.18 nmol/min per nmol enzyme, respectively. This indicates that rHv βII hydrolyses mannooligosaccharides more rapidly than Os3BGlu7.

4.6 Inhibition of rHv βII by pNP-β-D-thioglucoside and pNP-β-D-thiomannoside

The inhibition study of rHv βII was performed with the competitive inhibitors *p*NP-β-D-thioglucoside and *p*NP-β-D-thiomannoside. The *p*NP-β-D-thioglucoside

inhibited the hydrolysis of *p*NPGlc with a K_i of 0.17 mM and the apparent K_m of rHv βII towards *p*NPGlc increased from 0.5 to 0.95 mM at 200 μM of pNP-β-D-thioglucoside. The pNP-β-D-thiomannoside inhibited the hydrolysis of *p*NPMan with a K_i of 200 μM, and the apparent K_m increased from 0.2 to 0.4 mM, at 200 μM *p*NP-β-D-thiomannoside. Czjzek et al. (2001) proposed that the conformation of glucose residues at binding in the active site before hydrolysis is a $^1S_3$ skew boat conformation. The attempt to identify the conformation of the substrate at transition state in maize β-glucosidase failed, because the structure of the *p*NP-β-D-thioglucosidase bound to the enzyme could not be determined. However, the determination of the enzyme-substrate intermediate structure in golgi α-mannosidase II using α-(1,3)-linked thiomannoside showed that conformational changes of the bound mannoside was changed to a high-energy $B_{2,5}$ conformation (Zhong et al., 2008).

4.7 Protein sequence analysis and active sites of β-glucosidases

The putative catalytic amino acids in rHv βII, Os1BGlu1 and Os3BGlu8 were identified by multiple protein sequence analysis. The catalytic acid/base residues in rHv βII, Os1BGlu1 and Os3BGlu8 are E181, E194, and E177, respectively. The catalytic nucleophiles in rHv βII, Os1BGlu1 and Os3BGlu8 are E391, E403, and E387, respectively. The putative catalytic amino acids are located in two motifs, which are TFNEP and ITENG in Os3BGlu7. In rHv βII, Os1BGlu1 and Os3BGlu8 the first motif is TFNEP like Os3BGlu7, but the second motif is different. The second motif is LSENG in rHv βII and Os1BGlu1 and ISENG in Os3BGlu8. This suggests that the prediction of β-mannosidase being determined by the LS/AENG sequence

(Xu et al., 2004) may not be correct, because Os1BGlu1 which has this conserved motif does not hydrolyse *p*NPMan.

The multiple protein sequence alignment of rHv βII, Os1BGlu1, Os3BGlu8 and two other rice β-glucosidases (Os3BGlu7 and Os7BGlu26) showed that they share several conserved residues with other plant β-glucosidases (Barrett et al., 1995; Czjzek et al., 1997; Sue et al., 2006; Verdoqc et al., 2003). The positions of the conserved amino acids are in this order, rHv βII, Os7BGlu26, Os1BGlu1, Os3BGlu7, and Os3BGlu8. The amino acids which are in close contact with the glucose at the -1 site are strictly conserved among rHv βII and rice β-glucosidases are glutamine (34, 31, 47, 29, 30), histidine (135, 132, 148, 130, 131), asparagine (180, 177, 193, 175, 176), asparagine (318, 315, 330, 313, 314), tyrosine (320, 317, 329, 315, 316), tryptophan (438, 435, 450, 433, 434), glutamate (445, 442, 457, 440, 441) and tryptophan (446, 443, 458, 441, 442), respectively. The conserved amino acids involved in aglycone binding at the +1 and +2 subsites of the rHv βII and rice Os1BGlu1, Os3BGlu7, Os3BGlu8, and Os7BGlu26 β-glucosidases are tyrosine (98, 132, 149, 131, 132), arginine (183, 180, 196, 178, 179), leucine (188, 185, 201, 183, 184), leucine (247, 244, 257, 242, 243), histidine (272, 269, 284, 267, 268) and tryptophan (363, 360, 375, 358, 359).

By superposition of the homology models of rHv βII, Os1BGlu1, and Os3BGlu8 onto the crystal structure of Os3BGlu7, we found a series of amino acid residues that form the active sites of these β-glucosidases within 3Å distance of a cellopentaose bound in the Os3BGlu7 active site and vary within this group of enzymes. The active site figures of rHv βII, Os1BGlu1, and Os3BGlu8 are illustrated with the predicted electrostatic potential map in Figure 3.25. At the –1 subsite of rHv

βII, L246 corresponds to V241 in rice Os3BGlu7 β-D-glucosidase. At the +1 site, three amino acid residue differences were evident: V184, R447 and L448 in rHv βII correspond to I179, L442, and S443 in Os3BGlu7, respectively. At the +2 subsite, three amino acid residues in rHv βII, F194, H195, and V250, were different from the corresponding residues in Os3BGlu7, T189, N190, and N245. At the +3 subsite, N192 in rHv βII corresponds to A187 in Os3BGlu7. At the +4 subsite, rHv βII residues Q339 and F346 are different from the corresponding residues in Os3BGlu7, S334 and Y341, respectively. However, Os1BGlu1, which cannot hydrolyse *p*NPMan, is more similar to rHv βII, and matches it at each of the positions identified in the -1 an +1 sites, except for the conserved substitution of K for rHv βII R447 at the +1 subsite.

4.8 Mutagenesis of rHv βII

rHv βII and Os3BGlu7 share 64.5% protein sequence identity in protein sequence alignment, but they showed different substrate specificities. The ratio of specific activities toward *p*NPMan to *p*NPGlc of rHv βII is 3.5, while the ratio is 0.1 for Os3BGlu7. Mutations that decrease this specific activity ratio could confirm the residues predicted to affect substrate specificity based on protein sequence differences and protein homology modeling of Hv βII using the Os3BGlu7 crystal structure with cellopentaose as template. Here, four mutants changing the amino acids in rHv βII to the corresponding amino acids in Os3BGlu7 were constructed. By comparing the specifc *p*NPMan/*p*NPGlc activity ratio, A187L, L246V, and V250N showed decreased activity ratios (1.34, 1.95, and 2.23, respectively) compared to wild type rHv βII. However, the specific *p*NPGlc hydrolysis activity of the L246V mutant dropped to 1.56 nmol *p*NP/min per μg protein which is 2.35 times lower than the wild

type rHv βII, while the specific *p*NPGlc hydrolysis activity of the A187L mutant dropped to 0.59 nmol *p*NP/min per µg protein, which is 6.2 times lower than wild type rHv βII. Also, the specific *p*NPMan hydrolysis activity of the L246V mutant dropped to 3.04 nmol *p*NP/min per µg protein, which is 4.3 times lower than the wild type rHv βII, while the specific *p*NPMan hydrolysis activity of the A187L mutant dropped to 0.79 nmol *p*NP/min per µg protein, which is 17 times lower than that of wild type rHv βII. This indicates that A187 affects the hydrolysis of both *p*NPGlc and *p*NPMan, while L246 and V250 are crucial in *p*NPGlc hydrolysis. The V184I mutation showed an unexpected result, as the specific *p*NPGlc hydrolysis activity increased to 3.66 nmol *p*NP/min per µg protein and the specific *p*NPMan hydrolysis activity jumped to 44.1 *p*NP/min per µg protein, which is 3.4 times higher than the wild type rHv βII. From k_{cat}/K_m parameters, it is clear that the V184I and L246V mutants showed slightly increased *p*NPGlc k_{cat}/K_m values of 1.18 $mM^{-1}s^{-1}$ and 1.46 $mM^{-1}s^{-1}$ from 1.00 $mM^{-1}s^{-1}$in wildtype, while the k_{cat}/K_m of *p*NPMan values decreased to 2.67 $mM^{-1}s^{-1}$ and 3.4 $mM^{-1}s^{-1}$ from 12.67 $mM^{-1}s^{-1}$ in wildtype. Therefore, V184 and L246 are two amino acids in rHv βII which play roles in determining its selectivity for *p*NPMan hydrolysis. In Os3BGlu7 mutations, Chuenchor et al. (2008) studied the mutation of amino acids in Os3BGlu7 to the amino acids at the corresponding residues in rHv βII. I179V and N245V, which correspond to V184I and V250N in rHv βII, decreased the k_{cat}/K_m values for hydrolysis of *p*NPMan to 6.40 $mM^{-1}s^{-1}$ and 2.24 $mM^{-1}s^{-1}$ compared to wildtype Os3BGlu7 with k_{cat}/K_m value of 23.3 $mM^{-1}s^{-1}$. The decreased k_{cat}/K_m values of the V184I and V250N mutants should be the result of a slight change in the active site conformation, which accommodates *p*NPGlc to bind in a productive position, but made *p*NPMan bind less well in the productive position

rather than blocking the axial hydroxyl group at 2-position of the mannosyl residue. This is because the changing of L246 to V, which is one carbon shorter, seems unlikely to block the binding of a mannosyl residue at the productive site. Therefore, changing of *p*NPMan specificity in rHv βII to be *p*NPGlc specificity requires changing of amino acids at several positions and the changing of substrate specificity may require a change in the shape of the active site rather than change in a single amino acid residue or a few amino acid changes.

Previous studies have investigated differences in two plant β-glucosidases that share high protein sequence identity, including ZmGlu1 in maize and SbDhr1 in sorghum (Verdoucq et al., 2003), and TaGlu1 in wheat and ScGlu in rye (Sue et al., 2006). For ZmGlu1 and SbDhr1, which share 75% protein sequence identity, swapping of the C-terminal domain between ZmGlu1 and SbDhr1 gave rise to a chimeric ZmGlu1 with dhurrinase activity. Amino acid sequence comparison and homology modeling of ZmGlu1 and SbDhr1 revealed three amino acids, S462, S463, and F469, at the C-terminal of SbDhr1 which are involved in dhurrinase specificity (Czjzek et al., 2001). In a following study, the SbDhr1-V196F, L203F double mutations and SbDhr1 mutation of SbDhr1 led to a drastic decrease of dhurrin hydrolysis by decreasing the turnover rate to only 25%, while the counter mutants in ZmGlu1, the-F198V, F205L double mutant and the P377A single mutant, are not able to hydrolyse dhurrin. Later, comparison of the crystal structures of ZmGlu1 and SbDhr1 showed that these two β-glucosidases are different in their active site (Verdoucq et al., 2004). The active site of ZmGlu1 appears to be a flattened crater or slot, while the active site of SbDhr1 is wider and smaller. In ZmGlu1, aromatic sidechains of amino acids forming the aglycone binding site, W378, F198, F205, and

F466, are responsible for binding to DIMBOA or other aromatic aglycones by aromatic stacking and π-interactions, (Czjzek et al., 2000). This is different from SbDhr1, in which N259, F261, and S462 are crucial for aglycone recognition and binding via hydrophobic interactions, hydrogen bonding, and π-interactions. This suggests that interactions with the aglycone in plant GH1 family β-glucosidases is dominated by aromatic interactions with a help of hydrogen bonding in some cases.

In another case, site-directed mutagenesis was performed in β-glucosidases of wheat (TaGlu1) and rye (ScGlu1), which share 90% sequence identity, to change the preference of ScGlu1 from its natural substrate DIBOA-Glc to DIMBOA-Glc, the natural substrate of TaGlu1. However, the changes of amino acids in ScGlu to the corresponding amino acids in TaGlu, G464S, S465L, and F471Y, showed increased DIMBOA-Glc relative activity, while the relative activity to DIBOA-Glc, the preferred substrate of ScGlu, decreased. This suggests that the amino acid residues which control substrate specificities in rHv βII and rice Os3BGlu7 may reside at different regions, as in the cases of ZmGlu1 and SbDhr1, and TaGlu and ScGlu.

4.9 Functions of Hv βII, Os1BGlu1, and Os3BGlu8 in plants

β-Mannosidases in plants and microorganisms are involved in hydrolysing hemicelluloses into monosaccharides. Certain microorganisms use hemicellulose (heteroglycan) as carbon and energy sources. The highly variable hemicelluloses are hydrolysed by three enzymes. β-mannanase and β-mannosidase are responsible for hydrolysis of hetero-(1,4)-β-D-mannans, one of the major components of hemicelluloses, into simpler sugars that can readily be used as a carbon or energy source, while additional enzymes are required to remove side chain sugars that are

attached at various points on hetero-(1,4)-β-D-mannans. For example, galactomannans have galactose residues bound to the mannan backbone, and their removal is effected through the action of α-galactosidase. The characterization of thermophilic *Thermotoga neapolitana* and *Aspergillus niger* β-mannanase and α-galactosidase showed that they function in harmony to release monosaccharides as a carbon source (Duffaud et al., 1996; Ademark et al., 2001). The optimum pH values of β-mannosidase and α-galactosidase purified from cell extracts are similar, 7.7 for β-mannosidase, and 7.3 for α-galactosidase. The very high k_{cat} of 4070 s^{-1} and high k_{cat}/K_m of 1454 $mM^{-1}s^{-1}$ of *T. neapolitana* β-mannosidase suggests that it is responsible for releasing of terminal mannosyl residues from β-mannans. The role of β-mannosidase in hydrolysis of hemicelluloses was suggested in several microorganisms which express this enzyme, including *Aspergillus niger* (Elbein et al., 1977) and *Trichoderm reesei* (Kulminskaya et al., 1999) .

GH family 1 β-mannosidase and β-glucosidase from *Pyrococcus furiosus* characterized (Bauer et al., 1996). The *P. furiosus* β-mannosidase and β-glucosidase share 46.5% protein sequence similarity, the size of both enzymes are similar, 59.0 kDa for β-mannosidase and 54.6 kDa for β-glucosidase. However, they differ in substrate hydrolysis. The *P. furiosus* β-mannosidase showed highest activity in *p*NPMan hydrolysis, but *p*NPGlc was hydrolysed with just 4.7% relative activity, while the β-glucosidase, which hydrolysed *p*NPGlc best, had only 3.6% relative activity to *p*NPMan. The determination of K_m and k_{cat}/K_m also showed that the β-mannosidase hydrolysed *p*NPMan with low K_m and high k_{cat}/K_m, while the β-glucosidase hydrolysed *p*NPGlc with low K_m and high k_{cat}/K_m.

In tomato, β-mannosidases and two other enzymes, β-mannanase and α-galactosidase are involved in the hydrolysis of galactomannans (Mo and Bewley, 2002), which are particularly abundant in the primary cell walls of Solanaceous species (O'Neil and York, 2003). Mo and Bewley (2002) showed that the both enzymes increased in activity prior to the completion of germination, particularly in the micropylar endosperm, and both increase in the lateral endosperm following germination. Tomato β-mannanase hydrolysed the backbone into mannobiose and mannotriose, which were hydrolysed to mannose by β-mannosidase. The expression of these two enzymes was affected by gibbellin deficiency, which resulted in no germination.

The rHv βII can hydrolyse several types of glycosides, including cyanogenic glucosides, hormonal glucosides, isoflavonoids, and lignin precursors. However, the synthesis of rHv βII in germinating barley seeds and the storage of epiheterodendrin, a cyanogenic glucoside, in barley leaves (Nielsen et al., 2006) suggests that rHv βII is not responsible for cyanogenesis in response to pest invasion. Towards oligosaccharides, rHv βII is specific to β-(1,2)-, (1,3)-, and (1,4)- linkages. Therefore, rHv βII appears to act in remodelling of the cell wall during germination by breaking-down oligosaccharides that are released from β-D-mannans and β-D-glucans (Leah et al., 1995; Hrmova et al., 1996, 1998, 2006). Hrmova et al. (2006) found that barley Hv βII works in a concerted pattern with HvMAN1, a barley β-mannanase, in hydrolysis of locus-bean gum galactomannan, to release mannosyl residues. First the HvMAN1 hydrolysed locus-bean gum galactomannan into mannobiose and mannotriose, which were further hydrolysed into mannose by Hv βII, suggesting that Hv βII and HvMAN1 work in a concerted pattern in hydrolysis of galactomanan,

which is a backbone in hemicellulose. Unlike tomato β-mannosidase, the activity of Hv βII did not increase in the presence of gibberellic acid. This may be because Hv βII was synthesized two weeks before maturation and is stored in the endosperm of the dry dormant seed (Simos et al., 1994).

Barley rHv βII hydrolysed mannooligosaccharides with increasing relative rates as the DP increased from 2-6. The β-mannosidase from *Bacillus* sp. also showed increased activity toward mannooligosaccharides as DP increased from 2 to 4 (Akino et al., 1988). However, the β-mannosidase from *T. reesei* showed decreased activity as the DP increased from 2 to 4 (Kulminskaya et al., 1999).

Opassiri et al. (2006) identified the expression of rice β-glucosidases by searching the dbEST database with the rice GH1 cDNA sequences. The Os1BGlu1 matched 13 ESTs, while the Os3Bglu8, which has highest similarity to Os3BGlu7, showed higher abundance, with 77 ESTs clones, which is the second most of any GH1 gene behind to Os3BGlu7, which has 326 ESTs. From the analysis, Os1BGlu1 and Os3BGlu8 are expressed in shoot and panicle at tillering stage and they respond to abscisic acid treatment. The Os3BGlu8 is also expressed in shoot and panicle during flowering stage and it responds to benzyl amino purine, a cytokinin analogue, in callus and cold stress in shoot. This suggests that Os1BGlu1 and Os3BGlu8 are responsible for the cell wall remodelling in several developmental stages, and are controlled by hormones. From protein sequence alignment, Os1BGlu1 and Os3BGlu8 showed 62.9% and 66.7% protein sequence identity to Os3BGlu7. This high degree of identity of Os1BGlu1 and Os3BGlu8 to Os3BGlu7 suggests that Os1BGlu1 and Os3BGlu8 could be products from gene duplication which is frequently observed among glycosyl hydrolases (Henrissat, 1991). Henrissat (1991) proposed that the

enzyme produced from the original gene copy would continue hydrolysing the original substrate, while duplicate gene copies could constitute templates for constructing enzymes with activity directed to a new, but stereo-chemically similar substrate. Therefore, the Os3BGlu7, Os1BGlu1 and Os3BGlu8 could have a common predecessor, but may have since evolved different functions.

In this study, the barley rHv βII, along with Os1BGlu1 and Os3BGlu8, were expressed and purified. The rHv βII showed that it is almost identical to Hv βII isolated from seed in terms of substrate specificity. Compared to β-mannosidases from microorganisms, plants, and animals, rHv βII showed the broadest substrate specificity as it hydrolysed saccharides with β-(1,2)-, β-(1,3)-, and β-(1,4)-D-linkages. The hydrolysis by rHv βII of a broad range of glycosides, including cyanogenic glucosides, alcoholic glucosides, isoflavonoid glucoside, lignin precursors, and pyridoxine glucoside suggests that rHv βII is the β-mannosidase with the broadest substrate specificity that has ever been reported. The lack of β-mannosyltransferase activity to synthesize β-mannooligosaccharides in rHv βII suggests that the main function of barley rHv βII is hydrolysis, not synthesis of saccharides. This data also suggests that experiments to confirm the substrate specificity of glycosyl hydrolases is needed to confirm the prediction of functions by phylogenetic tree and multiple protein sequence analysis.

CHAPTER V

CONCLUSION

In this study, the barley β-glucosidase, rHv βII, and two rice β-glucosidases, Os1BGlu1 and Os3BGlu8, were characterized. The mRNA encoding mature rHv βII was purified from germinating barley seeds and was used as a template in cloning of the cDNA encoding mature rHv βII. The cDNA encoding mature rHv βII was cloned into the pET32a(+) expression vector and rHv βII was successfully expressed in *E. coli* strain Origami (DE3) as a 75 kDa fusion protein containing hexahistidine tag and thioredoxin on the N-terminus. The recombinant rHv βII was purified using Co^{2+} IMAC and the N-terminal fusion protein was cleaved off from recombinant rHv βII by enterokinase digestion and removed by reloading the enterokinase-digested rHv βII over a Co^{2+} IMAC column. The 55 kDa rHv βII was obtained with at least 95% purity. The determined N-terminal amino acid sequences exactly match the amino acid sequence of fusion protein on the N-terminus, which showed that rHv βII is expressed as the expected fusion protein and the tryptic peptide identified from mass spectrophotometry covered 49.6% of the entire rHv βII protein sequence.

The cDNAs encoding mature Os1BGlu1 and Os3BGlu8 β-glucosidases were amplified using full-length cDNA clones as templates. The recombinant Os1BGlu1 and Os3BGlu8 β-glucosidases were expressed as 75 kDa proteins in the same system as rHv βII. The recombinant Os3BGlu8 was first purified by Co^{2+} IMAC column, followed by Q-sepharose (ion-exchange chromatography) and phenyl sepharose

(hydrophobic interaction chromatography). The recombinant Os1BGlu1 was purified using the methods described for Os3BGlu8, followed by removal of the N-terminal fusion protein as described for rHv βII.

The rHv βII enzyme can hydrolyze several *p*NP-glycosides, including *p*NPGlc, *p*NPMan, *p*NP-galactose, *p*NP-fucose, and *p*NP-arabinose. rHv βII showed higher specific activity in hydrolysis of *p*NPMan than of *p*NPGlc. rHv βII hydrolyzed disaccharides with (1,2)-, (1,3)-, and (1,4)-β-linkages. Towards natural glucosides, rHv βII can hydrolyze cyanogenic glucosides (epiheterodendrin, dhurrin, D-amygdalin, sambunigrin, and tetraphyllin), isoflavonoid glucosides (daidzin, genistin, and glycitin), phenolic alcohol glucoside (salicin and esculin), and the vitamin glucoside pyridoxine glcoside. In hydrolysis of cellooligosaccharides with DP of 2-6, rHv βII showed higher specific activity in hydrolysis of cellobiose than cellotriose, and the specific activity increased as the DP increased from 4-6. The characterization of rHv βII confirmed that it is highly identical to Hv βII, as they both preferred *p*NPMan to *p*NPGlc and had higher specific activity to cellobiose than cellotriose.

The characterization of the rice isozymes showed that Os1BGlu1 does not have β-mannosidase activity which is different from the prediction from the phylogenetic tree analysis, in which Os1BGlu1 was closest to rHv βII. This suggests that prediction of substrate specificity based on phylogenetic analysis should be tested by substrate specificity experiments. Os3BGlu8 hydrolyzed *p*NPGlc with higher specific activity compared to *p*NPMan, like Os3BGlu7. Moreover, Os1BGlu1 and Os3BGlu8 can hydrolyze cellooligosaccharides with DP 2-6 with increasing specific activity as the DP increased from 2-6 like Os3BGlu7.

By comparing the kinetic parameters of rHv βII, Os1BGlu1, and Os3BGlu8, it was found that rHv βII is the most efficient β-glucosidase in hydrolysis of *p*NPMan, as it showed highest k_{cat}/K_m value compared to rice Os1BGlu1 and Os3BGlu8, while Os3BGlu8 is the most efficient β-glucosidase as it had the highest k_{cat}/K_m value in hydrolysis of *p*NPGlc. In hydrolysis of cellooligosaccharides with DP 2-6, rHv βII is more efficient in cellobiose hydrolysis compared to cellotriose, as shown by its higher k_{cat}/K_m for cellobiose, while the k_{cat}/K_m values increased as the DP of cellooligosaccharides increased from 3-6. For Os1BGlu1 and Os3BGlu8, they showed increased k_{cat}/K_m values as the DP of cellooligosaccharides increased from 2-6. The subsite affinities of barley rHv βII, Os1BGlu1, and rice Os3BGlu8 are different at the +1 and +2 subsites. At the +2 subsite, negative affinity was determined in rHv βII, while very high affinities were determined in Os1BGlu1 and Os3BGlu8. At the +1 subsite, rHv βII has higher affinity than Os1BGlu1 and Os3BGlu8. At the -1, +3, +4, and +5 subsites, rHv βII, Os1BGlu1 and Os3BGlu8 showed similar affinities. The inhibition study showed that *p*NP-thioglucoside can inhibit the hydrolysis of *p*NPGlc by rHv βII, resulting in the increased of K_m from 0.5 mM to 0.95 mM at an inhibitor concentration equal to the K_i with the K_i of 0.17 mM, and *p*NP-thiomannoside can inhibit the hydrolysis of *p*NPMan resulting in the increased of K_m from 0.25 mM to 0.4 mM at a concentration equal to its K_i of 0.2 mM.

The rHv βII and rice Os3BGlu7 can hydrolyze mannooligosaccharides. The rHv βII and Os3BGlu7 showed increasing hydrolysis rate as the DP increased from 2-6. By comparing the specific activities, rHv βII showed higher specific hydrolysis rate compared to Os3BGlu7. The rHv βII and Os3BGlu7 enzymes can also catalyze the

transglycosylation reaction using *p*NPGlc and cellobiose as substates, but not with *p*NPMan and β-1,4-mannobiose as substrates.

Mutations were made to attempt to the specific *p*NPMan/*p*NPGlc decrease activity ratio of wildtype rHv βII by changing the active site amino acid residues in rHv βII to corresponding amino acids in Os3BGlu7. Thea L246V mutant had a low specific *p*NPMan/*p*NPGlc activity ratio to 1.95 while the V250N mutant had a similar ratio of 2.23. The A187L mutant showed the lowest ratio of 1.34, but was considered an inactive mutant as it had very low specific activity towards both *p*NPGlc and *p*NPMan. The V184I mutant gave an unexpected result as it had higher specific activity toward *p*NPGlc, resulting in a higher specific *p*NPMan/*p*NPGlc activity ratio of 8.02.

The determination of the kinetic parameters of the V184I and L246V rHv βII mutants toward *p*NPGlc and *p*NPMan confirmed the results from the specific *p*NPMan/*p*NPGlc activity ratio as the K_m values of *p*NPGlc for the L246V mutant is higher (1.06 mM) than that of the V184I mutant (0.25 mM), while the opposite trend was seen for the K_m values for *p*NPMan of L246V (2.32 mM) and V184I (0.27 mM).

In this study, the rHv βII which is expressed in germinating barley seed and two rice β-glucosidases, Os1BGlu1 and Os3BGlu8, were characterized and found to have different activities toward *p*NPGlc, *p*NPMan, and cellooligosaccharides, despite their sequence similarity. The rHv βII hydrolyzes variety of substrates including glycosides, saccharides with different linkages and DP, and various types of plant glycosides. Therefore, rHv βII is a plant β-mannosidase which showed very broad substrate specificity. The attempt to decrease β-mannosidase activity and increase β-glucosidase activity of rHv βII by single mutations to make it more similar to

Os3BGlu7 showed that single mutations are not enough to account for differences between related plant β-glucosidases and β-mannosidases, therefore, multiple mutations to change the shape of the active site may be required.

REFERENCES

Ademark, P., Vroes, Pd., Hagglund, P., Stalbrand, H., Visser, J. (2001). Cloning andcharacterization of *Aspergillus niger* genes encoding an α-galactosidase and a β-mannosidase involved in galactomannan degradation. **Eur. J. Biochem.** 268: 2982-2990.

Akino, T., Nakamura, N., Horikoshi, K. (1988). Characterization of β-mannosidase of an alkalophilic *Bacillus* sp. **Agric. Biol. Chem.** 52: 1459-1464.

Akiyama, T., Kaka, H., Shibuya, N. (1998). A cell wall-bound β−glucosidase from germinated rice: purification and properties. **Phytochemistry** 48: 49-54.

Babcock, G. D., Esen, A. (1994). Substrate specificity of maize β-glucosidase. **Plant Sci.** 101: 31-39.

Baker, N. A., Sept, D., Joseph, S., Holst, M. J., McCammon, J. A. (2001). Electrostatics of nanosystems: Application to microtubules and the ribosome. **Proc. Natl. Acad. Sci** 98: 10037-10041.

Barleben, L., Paniikar, S., Ruppert, M., Koepke, J., Stöckigt, J. (2007). Molecular architecture of strictosidine glucosidase: the gateway to the biosynthesis of the monoterpenoid indole alkaloid family. **Plant Cell** 19: 2886-2897.

Barrett, T., Suresh, C. G., Tolley, S. P., Dodson, E. J., Hughes, M. A. (1995). The crystal structure of a cyanogenic β-glucosidase from white clover, a family 1 glycosyl hydrolase. **Structure** 3: 951-960.

Bauer, M. W., Bylina, E. J., Swanson, R. V., Kelly, R. M. (1996). Comparison of a β-glucosidase and a β-mannosidase from the hyperthermophilic archaeon *Pyrococcus furiosus*. **J. Biol. Chem.** 271: 23749-23755.

Bendtsen, J. D., Nielsen, H., Heijine, G. V., Brunak, S. (2004). Improved prediction of signal peptides: SignalP 3.0. **J. Mol. Biol.** 340: 783-795.

Berrin, J. G., Czjzek, M., Kroon, P. A., McLauchlan, W. R., Puigserver, A., Williamson, G., Juge, N. (2003). Substrate (aglycone) specificity of human cytosolic β-glucosidase. **Biochem. J.** 373: 41-48.

Berrin, J. G., McLauchlan, W. R., Needs, P., Williamson, G., Puigserver, A. (2002). Functional expression of human liver cytosolic β-glucosidase in *Pichia pastoris*. **Eur. J. Biochem.** 269: 249-258.

Boerjan, W., Ralph, J., Baucher, M. (2003). Ligin biosynthesis. **Annua. Rev. Plant Biol.** 54: 519-546.

Bourderioux, A., Lefoix, M., Tatibouet, D., Cottaz, S., Arzt, S., Burmeister, W. P., Rollin, P. (2005). New insights into enzyme-substrate interactions by use of simplified inhibitors. **Org. Biomol. Chem.** 3: 1872-1879.

Bradford, M. M. (1976). A rapid and sensitive method for the quantitation of microgram quantities of protein utilizing the principle of protein-dye binding. **Anal. Biochem.** 72: 248-254.

Bryan, L., Schmutz, S., Hodges, S. D., Snyder, F. F. (1990). Bovine β-mannosidase deficiency. **Biochem. Biophys. Res. Commun.** 173: 491-495.

Brzobohaty, B., Moore, I., Kristoffersen, P., Bako, L., Campos, N., Schell, J., Palme, K. (1993). Release of active cytokinin by a beta-glucosidase localized to the maize root meristem. **Science** 262: 1051-1054.

Burmeister, W. P., Cottaz, S., Driguez, H., Tori, R., Palmieri, S., Henrissat, B. (1997). The crystal structures of *Sinapis alba* myrosinase and a covalent glycosyl-enzyme intermediate provide insights into the substrate recognition and active-site machinery of an S-glycosidase. **Structure** 5: 663-675.

Burmeister, W. P., Cottaz, S., Rollin, P., Vasella, A., Henrissat, B. (2000). High resolution X-ray crystallography shows that ascorbate is a cofactor for myrosinase and substitutes for the function of the catalytic base. **J. Biol. Chem.** 275: 393385-393393.

Carpita, N. C., Gibeaut, D. M. (1993). Structural models of primary-cell walls in flowering plants-consistency of molecular-structure with the physical-properties of the walls during growth. **Plant J.** 3: 1-30.

Chen, H., Leipprandt, J. R., Travis, C. E., Sopher, B. L., Jones, M. Z., Cavanagh, K. T., Friderici, K. H. (1995). Molecular cloning and characterization of bovine β-mannosidase. **J. Biol. Chem.** 270: 3841-3848.

Choi, S. Y., Ko, H. C., Ko, S. Y., Hwang, J. H., Park, J. G., Kang, S. H., Han, S. H., Yun, S. H., Kim, S. J. (2007). Correlation between flavonoid content and the NO production inhibitory activity of peel extracts from various citrus fruits. **Biol. Pharm. Bull.** 30: 772-778.

Chuankhayan, P., Hua, Y., Svasti, J., Sakdarat, S., Sullivan, P. A., Ketudat Cairns, J. R. (2005). Purification of an isoflavinoid 7-O-β-apiosyl-glucosidase β-glucosidase and its substrates from *Dalbergia nigrescens* Kurz. **Photochemistry** 66: 1880-1889.

Chuenchor, W., Pengthaisong, S., Robinson, R. C., Jirundon, Y., Esen, A., Chen, C-J., Opassiri, R., Svasti, J., Ketudat Cairns, J. R. (2008). Structural insights into

rice BGlu1 β−glucosidase oligosaccharide hydrolysis and transglycosylation. **J. Mol. Biol.** 377: 1200-1215.

Cicek, M., Esen, A. (1998). Structure and expression of a dhurrinase (β-glucosidase) from sorghum. **Plant Physiol.** 116: 1469-1478.

Coutinho, P. M., Henrissat, B. (1999). Carbohydrate-active enzymes: an integrated database approach. In H. J. Gilbert, G. Davies, B. Henrissat, B. Svensson, eds, **Recent advances in carbohydrate bioengineering.** The Royal Society of Chemistry, Cambridge, pp 3-12.

Czjzek, M., Cicek, M., Zamboni, V., Bevan, D. R., Henrissat, B., Esen, A. (1997). The mechanism of substrate (aglycone) specificity in *β*-glucosidases is revealed by crystal structures of mutant maize β-glucosidase-DIMBOA, -DIMBOAGlc, and -dhurrin complexes. **Proc. Natl. Acad. Sci.** 97: 13555-13560.

Davies G., Henrissat, B. (1995). Structure and mechanisms of glycosyl hydrolases. **Structure** 3: 853-859.

Davies, G., Mackenzie, L., Varrot, A., Dauter, M., Brzozowski, M., Schulein, M., Withers, S. G. (1998). Snapshots along the enzymatic reaction coordinate: analysis of a retaining β-glycoside hydrolase. **Biochemistry** 37: 11707-11713.

Davies, G. J., Ducros, V. M. A., Varrot, A., Zechel, D. L. (2003). Mapping the conformational itinerary of β-glycosidases by X-ray crystallography. **Biochem. Soc. Trans.** 31: 523-527.

Dietz, K-L., Sauter, A., Wichert, K., Messdaghi, D., Hartung, W. (2000). Extracellular β−glucosidase activity in barley involved in the hydrolysis of ABA glucose conjugate in leaves. **J. Exp. Biol.** 51: 937-944.

Duffaud, G. D., McCutchen, C. M., Leduc, P., Parker, K. N., Kelly, R. M. (1996). Purification and characterization of extremely thermostable β-mannanase, and β-mannosidase, α-galactosidase from the hyperthermophilic eubacterium *Thermotoga neapolitana* 5068. **Appl. Environ. Microb.** 63: 169-177.

Ehlting, J., Mattheus, N., Aeschliman, D. S., Li, E., Hamberger, B., Cullis, I. C., Zhuang, J., Keneda, M., Mansfield, S. D., Samuels, L., Ritland, K., Ellis, B. L., Bohlmann, J., Douglas, C. J. (2005). Global transcript profiling of primary stems from *Arabidopsis thaliana* identifies candidate genes for missing links in lignin biosynthesis and transcriptional regulators of fiber differentiation. **Plant J.** 42: 618-640.

Elbein, A. D., Adya, S., Lee, Y. C. (1977). Purification and properties of a β-mannosidase from *Aspergillus niger*. **J. Biol. Chem.** 252: 2026-2031.

Escamilla-Tevino, L. L., Chen, W., Card, M. L., Shih, M. C., Cheng, C. L., Poulton, J. E. (2006). *Arabidopsis thaliana* β-glucosidases BGLU45 and BGLU46 hydrolyse monolignol glucosides. **Phytochemistry** 67: 1651-1660.

Esen, A. (1992). Purification and partial characterization of maize (*Zea mays L.*) β-glucosidase. **Plant Physiol.** 98: 172-182.

Esen, A. (1993). β-glucosidase: Overview in **β-Glucosidases:Biochemistry and Molecular Biology.** American Chemical Society, Washington, DC, pp 1-26.

Fan, T-M., Conn, E. E. (1988). Isolation and characterization of two cyanogenic β-glucosidases from flax seeds. **Arch. Biochem. Biophys.** 243: 361-373.

Ferreira, A. H. P., Marana, S. R., Terra, W. R., Ferreira, C. (2001). Purification, molecular cloning, and properties of a β-glycosidase isolated from midgut lumen of *Tenebrio molitor* (Coleoptera) larvae. **Insect Biochem. Mol. Biol.** 31: 1065-1076.

Fischer, L. G., Santos, D., Serafin, C., Malherios, A., Monache, F. D., Monache, G. D., Filho, V. C., Souza, M. M. (2008). Further antinociceptive properties of extracts and phenolic compounds from *Plinia glomerata* (Myrtaceae) leaves. **Biol. Pharm. Bull.** 31: 235-239.

Fujiki, Y., Yoshikawa, Y., Sato, T., Inada, N., Ito, M., Nishida, I., Watanabe, A. (2001). Dark-inducible genes from *Arabidopsis thaliana* are associated with leaf senescence and repressed by sugars. **Physiologia. Plantarum.** 111: 345-352.

Fujimoto, H., Isomura, M., Ajisaka, K. (1997). Syntheses of alkyl β-D-mannopyransides and β-1,4-linked oligosaccharides using β-mannosidase from *Rhizopus niveus*. **Biosci. Biotech. Biochem.** 61: 164-165.

Gabrys, B., Tjallingii, W. F. (2002). The role of sinigrin in host plant recognition by aphids during initial plant penetration. **Entomol. Exp. Appl.** 104: 89-93.

Gopalan, V., Daniels, L. B., Glew, R. H., Claeyssens, M. (1989). Kinetic analysis of the interaction of alkyl glycosides with two human β-glucosidases. **Biochem. J.** 262: 541-548.

Grover, A. K., Macmurchie, D. D., Cushley, R. J. (1977). Studies on almond emulsin β-glucosidase, isolation and characterization of a bifunctional isozyme. **Biochim. Biophys. Acta.** 482: 98-108.

Guntert, P., Dotsch, V., Wider, G., Wuthric, H. K. (1992). Processing of multi-dimensional NMR data with the new software PROSA. **J. Biomol. NMR** 2: 619-629.

Ha, M. A., Apperley, D. C., Jarvis, M. C. (1997). Molecular rigidity in dry and hydrated onion cell walls. **Plant Physiol.** 115: 593-598.

Henrissat, B. (1991). A classification of glycosyl hydrolases based on amino acid sequence similarities. **Biochem. J.** 280: 309-316.

Henrissat, B., Bairoch, A. (1993). New families in the classification of glycosyl hydrolases based on amino acid sequence similarities. **Biochem. J.** 293: 781-788.

Henrissat, B., Davies, G. (1996). Updating the sequence-based classification of glycosyl hydrolases. **Biochem. J.** 316: 695-696.

Hiromi, K., Nitta, Y., Namura, C., Ono, S. (1973). Subsite affinities of glucoamylase: examination of the validity of the subsite theory. **Biochim. Biophys. Acta** 302: 362-375.

Hrmova, M., Burton, R. A., Buely, P., Lahnstein, J., Fincher, G. B. (2006a). Hydrolysis of (1,4)-β-mannans in barley (*Hordeum volgare* L.) is mediated by the concerted action of (1,4)-β-mannan endohydrolase and β-D-mannosidase. **Biochem J.** 399: 77-90.

Hrmova, M., Burton, R. A., Biely, P., Lahnstein, J., Fincher, G. B. (2006b). Hydrolysis of (1,4)-β-mannans in barley (*Hordeum vulgare* L.) is mediated by the concerted action of (1,4)-β-mannan endohydrolase and β-D-mannosidase. **Biochem J.** 399: 77-90.

Hrmova, M., Harvey, A. J., Wang, J., Shirley, N. J., Jones, G. P., Stone, B. A., Høji, P. B., Fincher, G. B. (1996). Barley β–D-glucan exohydrolases with β–D-glucosidase activity. **J. Biol. Chem.** 271: 5277-5286.

Hrmova, M., MacGregor, E. A., Biely, P., Stewart, R. J., Fincher, G. B. (1998). Substrate binding and catalytic mechanism of a barley β–D-glucosidase/(1,4)-β–D-glucan exohydrolase. **J. Biol. Chem.** 273: 11134-11143.

Jolly, R. D., Thompson, K. G., Bayliss, S. L., Vidler, B. M., Orr, M. B., Bole, P. L. (1990). β-mannosidosis in a salers calf: a new storage disease of cattle. **N. Z. Vet. J.** 38: 102-105.

Kaufman, P. B., Cseke, L. J., Warber, S., Duke, J. A. (1998). **Natural products from plants.** CRC Press.

Kawasaki, S., Borchert, C., Deyholos, M., Wang, H., Brazille, S., Kawai, K., Galbraith, D., Bohnert, H. J. (2001). Gene expression profiles during the initial phase of salt stress in rice. **Plant Cell** 13: 889-905.

Kikuchi, S., Satoh, K., Nagata, T., Kawagashira, N., Doi, K., Kishimoto, N., Yazaki, J., Ishikawa, M., Yamada, H. (2003). Collection, mapping, and annotation of over 28,000 cDNA clones from *Japonica* rice. **Science** 301: 376-379.

Kitajima, J., Okamura, C., Ishikawa, T., Tanaka, Y. (1998). Coumarin glycisides of *Glehnia littoralis* root and rhizoma. **Chem. Pharm. Bull.** 46: 1404-1407.

Koike, H. (1954). Studies on carbohydrates of insects. I. Distribution of carbohydrases in several insects. **Zool. Mag.** 63: 228-234.

Koshland, D. E. (1953). Sterochemistry and the mechanism of enzymatic reactions. **Biol. Rev.** 28: 416-436.

Kulminskaya, A. A., Eneiskaya, E. V., Isaeva-Ivanova, L. S., Savel'ev, A. N., Sidorenko, I. A., Shabalin, K. A., Golubev, A. M., Neustroev, K. N. (1999). Enzymatic activity and β-galactomannan binding property of β-mannosidase from *Trichoderm reesei*. **Enz. Micro. Tech.** 25: 372-377.

Laemmli. (1970). Cleavage of structural proteins during assembly of head of bateriophage-T_4. **Nature** 227: 680-685.

Laskowski, R. A., MacArthur, M. W., Moss, D. S., Thornton, J. M. (1993). PROCHECK: a program to check the stereochemical quality of protein structures. **J. Appl. Crytstallogr.** 26: 283-291.

Lawson, S. L., Wakarchuk, W. W., Withers, S. G. (1996). Effects of both shortening and lengthening the active site nucleophile of *Bacillus circulans* xylanase on catalytic activity. **Biochemistry** 35: 10110-10118.

Lawson, S. L., Wakarchuk, W. W., Withers, S. G. (1997). Positioning the acid/base catalyst in a glycosidase: studies with *Bacillus circulans* xylanase. **Biochemistry** 36: 2257-2265.

Leah, R., Kigel, J., Svendsen, I., Mundy, J. (1995). Biochemical and molecular characterization of a barley seed β-glucosidase. **J. Biol. Chem.** 270: 15789-15797.

Lee, K. H., Piao, H. L., Kim, H. Y., Choi, S. M., Hartung, W., Hwang, I., Kwak, J. M., Lee, I. J., Hwang, I. (2006). Activation of glucosidase via stress-induced polymerization rapidly increases active pools of abscisic acid. **Cell** 126: 1109-1120.

Li, X., Ljungdahl, L. G., Ximenes, E. A., Chen, H., Felix, C. R., Cotta, M. A., Dies, B. S. (2004). Properties of a recombinant β-glucosidase from the polycentric anaerobic fungus *Orpinomyces* PC-2 and its application for cellulose hydrolysis. **Appl. Biochem. Biotech.** 113: 233-250.

Lin, L. H., Lee, L. W., Sheu, S. Y., Lin, P. Y. (2004). Study on the stevioside analogues of steviolbioside, steviol, and isosteviol 19-alkyl amide dimers: synthesis and cytotoxic and antibacterial activity. **Chem. Pharm. Bull.** 52: 1117-1122.

Lobov, S. V., Kasai, R., Ohtani, K., Tanaka, O., Yamasaki, K. (1991). Enzymatic production of sweet stevioside derivatives: transglucosylation by glucosidases. **Agric, Biol. Chem.** 55: 2929-2965.

Makropoulou, M., Christakopoulos, P., Tsitsimpikou, C., Kekos, D., Kolisis, F. N., Macris, B. J. (1998). Factor affecting the specificity of β-glucosidase from *Fusarium oxysporum* in enzymatic synthesis of alkyl-β-D-glucosides. **Inter. J. Biol. Macromol.** 22: 97-101.

Matsui, K., Eguchi, K., Tetsuka, T. (2008). A novel gene that diverts the anthocyanin biosynthesis pathway towards the production of proanthocyanidins in common buckwheat (*Fagopyyrum esculentum*). **Breeding Science** 58: 143-148.

Mattiacci, L., Dicke, M., Posthumus, M. A. (1995). β-glucosidase: an elicitor of herbivore-induced plant odor that attracts host-searching parasitic wasps. **Proc. Natl. Acad. Sci.** 92: 2036-2040.

McCann, M. C., Robert, K. (1994). Changes in cell-wall architecture during cell elongation. **J. Exp. Bot.** 45: 1683-1691.

Mo, B., Bewley, J. D. (2002). β-Mannosidase (EC 3.2.1.25) activity during and following germination of tomato (*Lycopersicon esculentum* Mill.) seeds. Purification, cloning and characterization. **Planta** 215: 141-152.

Nambisan, B. (1999). *Cassava* latex as a source of linamarase for determination of linamarin. **J. Agric. Food. Chem.** 47: 372-373.

Newcomer, W. S. (1952). The occurrence of β-glucosidase in digestive juice of *Porcellio* and *Armadillidium*. **Anat. Rec.** 113: 536.

Newcomer, W. S. (1954). The occurrence of β-glucosidase in digestive juice of cockroach. **J. Cell. Comp. Physiol.** 43: 79-86.

Newcomer, W. S. (1956). Digestive carbohydrates of the wood louse, *Porcellio*. **Physiol. Zool.** 29: 157-162.

Nielsen, K. A., Hrmova, M., Nielsen, J. N., Forslund, K., Ebert, S., Olsen, C. E., Fincher, G. B., Moller, B. L. (2006). Reconstitution of cyanogenesis in barley (*Hordeum vulgare L.*) and its implications for resistance against the barley powdery mildrew fungus. **Planta** 223: 1010-1023.

Niemeyer, H. M. (1988). Hydroxamic acid (4-hydroxyl-1,4-benzoxazin-3-ones) defense chemicals in the Gramineae. **Phytochemistry** 27: 3349-3358.

O'Neil, M. A., York, W. S. (2003). The composition and structure of plant primart cell wall. In J. K. C. Rose, ed, **The Plant Cell Wall.** Blackwell Publishing, Oxford, UK.

Opassiri, R., Hua, Y., Wara-aswapati, O., Akiyama, T., Svasti, J., Esen, A., Ketudat Cairns, J. R. (2004). β−glucosidase, exo-β-glucanase and pyridoxine transglucosylase activities of rice BGlu1. **Biochem. J.** 379: 125-131.

Opassiri, R., Ketudat Cairns, J. R., Akiyama, T., Wara-aswapati, O., Svasti, J., Esen, A. (2003). Characterization of a rice β−glucosidase highly expressed in flower and germinating shoot. **Plant. Sci.** 165: 627-638.

Opassiri, R., Pomthong, B., Onkoksoong, T., Akiyama, T., Esen, A., Ketudat Cairns, J. R. (2006). Analysis of rice glycosyl hydrolase family I and expression of Os4bglu12 β-glucosidase. **BMC Plant Biol.** 6: 33.

Rantwijk, F. V., Oosterom, M. W., Sheldon, R. A. (1999). Glycosidase-catalysed synthesis of alkyl glycosides. **J. Mol. Catal. B: Enzym.** 6: 511-532.

Robinson, D. (1956). The fluorimetric determination of β-glucosidase : its occurrence in the tissues of animals, including insects. **Biochem. J.** 63: 39-44.

Sabini, E., Sulzenbacher, G., Dauter, M., Dauter, Z., Jorgensen, P. L., Schulein, M., Dupont, C., Davies, G., Wilson, S. (1999). Catalysis and specificity in enzymatic glycoside hydrolysis: a ^{2,5}B conformation for the glycosyl-enzyme intermediate revealed by the structure of the *Bacillus agaradhaerens* family 11 xylanase. **Chem. Biol.** 6: 483-492.

Sali, A., Blundell, T. L. (1993). Comparative protein modelling by satisfaction of spatial restraints. **J. Mol. Biol.** 234: 779-815.

Sambrook, J., MacCallum, P., Russel, D. (2001). **Molecular Cloning: a Laboratory Manual (Third Edition).** Cold Spring Harbor Laboratory Press.

Samuels, L., Rensing, K. H., Douglas, C. J., Mansfield, S. D., Dharmawardhana, D. P., Ellis, B. L. (2002). Cellular machinery of wood production: differentiation of secondary xylem in *Pinus contorta* var. *latifolia*. **Planta** 216: 72-82.

Schlieman, J. (1984). Hydrolysis of conjugated gibberellins by β-glucosidase genes from dwarf rice (*Oryza sativa* L. cv. Tan-ginbozu). **J. Plant. Physiol.** 116: 123-132.

Selmar, D., Lieberei, R., Biehl, B., Voigt, J. (1987). Hevea linamarase- A nonspecific β-glycosidase. **Plant Physiol.** 83: 557-563.

Shahravan, S. H., Qu, X., Chan, I-S., Shin, J. A. (2008). Enhancing the specificity of the enterokinase cleavage reaction to promote efficient cleavage of a fusion tag. **Protein Expr. Purif.** 59: 314-319.

Sidhu, G., Stephen, G., Nguyen, T., McIntosh, L. P., Ziser, L., Brayer, G. D. (1999). Sugar ring distortion in the glycosyl-enzyme intermediate of a family G/11 xylanase. **Biochemistry** 38: 5346-5354.

Simos, G., Panagiotidis, C. A., Skoumbas, A., Choli, D., Ouzounis, C., Georgatsos, J. G. (1994). Barley β-glucosidase: expression during seed germination and maturation and partial amino acid sequences. **Biochim. Biophys. Acta.** 1199: 52-58.

Solovicová, A., Juraj, G., Hostinová, E. (1996). High-yield production of *Saccharomycopsis fibuligera* in *Escherichia coli*, refolding, and comparison of the nonglycosylated and glycosylated enzyme forms. **Biochem. Biophys. Res.** 224: 790-795.

Stephen, M. A. (1982). Other plant polysaccharides. **In GO Aspinall ed. in The Polysaccharides.** Academic Press, New York, USA.

Su, J., Wu, Z. J., Zhang, W. D., Zhang, C., Li, H. L., Lui, R. H., Shen, Y. H. (2008). Two new bis-coumarin glycosides from *Daphne giraldii* nitsche. **Chem. Pharm. Bull.** 56: 589-591,

Sue, M., Ishihara, A., Iwamura, H. (2000a). Purification and characterization of a hydroxamic acid glucoside β-glucosidase from wheat (*Triticum aestivum* L.) seedlings. **Planta** 210: 432-438.

Sue, M., Ishihara, A., Iwamura, H. (2000b). Purification and characterization of a β-glucosidase from rye (*Secale cereale* L.) seedlings. **Plant Sci.** 155: 67-74.

Sue, M., Yamazaki, K., Yajima, S., Nomura, T., Matsukawa, T., Iwamura, H., Miyamoto, T. (2006). Molecular and structural characterization of hexameric β-D-glucosidases in wheat and rye. **Plant Physiol.** 141: 1237-1247.

Svasti, J., Phongsak, T., Sarnthima, R. (2003). Transglucosylation of teritary alcohols using cassava β-glucosidase. **Biochem. Biophy. Res.** 305: 470-475.

Thorlby, G., Fuorrier, N., Warren, G. (2004). The sensitivity to freezing2 gene required for freezing tolerance in *Arabiopsis thaliana,* encodes a β−glucosidase. **Plant Cell** 16: 2192-2203.

Thompson, J. D., Higgin, D. G., Gibson, T. J. (1994). CLUSTAL W: improving the sensitivity of progressive multiple sequence alignment through sequence weighting, positions-specific gap penalties and weight matrix choice. **Nucleic Acids Res.** 22: 4673-4680.

Verdoucq, L., Czjzek, M., Moriniere, J., Bevan, D. R., Esen, A. (2003). Mutational and structural analysis of agylcone specificity in maize and sorghum β-glucosidases. **J. Biol. Chem.** 278: 25055-25062.

Verdoucq, L., Moriniere, J., Bevan, D. R., Esen, A., Vasella, A., Henrissat, B., Czjzek, M. (2004). Structural determinants of substrate specificity in family 1 β-glucosidases: novel insights from the crystal structure of sorghum dhurrinase-1, a plant β-glucosidase with strict specificity, in complex with its natural substrate. **J. Biol. Chem.** 279: 31796-31803.

Wang, Q., Trimbur, D., Graham, R., Warren, R. A. J., Wither, S. G. (1995). Identification of the acid/base catalyst in *Agrobacterium faecalis* β-Glucosidase by kinetic analysis of mutants. **Biochemistry** 34: 14554-14562.

Warzecha, H., Gerasimenko, I., Kutchan, T., Stöckigta, J. (2000). Molecular cloning and functional bacterial expression of a plant glucosidase specifically involved in alkaloid biosythesis. **Phytochemistry** 54: 657-666.

Withers, S. G. (2001). Mechanisms of glycosyl transferases and hydrolases. **Carb. Polymers** 44: 325-337.

Withers, S. G., Rupitz, K., Trimbur, D., Warren, A. J. (1992). Mechanistic consequences of mutation of the active site nucleophile Glu 358 in *Agrobacterium* β-glucosidase. **Biochemistry** 31: 9979-9985.

Withers, S. G., Street, I. P. (1988). Identification of a covalent α-D-glucopyranosyl enzyme intermediate formed on a β-glucosidase. **J. Am. Chem. Soc.** 110: 8551-8553.

Withers, S. G., Warren, R.A. J., Street, I. P., Rupitz, K., Kempton, J. B., Aebersold, R. (1990). Unequivocal demonstration of the involvement of a glutamate residue as a nucleophile in the mechanism of a retaining glycosidase. **J. Am. Chem. Soc.** 112: 5887-5889.

Xu, Z., Escamilla-Treviño, L. L., Zeng, L., Lalgordar, M., Bevan, D. R., Winkel, S. J., Mohamed, A., Ceng, C-L., Shih, M-C., Poulton, J. E., Esen, A. (2004). Functional genomic analysis fo *Arabidopsis thaliana* glycoside hydrolase family 1. **Plant Mol. Biol.** 55: 343-367.

Yag, A., Washida, Y., Takata, N., Nishioka, I. (1972). Studies on *Hydrangea* species I. phenolic components of *Hydrangea serrata* Seringe var. *thunbergii* Sugimoto. **Chem. Pharm. Bull.** 20: 1755-1761.

Yokosuka, A., Mimaki, Y. (2007). Steroidal glycosides from *Agave utahensis*. **Chem. Pharm. Bull.** 55: 145-149.

Zechel, D. L., Withers, S. G. (2000). Glycosidase mechanism: anatomy of finely tuned catalyst. **Acc. Chem. Res.** 33: 11-18.

Zhong, W., Kuntz, D. A., Ember, B., Sigh, H., Moremen, K. W., Rose, D. R., Boons, G-J. (2008). Probing of the substrate specificity of Golgi α-mannosidase II by use of synthetic oligosaccharides and a catalytic nucleophile mutant. **J. Am. Chem. Soc.** 130: 8975-8983.

Zouhar, J., Vevodova, J., Marek, J., Damborsky, J., Su, X-D., Brzobohaty, B. (2001). Insights into the functional artchitecture of the catalytc center of a maize β-glucosidase Zm-p60.1. **Plant Physiol.** 127: 973-985.

CIRRICULUM VITAE

NAME Mr. Teerachai Kuntothom

DATE OF BIRTH 21 March 1977

PLACE OF BIRTH Khon Kaen, Thailand

INSTITUTION ATTENED

Khon Kaen University

Khon Kaen, Thailand, 1998-2001,

Bachelor of Science (Biology)

Mahidol University

Bangkok, Thailand, 1998-2001,

Master of Science (Molecular Biology and Genetic Engineering)

AWARDS AND SCHOLARSHIPS

The Development and Promotion of Science and Technology Talents Projects of Thailand (DPST) Scholarship, 1994-2008